MASTERARBEIT | MASTER'S THESIS

Titel | Title

ICAM-1- and IL-16-induced Proteome Dynamics of Murine Dorsal Root Ganglia: Unveiling Pathways Contributing to TRPA1 Sensitisation in Postsurgical Pain

verfasst von | submitted by

Gudrun Viktoria Hartl BSc

angestrebter akademischer Grad | in partial fulfilment of the requirements for the degree of

Magistra pharmaciae (Mag. pharm.)

Wien | Vienna, 2025

Studienkennzahl lt. Studienblatt | Degree programme code as it appears on the student record sheet:	UA 066 605
Studienrichtung lt. Studienblatt | Degree programme as it appears on the student record sheet:	Masterstudium Pharmazie
Betreut von | Supervisor:	Univ.-Prof. Manuela Schmidt Ph.D.

Abstract

The development of acute and chronic postsurgical pain (CPSP) is driven by neuroinflammatory processes, yet the mechanisms promoting nociceptor sensitisation remain incompletely understood. Intercellular adhesion molecule-1 (ICAM-1) and interleukin-16 (IL-16) have been linked to multiple pain- and injury-related conditions, and recent evidence shows that both mediators enhance neuronal responses to transient receptor potential ankyrin 1 (TRPA1) activation, suggesting TRPA1 sensitisation. However, the underlying molecular pathways remain unclear.

This study therefore investigated how ICAM-1 and IL-16 alter the proteome of dorsal root ganglia (DRG), and which pathways may contribute to TRPA1 sensitisation. Murine DRG cultures were stimulated with ICAM-1 or IL-16 for two hours and differentially expressed proteins (DEPs) and associated pathways were analysed. Both stimuli altered coagulation, complement and extracellular matrix (ECM) remodelling pathways, characterised by reduced levels of coagulation- and complement-related proteins and overexpression of structural ECM components. Although IL-16 influenced wound healing processes more directly, the findings indicate that both mediators promote early ECM remodelling.

Comparative analysis revealed distinct signalling mechanisms for each mediator: ICAM-1-specific DEPs engaged toll-like receptor 2/4 (TLR2/4) pathways coupled to canonical nuclear factor kappa-light-chain-enhancer of activated B cells (NF-κB) signalling, whereas those unique to IL-16 stimulation were associated with tumour necrosis factor (TNF)-mediated pathways as well as non-canonical NF-κB signalling. IL-16 also promoted the synthesis of pro-inflammatory cytokines TNF and IL-6, which may subsequently drive arachidonic acid and prostaglandin production, potentially enhancing TRPA1 sensitisation.

Together these findings highlight ICAM-1 and IL-6 as upstream regulators of distinct, yet converging inflammatory pathways in DRGs, offering new insights into early molecular mechanisms that may drive TRPA1 sensitisation in the development of chronic postsurgical pain.

Zusammenfassung

Die Entstehung akuter und chronischer postoperativer Schmerzen wird durch neuro-inflammatorische Prozesse beeinflusst, doch die Mechanismen der Nozizeptor-Sensibilisierung sind noch nicht vollständig verstanden. Das intercellular adhesion molecule-1 (ICAM-1) und Interleukin-16 (IL-16) wurden bereits mit verschiedenen schmerz- und verletzungsassoziierten Erkrankungen in Verbindung gebracht. Neuere Erkenntnisse zeigen, dass beide Mediatoren neuronale Antworten auf die Aktivierung des transient receptor potential ankyrin 1 (TRPA1) verstärken und somit eine TRPA1 Sensibilisierung begünstigen könnten, doch die zugrundeliegenden molekularen Signalwege sind weitgehend ungeklärt.

Diese Studie untersuchte daher, wie ICAM-1 und IL-16 das Proteom von Spinalganglien (DRG) verändern und welche Mechanismen zur Sensibilisierung von TRPA1-Kanälen beitragen könnten. Murine DRG-Kulturen wurden zwei Stunden mit ICAM-1 bzw. IL-16 stimuliert und differentiell exprimierte Proteine (DEPs) sowie zugehörige Signalwege analysiert. Beide Stimuli beeinflussten Koagulations-, Komplement- und Umbauprozesse der extrazellulären Matrix (ECM), gekennzeichnet durch eine verringerte Expression von Gerinnungs- und Komplementproteinen und eine Überexpression struktureller ECM-Komponenten. Obwohl IL-16 einen direkteren Einfluss auf Wundheilungsprozesse zeigte, deuten die Ergebnisse darauf hin, dass beide Mediatoren den Beginn des ECM-Umbaus begünstigen.

Der Vergleich beider Gruppen zeigte, dass ICAM-1-spezifische DEPs an Toll-like Rezeptor 2/4 (TLR2/4)-Signalwegen beteiligt waren, die mit der kanonischen Aktivierung des nuclear factor kappa-light-chain-enhancer of activated B cells (NF-κB) gekoppelt sind. Im Gegensatz dazu, waren IL-16 spezifische DEPs mit tumour necrosis factor (TNF)-vermittelten Signalwegen sowie nicht-kanonischen NF-κB Signalübertragung verbunden. Zudem begünstigten IL-16-induzierte Proteine die Synthese der pro-inflammatorischen Zytokine TNF und IL-6, die nachgeschaltet die Produktion von Arachidonsäure und Prostaglandinen steigern und so zur TRPA1 Sensibilisierung beitragen könnten.

Zusammen zeigen diese Ergebnisse, dass ICAM-1 und IL-16 unterschiedliche, aber konvergierende Entzündungswege in den DRGs regulieren. Sie liefern außerdem neue Einblicke in die frühen molekularen Mechanismen, die zur TRPA1 Sensibilisierung bei der Entwicklung chronischer postoperativer Schmerzen beitragen könnten.

Table of Contents

List of Figures

List of Tables

List of Abbreviations

AA	arachidonic acid
Ahsg	alpha-2-HS-glycoprotein
Ambp	alpha-1 microglobulin/ bikunin precursor
Apoa1	apolipoprotein A-I
Arg2	arginase-2, mitochondrial
ATP	adenosine triphosphate
Bgn	biglycan
BP	biological processes
C1qtnf3	complement C1q tumour necrosis factor-related protein 3
CC	cellular components
Ccn2	cellular communication network factor 2
CD4	cluster of differentiation 4
Cfi	complement factor I
CGRP	calcitonin-gene related peptide
CNS	central nervous system
Col1a1	collagen (I) alpha-1 chain
Col1a2	collagen (I) alpha- 2 chain
CPSP	chronic postsurgical pain
CV	coefficient of variation
Cxcl10	C-X-C motif chemokine 10
Cxcl12	stromal cell-derived factor 1
Cyp2j6	cytochrome P450 2J6
DAMP	danger-associated molecular pattern
DEP	differentially expressed protein
Dhx33	ATP-dependent RNA helicase DHX33
DMNC	Density of Maximum Neighbourhood Component
DRG	dorsal root ganglia
Dusp15	dual specificity protein phosphatase 15
ECM	extracellular matrix
Ecm1	extracellular matrix protein 1
ERK1/2	extracellular signal-regulated kinases 1 and 2
FC	fold change
Fgb/ Fgg	fibrinogen beta/ gamma chain
Fgfr3	fibroblast growth factor receptor 3
Fyn	tyrosine protein kinase Fyn
Gal	galanin
Glrx	glutaredoxin
GO	gene ontology

Gpb5	glycoprotein hormone beta-5
Htra1	high-temperature requirement A serine protease 1
ICAM-1	intercellular adhesion molecule-1
Ifitm3	interferon-induced transmembrane protein 3
IFN-γ	interferon-γ
IKK	IκB kinase
IL	interleukin (IL-1β, IL-2, IL-6, IL-16, IL-17)
Ilrun	protein ILRUN
IRAK1/2/4	interleukin-1 receptor-associated kinase 1/2/4
JAK	janus kinase
Kit	mast/stem cell growth factor receptor Kit
LPS	lipopolysaccharide
Lyn	tyrosine protein kinase Lyn
MAPK	mitogen-activated protein kinase
MCC	Maximal Clique Centrality
MF	molecular function
Mif	macrophage migration inhibitory factor
MMP	matrix metalloproteinase
MyD88	myeloid differentiation primary-response protein 88
NaV	voltage-gated sodium channel (Nav1.7, Nav1.8)
NF-κB	nuclear factor kappa-light-chain-enhancer of activated B cells
NGF	nerve growth factor
NIK	NF-κB-inducing kinase
NIL-IL-16	neuronal Interleukin-16
NO	nitric oxide
Otud5	OTU domain-containing protein 5
Pde4d	3',5'-cyclic-AMP phosphodiesterase 4D
Per1	Period circadian protein homolog 1
PG	Prostaglandin
PKA/C	protein kinase A/C
Pla2g4a	phospholipase A2 group IVA
Polr3f	DNA-directed RNA polymerase III subunit RPC6
Postn	periostin
PPI	protein-protein-interaction
Prg4	proteoglycan 4
Prkca	protein kinase C alpha type
Ptpn6	tyrosine-protein phosphatase non-receptor type 6
Pzp	pregnancy zone protein
Rac1	Ras-related protein Rac1
ROS	reactive oxygen species

S1P	sphingosine-1-phosphate
SCI	spinal cord injury
Serpind1	heparin cofactor 2
SGC	satellite glial cell
Smad1/5	mothers against decapentaplegic homolog 1/5
Sphk1	sphingosine kinase 1
Src	proto-oncogene tyrosine-protein kinase Src
STAT	signal transducer and activator of transcription
TAK1	TGF-β-activated kinase 1
Tank	TRAF family member-associated NF-kappa-B activator
TGF-β	transforming growth factor-β
Thbs1	thrombospondin-1
Tifa	TRAF-interacting protein with FHA domain-containing protein A
TIRAP	TIR domain-containing adaptor protein
TLR2/4	toll-like receptor 2/4
TNF-α	tumour necrosis factor-α
TRAF2/3	TNF receptor-associated factor 2/3
Traf6	TNF receptor-associated factor 6
Trex1	three-prime repair exonuclease 1
TRPA1	transient receptor potential ankyrin 1
TRPV1	transient receptor potential vanilloid 1
Zbtb20	zinc finger and BTB domain-containing protein 20

1. Introduction

1.1. Postoperative Pain

1.1.1. Acute and Chronic Postsurgical Pain (CPSP)

Pain is an "unpleasant sensory and emotional experience associated with actual or potential tissue damage" according to The International Association for the Study of Pain (IASP). Acute pain is the body's response to tissue damage, illness of inflammation. It is a protective mechanism that plays a key role in survival as it facilitates healing after e.g. an operation.[1] However, if it lasts beyond the healing process, (> three months after surgery or tissue trauma) acute pain can become chronic.[2]

In Europe alone, there are more than 50 million surgeries a year.[3] Around four out of five patients suffer from acute pain after surgery, the majority being moderate to severe [pain]. Inadequate treatment is associated with an increased risk of developing chronic postsurgical pain (CPSP).[4]

Currently, opioids and regional anaesthetics are used to treat acute pain after surgeries. These limited treatment options however, can cause severe adverse effects, including chronic opioid use.[5] Therefore, it is important to discover mechanisms involved in postsurgical pain to develop novel therapeutics that cause less adverse effects than current drugs, and translate these findings from research into practice.[6]

1.1.2. Dorsal Root Ganglia (DRG) and their Role in Pain

The dorsal root ganglia (DRGs) in the peripheral nervous system contain the cell bodies of nociceptors and other primary sensory neurons along with immune cells (macrophages and satellite glial cells) and endothelial cells.[7] Under chronic pain conditions, the number of primary and secondary immune cells within DRGs has been shown to increase.[8]

Nociceptors express different molecular sensors, including transient receptor potential channels (e.g. TRPA1, TRPV1), G-protein coupled receptors (GCPRs), voltage-gated sodium channels (e.g. Nav1.7, Nav1.8) and mechanosensitive Piezo channels. These receptors detect peripheral physical stimuli (mechanical injuries, temperatures) and chemical molecules that

foster inflammation. Damaged cells and nearby immune cells secrete inflammatory substances including prostaglandins (PGs), H+, bradykinin, tumour necrosis factor-α (TNF-α), interleukin-1β (IL-1β) and chemokines.[9,10] Noxious stimuli are transduced into electrical signals at the peripheral nociceptive nerve terminals, and the resulting action potentials are transmitted via Aδ- and C-fibres to the dorsal horn of the spinal cord, where they synapse with second-order neurons. The release of glutamate and substance P triggers these neurons, which relay the signal to higher brain structures. Myelinated Aδ-fibres conduct signals rapidly, causing sharp and localised pain, whereas unmyelinated slow-conducting fibres mediate dull and diffuse pain.[7,9]

Continuous stimulation of peripheral nociceptors promotes neuroplastic changes that increase pain sensitivity. The release of pro-inflammatory mediators from primary afferent fibres stimulates mast cell-mediated histamine secretion, which triggers the release of substance P and calcitonin-gene related peptide (CGRP) from C-fibres, producing neurogenic inflammation. These mediators lower the activation threshold of TRP channels and modulate NaV channels and protein kinases (PKA, PKC), resulting in peripheral sensitisation. Peripheral glutamate release from C-fibres depolarises dorsal horn neurons, removes the Mg^{2+} block from NMDA receptors, and allows normally non-noxious Aβ-fibre input to evoke pain (allodynia). Excitatory substances, nitric oxide (NO) and PGs also activate central glial cells, inducing cyclooxygenase-2 expression and the production of PGE2 and cytokines, lowering the thresholds in second-order neurons. Anti-nociceptive (GABA- and glycinergic) interneurons and descending serotonergic/ noradrenergic pathways normally modulate nociceptive signalling. However, dysfunction or loss of these inhibitory systems promotes central sensitisation, driving chronic pain and hyperalgesia (increased pain sensitivity).[9]

1.1.3. Neuroimmune System in Postoperative Pain

Injury or infection triggers inflammatory responses, characterised by pain, redness, oedema, warmth and loss of function. Within the central nervous system (CNS), the corresponding innate immune response to such noxious stimuli, referred to as neuroinflammation, fosters regeneration and healing, but can also drive the development of CPSP.[10–12]

The central nervous and immune system are tightly interconnected through bidirectional signalling pathways. Consequently, pain is not only a characteristic of inflammation, but also regulates immune responses.[10] Mediators secreted by immune cells regulate nociceptor activity and sensitisation and inflammatory conditions lower nociceptive thresholds, thereby inducing hyperalgesia. Nociceptors, on the other hand, modulate immune responses through the release of neuropeptides and neurotransmitters.[8] For instance, TRPA1 and TRPV1 activation promotes the secretion of Substance P and calcitonin gene-related peptide (CGRP), increasing nociception as well as neurogenic inflammation.[10]

In response to injury, macrophages produce cytokines, lipids and growth factors that can directly active nociceptive sensory neurons.[10] The release of Substance P from murine macrophages triggers extracellular signal-regulated kinases 1 and 2 (ERK1/2) and mitogen-activated protein kinase (MAPK) pathways. Subsequent nuclear factor kappa-light-chain-enhancer of activated B cells (NF-κB) signalling promotes the synthesis of TNF-α, IL-1β and IL-6. As a result, additional immune cells (macrophages, neutrophils, T cells) are recruited, and leukocytes migrate from the periphery to injured tissue, thereby prolonging inflammation. Mast cells further sensitise nociceptors by releasing cytokines, histamine and nerve growth factor (NGF).[10,13] The complement system, another component of the primary immune response, also modulates nociception. Elevated levels of complement factors C5/ C5a and the G-protein coupled receptor C5aR1 have been found in animal models of postsurgical and neuropathic pain. Shutov et al. showed that C5a signalling induces thermal hyperalgesia, by interacting with NGF-releasing macrophages that regulate TRPV1 receptors.[14]

Neuroinflammation, characterised by glial cell activation, release of pro-inflammatory substances and vascular alterations, plays a crucial role in the progression of acute to chronic postsurgical pain. Increased vascular permeability facilitates immune cell infiltration (e.g. leukocytes) and changes in gene expression. As illustrated in *Figure 1*, primary and secondary immune cells as well as glial cells all promote the development of CPSP, by releasing substances that activate and sensitise nociceptors.[15]

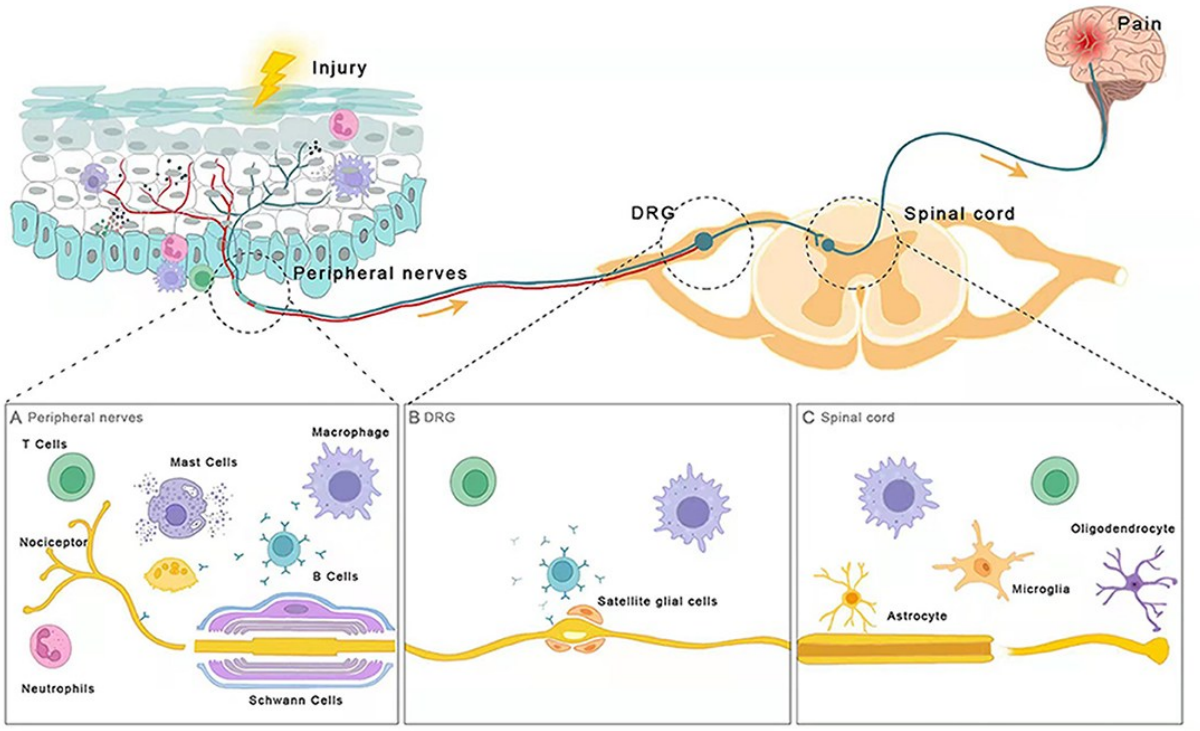

Figure 1: Immune cells involved in chronic pain following injury. *The nervous and immune system communicate via various signalling pathways. Primary immune cells (macrophages, neutrophils, mast cells), secondary immune cells (B and T lymphocytes) and glial cells (SGCs, microglia, astrocytes, oligodendrocytes) release substances that regulate the sensitivity and excitability of nociceptors. This promotes the transition from acute to chronic postsurgical pain. Figure taken from* $Yang\ et\ al$[15]

Activated glial cells, including microglia, astrocytes and satellite glial cells (SGCs), are important drivers of peripheral and central sensitisation.[2] They release ATP (adenosine triphosphate), glutamate and cytokines (IL-1β, IL-6, TNF) and express P2 purinergic receptors (P2Rs) that bind neuronal ATP. This enables glial cells to communicate with each other and adjacent neurons. Inflammation or nerve damage activates SGCs in sensory ganglia, where P2X7R-mediated phosphorylation of ERK (pERK1/2) induces TNF release, increasing neuronal excitability and contributing to the chronification of postsurgical pain.[16] Microglia are primary immune cells that have macrophage-like functions. They release and respond to pro-inflammatory cytokines, chemokines, reactive oxygen species (ROS) and secondary messengers (PGs and NO) that regulate nociceptive signalling pathways. Following injury, activated spinal microglia cause alterations in the synapses of the dorsal horn, which can lead to hyperalgesia.[12,17]

1.2. Inflammatory Markers

1.2.1. Intercellular Adhesion Molecule-1 (ICAM-1)

Intercellular adhesion molecules (ICAMs) mediate interactions between cells and play essential roles in inflammation and immunosurveillance.[18] They regulate the barriers of the endo- and epithelium and act as signalling receptors in inflammatory and healing processes.[19]

ICAM-1 (or CD54) is a cell surface glycoprotein of the immunoglobulin (Ig) superfamily, comprising five Ig domains (extracellular), one transmembrane domain and a C-terminal cytoplasmic tail (intracellular).[18,20] Six membrane-bound ICAM-1 isoforms and one soluble variant (sICAM-1) have been identified.[19] sICAM-1 can be generated via alternative splicing after transcription, or enzymatic cleavage of membrane ICAM-1 by disintegrin, metalloproteinases (ADAM10, ADAM17) and matrix metalloproteinases (MMP-2, MMP-9).[21]

While ICAM-1 is continuously expressed on immune, endothelial, epithelial and glial cells as well as neurons, upon inflammation it is often upregulated by pro-inflammatory stimuli (TNF-α, IL-1β, IFN-γ) via NF-κB activation.[20,22] Its upregulation also involves janus kinase-signal transducer and activator of transcription (JAK-STAT), MAPK and PKC signalling cascades.[22]

By binding the integrin lymphocyte function-associated antigen-1 (LFA-1), ICAM-1 mediates innate and adaptive immune system activation and leukocyte trafficking. It promotes the adhesion of leukocytes to the endothelium, facilitating their extravasation into inflamed tissue.[18,19] Elevated ICAM-1 expression also triggers microglial and astrocytic activation and the release of pro-inflammatory substances, thereby increasing the excitability of neurons and driving pain hypersensitivity and central sensitisation.[22]

Given its central role in inflammatory processes, ICAM-1 has been implicated in various neuroinflammatory and neurodegenerative diseases. Dysregulated expression contributes to the breakdown of the blood-brain barrier in conditions such as Morbus Alzheimer, multiple sclerosis, stroke and traumatic brain injury.[21,23] A recent transcriptomic and Mendelian randomisation study by Yuan et al. identified ICAM-1 as a potential biomarker and target in spinal cord injury (SCI). Seven days post-SCI, a significant increase of circulating ICAM-1 was observed, especially in patients with delayed wound healing and pressure ulcers. Functional enrichment analysis linked ICAM-1 to NF-κB signalling, cell adhesion, extracellular matrix (ECM)-receptor interactions, response to lipopolysaccharides (LPS), and lymphocyte

proliferation, underscoring its dual role in inflammation control and tissue repair. Furthermore, multivariable Mendelian randomisation suggested a protective effect of ICAM-1 in SCI recovery.[24]

Soluble adhesion molecules have also been linked to multiple pain-related conditions.[25] In a study by Luchting et al., higher pain intensities were described by chronic pain patients with increased sICAM-1 serum levels. Changes in pain ratings further correlated with altered sICAM-1 expression, highlighting its potential as a biomarker.[26] the upregulation of serum sICAM-1 has also been linked to autoimmune diseases (e.g. rheumatoid arthritis, systemic lupus erythematosus, psoriasis), late-life depression, type 2 diabetes and a higher cardiovascular disease mortality rate. *Figure 2* shows numerous diseases that are associated with dysregulated ICAM-1 or sICAM-1 levels.[21,27]

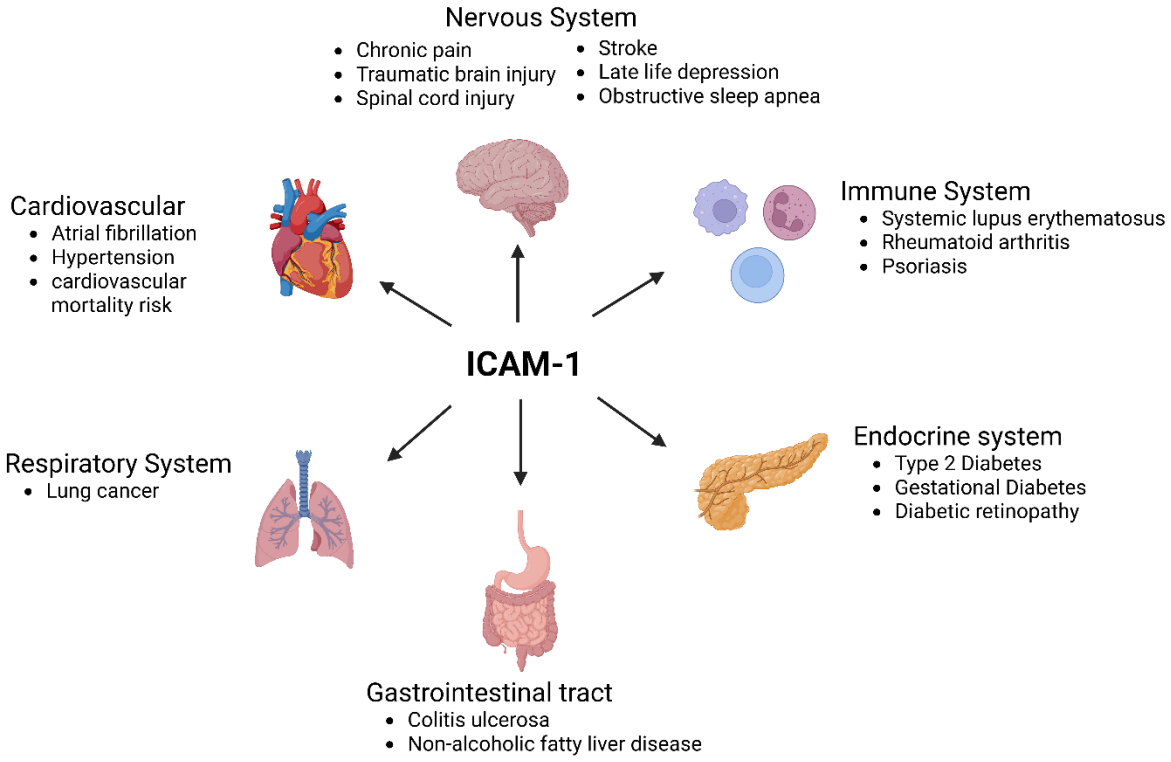

Figure 2: diseases associated with ICAM-1 or sICAM-1 dysregulation: *Figure adapted from Miller et al.[21] and created with BioRender (https://www.biorender.com/)*

1.2.2. Interleukin-16 (IL-16)

IL-16 is an immunoregulatory cytokine that fosters inflammation by controlling T-lymphocyte activation, growth and migration, cytokine production, and chemoattraction.[28] Two splice variants exist: IL-16 and the neuronal isoform NIL-16. The precursor pro-IL-16 is synthesised by multiple immune- and non-immune cells, including T helper cells (CD4+), cytotoxic T cells (CD8+), dendritic cells, macrophages, neutrophils, fibroblasts and microglia.[29] Upon stimulation, caspase-3 cleaves the precursor, releasing active IL-16 through a MAPK-dependent pathway, associated with the release of IL-1β. However, some circulating cells (e.g. CD8+ T lymphocytes, eosinophils and mast cells) carry pre-synthesised IL-16 and immediately release it upon stimulation with serotonin or histamine. The neuronal form NIL-16 is expressed in cerebellar and hippocampal neurons, regulates their excitability and is processed similarly via caspase-3 cleavage.[30]

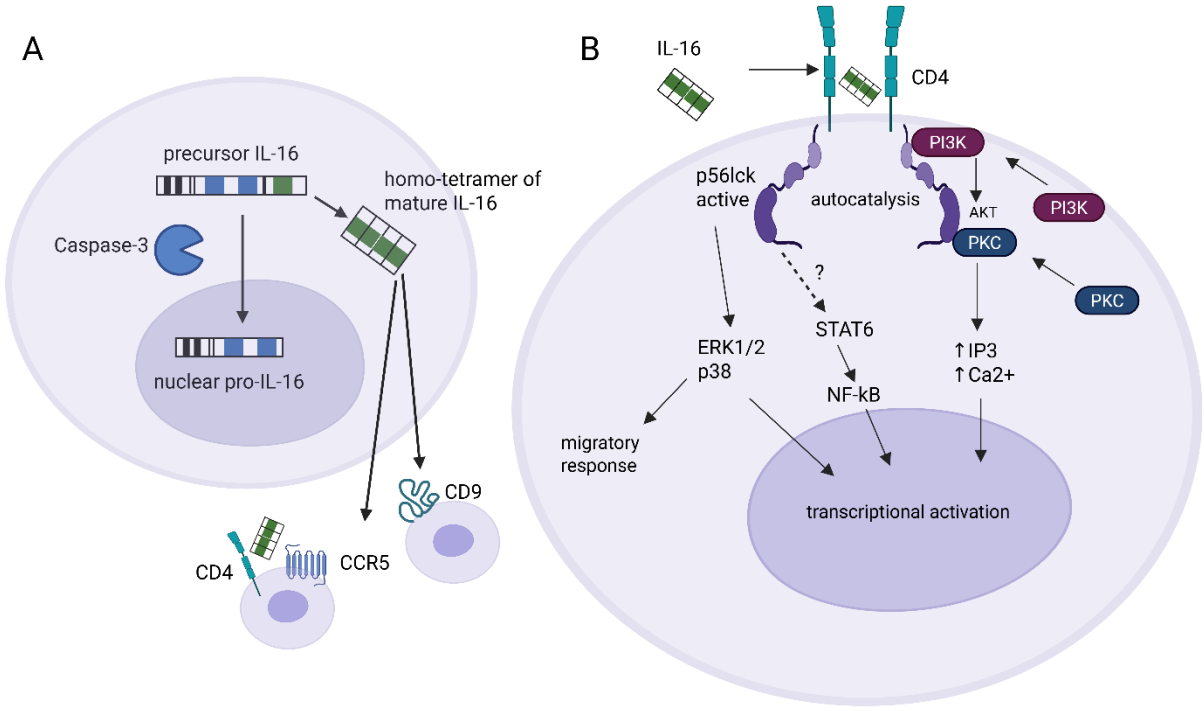

Figure 3: Processing and signalling of IL-16. *(A) IL-16 is cleaved by caspase-3 and homo-tetramers of mature IL-16 are released and bind to CD4, CD9 or CCR5. (B) IL-16 binding to CD4 leads to CD4 dimerization and autocatalysis. The activation of p56lck stimulates PI3K, ERK and p38, resulting in cell migration. Following PKC activation, IP3 and intracellular calcium are increased. All processes lead to the activation of transcription. Figure adapted from (A) Niewold et al.[30] and (B) Richmond et al.[31] and created with BioRender (https://www.biorender.com/)*

IL-16 signals through cluster of differentiation 4/ 9 (CD4, CD9) and CC chemokine receptor type 5 (CCR5) receptors, with CD4 regarded as the main target due to its wide expression on multiple immune, haematopoietic and neuronal cells. within the spinal cord, CD4 is expressed by microglia, adjacent neurons and astrocytes. After CD4 engagement, IL-16 stimulates the src-related tyrosine kinase p56lck, promoting PKC translocation. This activates signalling pathways in the target cells involving intracellular Ca^{2+}, Inositol 1,4,5-trisphosphate (IP3) and phosphoinositide 3-kinase (PI3K), as shown by *Figure 3*. IL-16-CD4 binding also activates STAT6, however the subsequent signalling cascades and cellular effects are not yet known.[30,31]

Elevated levels of circulating IL-16 have been associated with pain, inflammation, infection, autoimmune diseases as well as cancer, highlighting its potential as a drug target.[30] In rheumatoid arthritis, González-Rodríguez et al. demonstrated that locally and systemically administered IL-16 contributes to CC motif chemokine ligand 4 (CCL4)-evoked hyperalgesia after tissue injury. By binding CD4, IL-16 mediates the release of IL-1β, IL-6 or TNF-α, stimulating the production of PGs, which are known for their role in inflammatory peripheral sensitisation.[32] Similarly, a murine model of nociceptive pain linked IL-16 to the activation of astrocytes and glial cells, increased excitability of nociceptors and the progression of inflammatory pain.[30]

Beyond nociceptive pathways, IL-16 has been implicated in the pathogenesis of immune-mediated diseases. Hridi et al. reported its involvement in multiple sclerosis (MS), where IL-16 contributes to neuroinflammation via resident and infiltrating immune cells.[29] IL-16 positive T and B lymphocytes and dendritic cells have been detected in MS lesions, correlating with the extent of axonal damage. Even several psychiatric conditions (e.g. major depressive disorder, anxiety, insomnia) are related to levels of circulating IL-16 and Th1-mediated immune responses.[30]

1.3. Study Aim

The development of chronic postsurgical pain (CPSP) is known to have an inflammatory component. Elevated levels of ICAM-1 and IL-16 have been associated with various pathological and pain-related conditions. However, their effects on the proteomic profile of murine dorsal root ganglia have not yet been described. Recent work by Lea Weiß demonstrated that ICAM-1 and IL-16 stimulation increases the excitability of sensory neurons during perfusion with TRPA1 agonists. Nevertheless, the molecular mechanisms underlying TRPA1 sensitisation by these inflammatory markers remain uncertain.[33]

Therefore, the present study aimed to investigate the pathways through which ICAM-1, and IL-16 contribute to TRPA1 sensitisation in the context of postsurgical pain. For this purpose, murine DRG cell cultures were stimulated with ICAM-1 and IL-16 for two hours and a bulk proteomic approach was applied to identify changes in protein expression. By analysing differentially expressed proteins, we aimed to uncover signalling pathways affected by each mediator. Both treatments were examined individually and comparatively to identify overlapping as well as stimulus-specific mechanisms.

2. Materials and Methods

2.1. Materials

2.1.1. Experimental Mice

12 C57BL/6J wildtype mice were used in total. Six mice were bred in-house and used for IL-16 treatment. The other six used for the ICAM-1 stimulation experiment were purchased from Janvier Labs (Le Genest-Saint-Isle, France) and further bred in-house.

2.1.2. Reagents

Table 1: Reagents used for cell culture

Reagent	**Reference**	**Lot #**
Bovine Serum albumine (BSA)	Sigma-Aldrich	SLCM8620
Collagenase Type IV	Gibco	2820868
DMEM/F12 1:1 1X GlutaMax	Gibco	2916978
Horse serum	Gibco	1861232
Laminin	Invitrogen	2239271
Nerve Growth Factor (NGF)	R&D	HS5023111
Papain	Worthington	54D24436
Poly-D-Lysine (PDL)	Sigma-Aldrich	0000302807
70% Ethanol		

Table 2: Reagents used for Cell stimulation

Reagent	**Reference**	**Lot #**
ICAM-1 (10 ng/mL)	Sino Biological Inc.	LC16NO1012
IL-16 (100 ng/mL)	Invitrogen	ZK4545471
Lonza Water	AccuGene	21MB036

Table 3: Reagents used for Cell harvest and Whole Cell Lysis

Reagent	Reference	Lot #
cOmplete Protease Inhibitor Cocktail	Roche	74102800
Dithiothreitol 10 mM (DTT)	Sigma-Aldrich	Cas# 3483-12-3
Glycerol	Fisher	224125
Sodium dodecyl sulfate 20% (SDS)	Fisher Scientific	2929465
Tris-HCl 1M pH 7,4	AccuGENE	0000924725
Water LC-MS grade	Sigma-Aldrich	Z0911433406

Table 4: Reagents used for SP3

Reagent	Reference	Lot #
Acetonitrile (ACN)	Fisher Scientific	2484795
Ammonium bicarbonate (ABC)	Sigma Aldrich	BCCL4829
Ethanol gradient grade for liquid chromatography LiChrosolv®	Sigma Aldrich	1117272500
LC-MS grade LiChrosolv® Water	Sigma Aldrich	Z0911433406
NaOH 0.1 M	Fisher Scientific	2400759
Resuspension Buffer	PROMEGA	0000572520
Trypsin/ Lys-C Mix, Mass spec Grade (cell culture 1 & 2)	PROMEGA	0000586405
Trypsin/ Lys-C Mix, Mass spec Grade (cell culture 3-12)	PROMEGA	0000586405
2-Iodoacetamide (IAA)	Sigma Aldrich	0000305315
15mL SpeedBead magnetic carboxylate modified particles	Fisher Scientific	65152105050250
15mL SpeedBead magnetic carboxylate modified particles	Fisher Scientific	45152105050250

2.1.3. Consumables

Table 5: Consumables

Type	Specification	Source/ Manufacturer
Coverslips	Microscope cover glasses 12 mm ⌀	CarlRothGmbh
24 well plates	CELLSTAR® plate	Greiner Bio-One
Tubes	1.5mL Protein LoBind Tube	Eppendorf
	1.5 ml Microcentrifuge tube (autoclaved)	VWR
	15 mL Falcon CELLSTAR® tubes	Greiner Bio-One
	50 mL Falcon tubes	Greiner Bio-One
Paper	Indicator paper Rota® pH 1-12	VWR
	Weighing paper, 531 100 x 100 mm	VWR
Pipettes	Serological pipettes (5mL, 10mL, 50mL)	Fisher Brand
	Disposable Glass Pasteur Pipettes (2 mL)	VWR
Pipette tips	SurPhob® Filter tips 1-1000 µL	Biozym Scientific

2.1.4. Equipment

Table 6: Equipment

Type	Specification	Source/ Manufacturer
Analytical scale	AX124 M-pact	Satorius
Bioruptor	Bioruptor® Pico + Bioruptor® Cooler	Diagenode
Centrifuge	Centrifuge 5702	Eppendorf
	Ministar Micro Centrifuge	VWR
	HERAEUS FRESCO 17 Centrifuge	Thermo Scientific
Dissection tools	Cannulas (Henke-Ject 0.90x40mm 20Gx1 ½")	Henke Sass Wolf
	CO_2 chamber	
	Operating scissors	Fine Science Tools
	Dissecting scissors	
	Micro dissecting scissors	

	Micro dissecting spring scissors	
	Forceps	
	Micro dissecting tweezers	
	Rubber dissection disk	
	Styrofoam dissection board	
Freezer	Freezer Premium -20°C	Liebherr
	Inova U725 -80°C	Eppendorf
Fridge	Comfort	Liebherr
Incubator	HERAcell 150i CO2 incubator	Thermo Scientific
Magnetic rack	DynaMag 2	Invitrogen
Microscope	Stereo Microscope	Nikon
	Observer.Z1	Zeiss
Nano Photometer	Nanophotometer® N60	Implen
Pipettes	Pipetman P2, P20, P200, P1000	Gilson
	Pipettes 5, 10, 200, 1000 µL	Eppendorf
Pipettus	Pipette boy	Integra
Reagent Reservoir	Science Ware	
Sterile working bank	Safe 2020 Class II Biological Safety cabinet	Thermo Scientific
Spatulas		
Thermomixer	Thermomixer C	Eppendorf
Vacuum Hand Operator	Vacuboy	Integra
Vacuum Tube	Vacusafe	Integra
Vortexer	VWR international	VWR
Water bath	AQUAline – AL12 waterbath	Lauda

2.2. Methods

2.2.1. Experimental Design

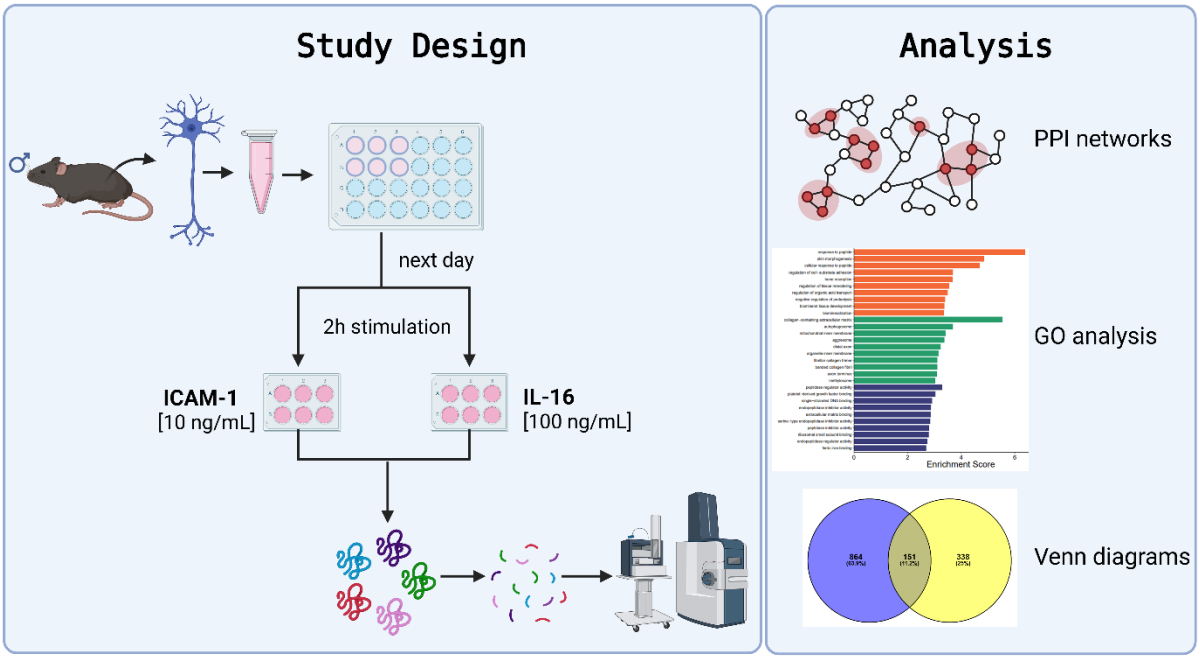

Figure 4: Experimental design of the study: *The murine DRGs of 12 mice were isolated and cultured. The wild-type cultures were stimulated with 10 ng/mL of ICAM-1 or 100 ng/mL of IL-16 for 2 hours. The cells were harvested, and proteins were extracted. Peptides were isolated and analysed using LC-MS/MS. Finaly, PPI networks with ICAM-1 and IL-16-induced DEPs were created, and functional enrichment analysis was performed. Figure created with BioRender (https://www.biorender.com/)*

In this study, the effects of ICAM-1 and IL-16 treatment on murine DRGS were examined on the proteome level. For this purpose, 12 male naïve C57BL/6J mice aged 10-12 weeks were used and at least 36 DRGs (5 lumbar, 12 thoracal and 1 cervical DRG on both sides) were isolated from each animal. Half of the mice were imported from Janvier Labs (Le Genest-Saint-Isle, France) and used for ICAM-1 treatment. The other six mice were in-house bred, and cell cultures were stimulated with IL-16.

One mouse was used per 6-well cell culture and on the following day, the treatment was added to three wells., while the other three served as controls. After a short stimulation of two hours, the cells were harvested and lysed to extract the proteins. Peptides were extracted using SP3 sample preparation (*Chapter 2.2.6*) and then analysed by mass spectrometry. Finaly, the received data were used to create protein-protein interaction networks and perform functional enrichment analysis. Lastly, shared as well as treatment-specific dysregulated proteins were further examined to identify shared and treatment-specific pathways that may contribute to TRPA1 sensitisation. *Figure 4* shows the experimental setup of this study.

2.2.2. Isolation of Dorsal Root Ganglia

Every mouse was euthanised in a CO_2 chamber and by checking the hind paw-reflex, their death was confirmed. The mouse was then placed on a Styrofoam dissection board, ventral side downwards. To disinfect and prevent displacement of fur, the animal was sprayed down with 70% Ethanol. After cutting off the head with operating scissors, the body was fixed with four cannulas. One was used to pin down each thigh, one was inserted at the top of the spine to stretch out the body, and another one at the base of the tail. Using forceps, the fur of the mouse was pulled up, and the first incision was made above the tail and removed by cutting on both sides towards the neck to expose the spine.

Using dissecting scissors, the spine was cut off at the base of the tail, before the hip bone was cut on both sides. Further incisions were made towards the neck, while also removing the organs and fatty tissue, to isolate the vertebral column.

The spine was placed on a rubber dissection disc and pinned down with eight cannulas: four on each side to stretch out the tissue. Starting at the cervical side going down towards the tail, the flesh was cut, while leaving the ribs intact. Under a microscope, the vertebrae were cut in the middle with micro dissecting scissors, to expose the spinal cord. Cutting the nerve fibres with micro dissecting spring scissors, the DRGs were extracted from the spinal foramen. At least 18 DRGs were isolated per side from each mouse; at least 5 lumbar, 12 thoracal and 1 cervical. Three DRGs were collected at a time and put into an Eppendorf tube containing 1 mL of serum free medium (DMEM/F12 1:1 1X GlutaMax), which was immediately used for the wild-type cell culture. The corpses and remaining tissue were disposed of in the freezer.

2.2.3. Wild-type DRG Cell Culture

A 24-well plate with six coverslips was used for each wild-typ DRG cell culture. 48 µL of Poly-D-Lysine (PDL) was put in the middle of each coverslip, before incubating the plate for 1.5 h at 37 °C and 5% CO_2. After removing the PDL, the coverslips were washed three times with around 500 µL DPBS. 1 mL of serum-free medium (DMEM/F12 1:1 1X GlutaMax) was put in an Eppendorf tube and another 2.5 mL in a Falcon. The other two Falcons were filled with 2 mL and 6 mL of medium with 10% horse serum. These steps were done at the beginning of each

week. The well plates were covered with parafilm and stored in the fridge until usage alongside the medium-containing tubes.

After each dissection, the isolated DRGs in serum-free medium were immediately transferred to a falcon containing 1 mL of Collagenase Type IV (12.5 mg/mL) and incubated for one hour. Every 15 min, the tube was lightly shaken to avoid lumping. Then, the suspension was triturated 12 times using a P1000 pipette tip, to mechanically break down the DRGs. 2.5 mL of serum-free medium as well as 500 µL of Papain (10 U/mL) were added, and the tube was incubated for another 30 min to digest the cells.

The cells were then centrifuged at 1000 rpm for 1 min, before the liquid was removed. One mL of medium with serum was added to resuspend the cells, which were then triturated 12 times. Another mL of medium as well as 2 mL of bovine serum albumin (BSA) were added, and the cells were centrifuged for 10 min at 1000 rpm. The viable cells were on the bottom, separated from cell debris by a medium and BSA layer. The cell debris layer, followed by the medium and BSA layer were removed. The cell pellet was resuspended in 120 µL of medium with horse serum and 100 ng/mL of NGF and 20 µL of the suspension were put on the middle of each coverslip. After incubating the plate for 20 min, 800 µL of NGF-containing medium were added to each well. The plate was then incubated overnight.

2.2.4. Treatment with ICAM-1 and IL-16

On the following day, the cultures were stimulated with ICAM-1 or IL-16 and incubated for two hours. For that purpose, three wells were treated with 200 µL of ICAM-1 (10 ng/mL) or IL-16 (100 ng/ mL). The other three wells served as controls and were filled with 200 µL of sterile water.

The stock solutions were prepared in advance by adding 200 µL of sterile water to the ICAM-1 and 100 µL to the IL-16 lyophilizate. One µL ICAM-1 and 5 µL IL-16 aliquots were stored in the -20°C freezer. On the day of each experiment, the ICAM-1 aliquot was diluted with 49 µL and IL-16 with 5 µL of sterile water. 8 µL of these dilutions were then added to 792 µL of sterile water.

As previously described by Lea Weiß, the concentrations and stimulation period led to an increase in neuronal excitability.[33] Therefore, the same conditions were used in this study.

2.2.5. Protein Extraction: Cell Harvest and Whole Cell Lysis (WCL)

After 2 hours of incubation, the cells of the wild-type cell culture were harvested and lysed to extract the proteins.

To harvest the cells, the medium of each well was carefully removed, and the cells were washed three times with around 500 µL of DPBS, which was prewarmed at 37°C in the water bath (AQUAline, Lauda-Königshofen, Germany). Each washing step was done very slowly to ensure the cells would not be removed from the coverslips. Then, the cells were incubated in 100 µL of lysis buffer for 10 minutes. The buffer was then pipetted up and down 10 times to detach the cells from the coverslips, before transferring everything to a LoBind Tube.

At the beginning of each week, the cOmplete Protease Inhibitor Cocktail tablet (Roche, Basel, Switzerland) was added to a 15 mL Falcon and 7.4 mL of LC-MS grade water were added, followed by 1 mL Tris-HCl (1M pH 7.4) and 500 µL of 5% Glycerol. Right before usage, 2.250 mL were transferred into a new Falcon and 25 µL of 10 mM dithiothreitol (DTT) and 250 µL of 20% SDS were added.

The order in which the cells were collected alternated to assure that the observed effects of the treatment were not due to a slightly longer or shorter stimulation time. One day, the treated cells from well 1A were harvested first, followed by the control from 1B. The next day it was the other way around (1B, then 1A).

After vortexing the tubes and a short spin down using a table centrifuge, the cells were lysed. For this purpose, the samples were sonicated in the Bioruptor (Diagenode, Seraing, Belgium) for 10 minutes at 4 °C and a low frequency with alternating 30 sec on- and off- periods. The tubes were vortexed again and put in the Thermomixer C (Eppendorf, Hamburg Germany) for 10 minutes at 70 °C and 1500 rpm. The vials were vortexed again and centrifuged for 5 min at 10,000 xg. The supernatant was transferred into a new LoBind tube and the samples were frozen at -20 °C until they were further processed.

2.2.6. Peptide Extraction: Single-pot, Solid-phase, Sample Preparation (SP3)

Single-pot, solid-phase-enhanced sample preparation (SP3) is a bead-based method to further process protein samples and optimise the sensitivity in downstream proteomics.[34] Reduction and alkylation steps in SP3 sample preparation assure that the proteins are digested efficiently. They also reduce the risk of disulfide bonds reforming after the proteins are broken down. However, a quenching agent is also essential to avoid overalkylation in order to minimise variability of identified and quantified proteins.[35] 12 samples a time were processed using the following protocol that was adapted from Hughes et al [34], as described by Xian et al.[36]

After the frozen protein samples were thawed on ice, 90 µL were pipetted in a new LoBind tube and vortexed and sonicated in the Bioruptor for 5 min (30s on and 30s off) at 4 °C and low frequency. To reduce the disulfide bonds of the proteins, 0.45 µL of 1M DTT were added to each vial. After vortexing them again, they were put in the Thermomixer for 30 min at 60°C and 1000 rpm. After reaching room temperature on ice, 10 µL of 20 mM IAA solution were added to each tube to alkylate the samples. The samples were vortexed and incubated in the dark for 30 min. Afterwards, another 0.5 µL of 1M DTT were added to avoid overalkylation.

10 µL of the pre-mixed SpeedBead carboxylate-modified magnetic particles (Cytiva, Marlborough, Massachusetts, USA) stock solution (Protein:bead ratio 1:10) was added to each LoBind tube. To ensure that the beads would bind the proteins, 111 µL of absolute EtOH was pipetted onto the bead mix and the samples were incubated for 5 min (24 °C, 1000 rpm) in the Thermomixer without closing the lid, followed by 2 min on the magnetic rack (DynaMag™-2 Magnet, Invitrogen by ThermoFisherScientific, Waltham, USA). The supernatant was discarded, followed by three washing steps with 400 µL of 80% EtOH (v/v). Each sample was reconstituted in 50 µL of Trypsin/Lys-C (Promega, Madison, Wisconsin, USA) solution (2 µL Tryps/LysC in buffer and 48 µL ABC solution). Finally, the vials were incubated for 18 hours at 37 °C and 950 rpm.

The next day, 950 µl of acetonitrile were added to each sample after a short spin down in the table centrifuge (MiniStar microcentrifuge, VWR, Radnor, Pennsylvania, USA). Then, they were incubated for 8 min at room temperature and put on the magnetic rack for another 2 min, before removing the supernatant. Another 900 µl of ACN were added and the tubes were

incubated on the magnetic rack for 2 min. The ACN was discarded, and the tubes were opened for 1 min, so the samples could dry.

For the peptide elution, the beads were reconstituted with 20 µL of LC-MS grade water and placed on the magnetic rack for another 2 min. The supernatant, which then contained the peptides, was saved in a new vial. To make sure that there were not any beads in the final peptide samples used for LC-MS/ MS analysis, the peptides were cleaned. Therefore, the tubes were centrifuged for 2 min at 17,000 xg and RT and put on the magnetic rack. Finally, the supernatant was transferred to a new LoBind tube and put on ice.

After measuring the peptide concentration of each sample at 205 nm using a Nanophotometer N60 (Implen GmbH, Munich, Germany), the samples were stored in the freezer at -20°C. Before further processing the samples using LC-MS/MS, they were acidified with formic acid (FA) to reach a concentration of 0.1%.

Preparation of Reagents

Bead-Mixture

The bead mixture was prepared in advance for all 72 samples. 10 µL of pre-mixed SpeedBead magnetic carboxylate modified particles were needed for each sample. Therefore, 360 µL of bead A as well as B were pipetted into a LoBind tube using a P1000 pipette. By shaking the mixture, the beads were brought into solution. The tube was then put on the magnetic rack, and the supernatant was discarded. The beads were washed twice with 720 µL of MS grade water (1:1 ratio of bead and water volume). 720 µL MS grade water was added to the clean beads, and the tube was lightly shaken. The bead mixture was stored in the fridge for the period of this experiment (3 weeks). Before each use, the mixture was shaken and brought into solution.

Ethanol

At the beginning of each week, 80% Ethanol was prepared using 40 mL of Ethanol gradient grade for liquid chromatography and 10 mL of MS grade water.

IAA and ABC

The 200 mM iodoacetamide (IAA) as well as the 50 mM ammonium bicarbonate (ABC) solutions were prepared freshly before the start of each experiment. The following formulas were used to calculate the needed volume of MS grade water.

200mM iodoacetamide (IAA): $\frac{2\ x\ IAA\ (g)}{0.073984} = mL\ H2O$

50mM ammonium bicarbonate (ABC): $\frac{40\ x\ ABC(g)}{0.15812} = mL\ H2O$

Since the ABC solution needs to reach a pH of 8, the Falcon was only filled with 80% of the water volume. After adjusting the pH by adding 0.1M NaOH, the rest of the water was added, and the Falcon was stored on ice. 672 µL of ABC-solution were pipetted into a new LoBind tube and put on ice. (later combined with enzyme). The LoBind tube containing the finished IAA solution was covered with aluminium foil and stored in the dark.

Trypsin/ Lys C mix

Since dissolved enzymes are less stable than their lyophilizates, the Trypsin/ Lys C mix was prepared just before use to maintain their proteolytic activity. During the 5 min incubation period in the Thermomixer, 20 µg of enzyme were dissolved in 20 µL of resuspension buffer (1 µg/µL) and immediately pipetted into a new 1.5 mL LoBind tube (on ice). Per sample, 50 µL of Tryps/LysC mix (2 µL) in ABC solution (48 µL) are needed. Therefore, 28 µL of Tryps/Lys C mix were then added to 672 µL of ABC-solution and stored on ice until needed. The remaining Tryps/LysC mix was stored in the -80°C freezer.

2.2.7. LC-MS/MS Set-up

LC-MS/MS was carried out by Feng Xian, PhD., as previously described by Grundtner et al.[37], Nanoflow reversed-phase liquid chromatography (Nano-RPLC) was carried out on a nanoElute system (Bruker Daltonik, Bremen, Germany). Via CaptiveSpray ion source, the LC system was linked to a timsTOF HT mass spectrometer (Bruker Daltonik).

After injecting 500 ng of peptides onto a C18 trap column (0.25 mm x 6 mm, Bruker Daltonik, Bremen Germany), they were separated using a C18 analytical column (PepSep, 1.5 µm, 25 cm x 75 µm, Bruker Daltonik) and a 60 min gradient. The mobile phase A consisted of 100%

water and 0.1% FA with a flow rate of 300 nL/ mL, which was increased to 400 nL/ min for the last 3 min. The flow rate of solvent B (100% acetonitrile and 0.1 FA) was increased linearly from 2% to 5% (for 3 min), then to 20% (over 42 min), to 35% (10 min), followed by an escalation to 95% within 0.5 min. For the last 5 min, a flow rate of 95% was maintained to guarantee that all hydrophobic peptides were eluted.

Each sample was analysed in data-independent acquisition (DIA) mode coupled with parallel accumulation serial fragmentation (PASEF). Precursors with a mass-to-charge ratio (m/z) from 300-1200 were analysed across 13 MS/MS ramps per cycle. This was accomplished with two or three quadrupole switches per ramp. One cycle within a 0.65-1.35 (1/k0) ion mobility range contained 34 MS/MS windows, with a determined isolation window (25 Da per step). The acquisition time was set to 100 ms per DIA-PASEF ramp, achieving a total time of circa 1.48 seconds per cycle. Lastly, the collision energy in DIA-PASEF mode was ramped linearly from 65 eV at 1/k0 = 1.6 to 20 eV at 1/k0 = 0.6.

2.2.8. Spectral Deconvolution with DIA-NN

Spectral deconvolution was performed by Lukáš Uhrík, PhD and Feng Xian, PhD. To process the data received from DIA-PASEF in library-free mode, DIA-NN 2.0.2 was used. A mus musculus proteome database with 17.070 protein entries (downloaded on 2021-07-08) was obtained from UniProt to predict the spectral library. Trypsin/P was used for in silico digestion. Per peptide, a maximum of two missed cleavages and two variable modifications (including N-terminal acetylation and methionine oxidation) were allowed, while the carbamidomethylation of Cysteine was a fixed modification setting. All peptides ranging from 5 to 30 amino acids in length were searched. The precursor charge was set to 2-4, the precursor ion m/z ranges to 350-1200 and the fragment ion m/z ranges to 100-1700. On the first run in the experiment, mass accuracy was automatically chosen. Protein interference correction was carried out using unique genes and the single-pass mode was chosen to classify neural networks. RT-dependent cross-run normalisation was performed with the high precision Quant UMS (Quantification using an Uncertainty Minimising Solution) option for the quantification. The R package DiaNN was used to process the main DIA-NN output. The q-value threshold was set to <0.01 at the precursor and gene group levels and the MaxLFQ intensities of all identified protein groups were extracted.

2.2.9. Data Analysis

RStudio (version 2024.12.1, build 563) was used to filter the differentially expressed proteins, quantified in ≥ 75% of samples, for significance and $\log_2$ fold change (FC). The thresholds were set for a p-value of ≤ 0.05 and an absolute $\log_2$ FC of ≥ 0.2. To identify overlapping and specific proteins, the list of DEPs of each cohort was merged and three conditions were assigned (ICAM-1, IL-16 and both).

The Search Tool for the Retrieval of Interacting Genes/ Proteins (STRING) 12.0 (https://string-db.org/) was used to create functional protein association networks. Cytoscape (v3.10.3) was used to visualise the protein networks using the stringApp (v2.2.0). *Mus musculus* was set as species, the confidence cutoff was set at 0.7 (high confidence) and *full STRING network* was selected as the network type.

The top 10 hub proteins were calculated using cytoHubba (v0.1) in Cytoscape (v3.10.3). It is common to use more than one algorithm to identify hub proteins and intersect the results, as described by Xiao et al.[38] Another paper by Chin et al. compared the most prominent cytoHubba plugins and found that Maximal Clique Centrality (MCC) identifies more essential high-degree as well as low-degree proteins than other methods. When combining MCC and Density of Maximum Neighbourhood Component (DMNC), different essential proteins can be obtained, which is advantageous when looking at a heterogeneous biological network.[39] Therefore, the top 10 proteins were computed based on MCC and DMNC, and intersected using VENNY 2.1.0 (https://bioinfogp.cnb.csic.es/tools/venny/). VENNY 2.1.0 was also used to visualise the overlapping proteins between both conditions and to determine the pathways (BPs) that were shared between ICAM-1 and IL-16-specific DEPs.

Functional enrichment analysis included the following gene ontology (GO) terms: biological processes (BP), cellular components (CC) and molecular functions (MF). The analysis and visualisation were performed on the SRplot (https://www.bioinformatics.com.cn/srplot) website.[40]

3. Results

3.1. Quality Control of Proteomics Data

In the present study, proteomic changes were examined in two experimental groups: ICAM-1 and IL-16-treated cultures, each compared to its respective control. To assess the quality and reproducibility of the experimental data, the coefficient of variation (CV) was calculated across all samples and within individual groups.

Figure 5 shows CVs below 20% in both the pooled dataset and across all conditions, indicating a high reproducibility of the proteomics data. The low CV of the pooled data reflects consistent technical replicates, while CVs < 20% for each condition demonstrate a high reproducibility among biological replicates. To further confirm instrumental stability and reproducibility across technical replicates, Pearson correlation coefficients were calculated for pooled samples. *Figure 6* displays high correlation coefficients (r > 0.98), reinforcing the reproducibility of the data. Overall, the low variability across both biological and technical replicates confirms that the data are reliable for subsequent analyses.

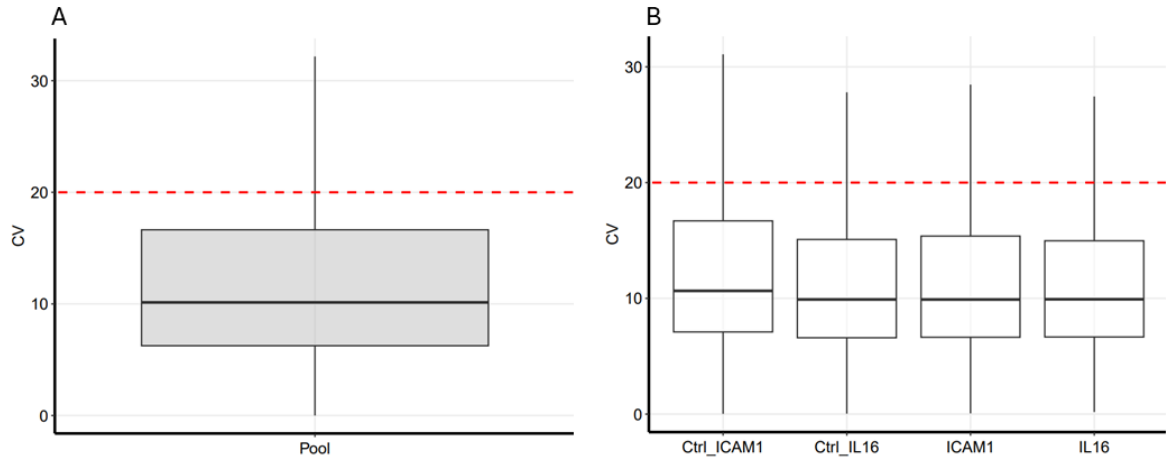

Figure 5: Coefficient of variation (CV): *The boxplots show the distribution of (A) pooled samples across all experimental groups (ICAM-1 treatment and control, IL-16 treatment and control) and (B) for each individual group. The red dashed line marks the CV value threshold of < 20%. All samples meet this criterium, indicating a high reproducibility.*

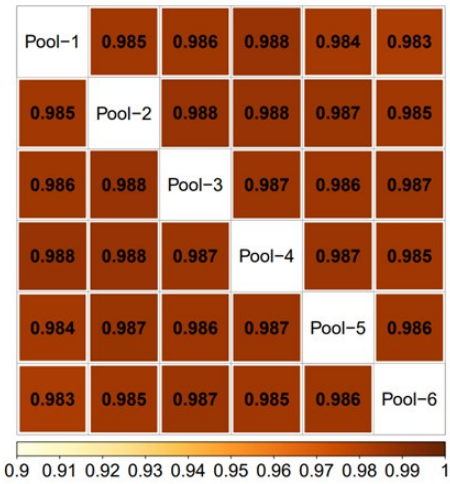

Figure 6: Pearson Correlation of pooled samples: *Correlation coefficients of r > 0.98 represents the technical stability and reproducibility of the data.*

3.2. Differentially Expressed Proteins (DEPs)

Following ICAM-1 and IL-16 stimulation, some proteins were up- or downregulated, relative to their vehicle control. These are referred to as differentially expressed proteins (DEPs). *Figure 7* presents the volcano plots for both treatments. The x-axis represents the $\log_2$ fold change (FC), where negative values indicate downregulation and positive values upregulation. To correct for multiple testing, the Benjamini-Hochberg correction was applied and the minus $\log_2$ p-value (or q-value) is shown on the y-axis.

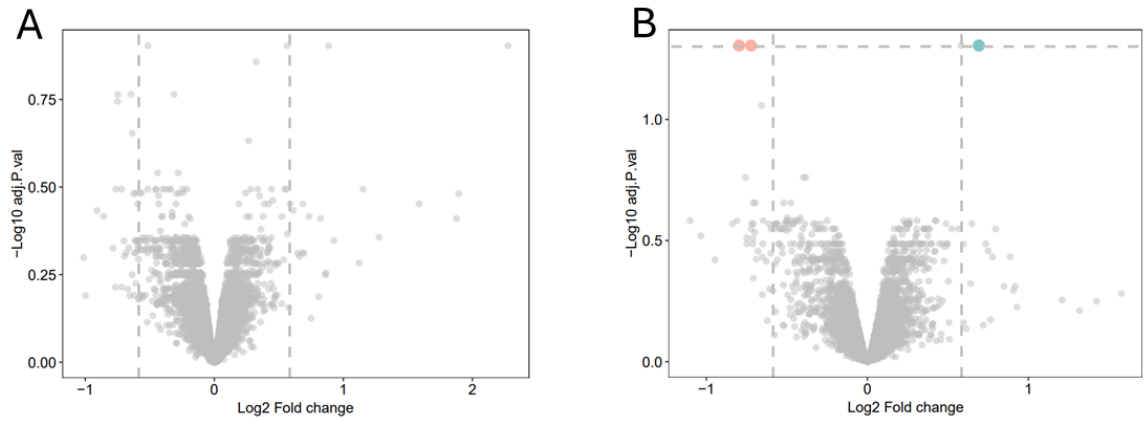

Figure 7: Volcano plots of differentially expressed proteins across experimental groups: *The plot shows the DEPs (A) after ICAM-1 and (B) IL-16 treatment. The $\log_2$ FC cutoff (on the x-axis) is set at ≥ 0.585 (FC ≥ 1.5 and FC ≤ 0.67). The q-value ($\log_{10}$ p value on the y-axis) has a threshold of < 0.05. The DEPs that follow these criteria are depicted in red and blue.*

When using a q-value cutoff of ≤ 0.05, few DEPs reached statistical significance. However, since some proteins may still be biologically or clinically relevant, a p-value of < 0.05 was used as the cutoff for downstream analyses. Additionally, a moderate threshold of $|\log_2 FC| \geq 0.2$, equivalent to a fold change of ≥ 1.1487 and ≤ 0.8706 was applied to define dysregulated proteins. Only proteins quantified in ≥ 75% of replicates within each experimental group were further analysed. After applying the above-mentioned cutoff criteria in RStudio (version 2024.12.1, build 563), the resulting lists of DEPs were imported into Cytoscape (v3.10.3) for network and functional analyses.

3.3. ICAM-1 PPI Network and Functional Enrichment Analysis

Before investigating the pathways and mechanisms following ICAM-1 treatment, the filtered list of 411 DEPs was imported into Cytoscape (v3.10.3), and a protein-protein-interaction (PPI) network was generated using the stringApp (v2.2.0). The complete PPI network (*SFigure 3*) comprises 313 nodes (112 upregulated and 201 downregulated), including 156 non-interacting singletons, and 281 edges.

To explore the potential biological functions of the DEPs within the PPI network, Gene Ontology (GO) analysis was performed across three categories: biological processes (BP), molecular function (MF) and cellular component (CC). Functional enrichment analysis and visualisation was conducted using SRplot (https://www.bioinformatics.com.cn/srplot). *Figure 8* depicts the top 10 significantly enriched GO results associated with DEPs following ICAM-1 stimulation. The GO terms with the highest enrichment score are listed first in each category.

Coagulation and complement activation through the alternative pathway were amongst the 10 most significantly enriched GO-BP terms. The CC term with the highest enrichment score was the collagen-containing extracellular matrix (ECM), which plays a critical role in haemostasis. Collagens are the most prevalent proteins of the ECM. They supply the walls of the vasculature with mechanical strength and stability and contribute to cell adhesion, migration, tissue scaffolding and repair. If the vascular walls are injured, they trigger platelet adhesion and aggregation by binding to platelet receptors.[41,42]

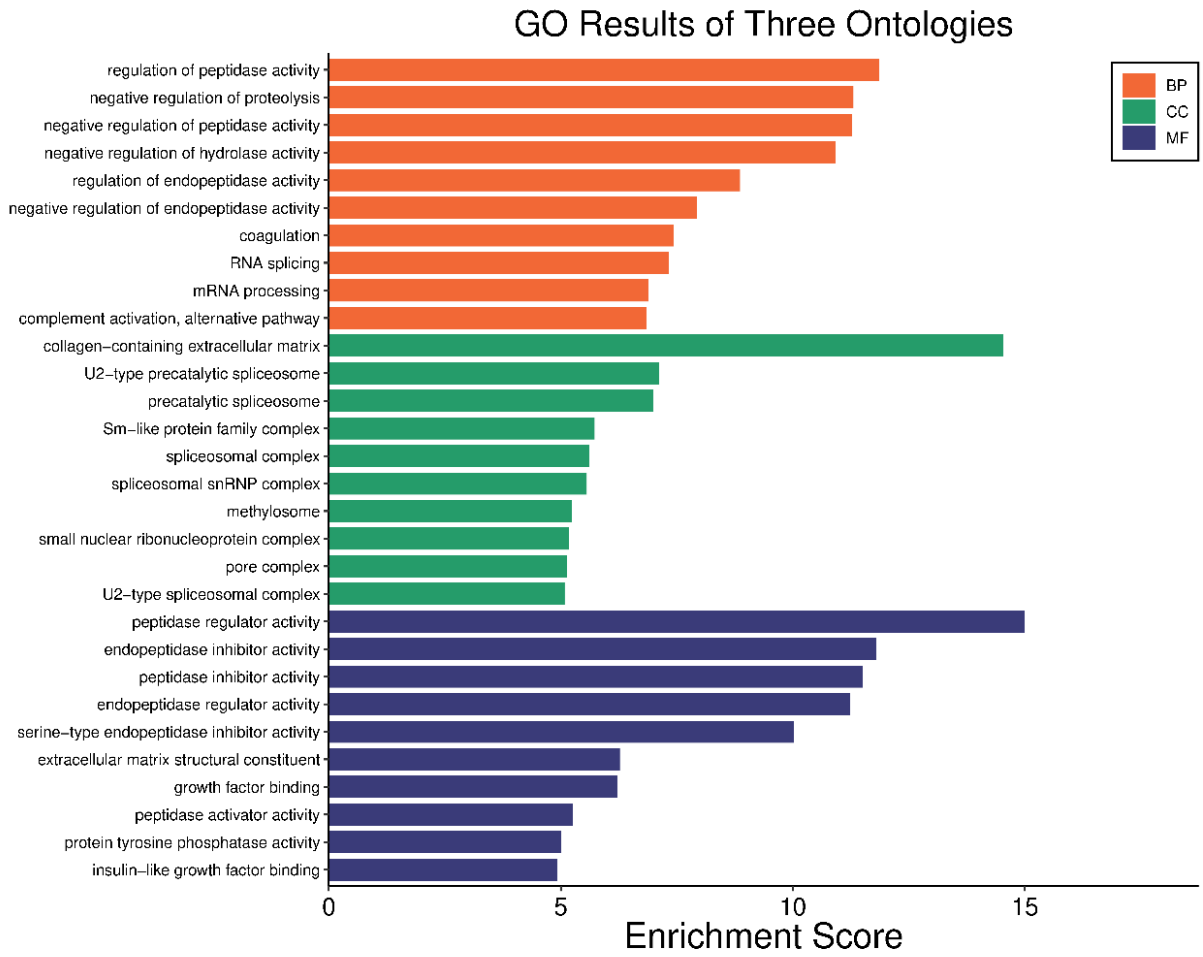

Figure 8: ICAM-1 – gene ontology of three categories: *biological process (BP in orange), cellular component (CC in green), molecular function (MF in blue). The 10 most significantly enriched GO terms of each category are arranged according to enrichment score, the most enriched term first. (Created with SRplot https://www.bioinformatics.com.cn/srplot)*

MF analysis further confirmed that some of the identified proteins contribute to the ECM's structural integrity. They also bind to growth factors, such as the insulin-like growth factor, which plays an important role in wound healing.[43] Studies have shown that there is a bidirectional link between coagulation cascades and immune pathways.[44] Therefore, it should be investigated further in the context of ICAM-1.

From the list of all significantly enriched GO terms, the first 10 BP, one CC and 9 MF terms with a direct link to coagulation and immune system processes were chosen for detailed analysis. Broader, non-specific terms were excluded. For instance, peptidase regulators participate in multiple processes including, but not limited to, blood coagulation and immune response, and were therefore not included.[45] In the CC category, only *collagen-containing ECM* was selected. *Table 7* lists the chosen GO terms, the number of associated DEPs and their corresponding p-values and enrichment scores.

Table 7: ICAM-1 group – coagulation- and immune system-related GO terms

Gene Ontology Term	*Number of DEPs*	*p-value*	*Enrichment Score*
Biological processes			
Coagulation	13	3.71E-08	7.43074
Complement activation alternative pathway	5	1.42E-07	6.84703
Blood coagulation	12	2.47E-07	6.60783
Haemostasis	12	2.98E-07	6.52563
Wound healing	16	1.45E-06	5.83750
Activation of immune response	16	1.71E-05	4.76687
Acute inflammatory response	8	2.06E-05	4.68699
Acute phase response	5	6.52E-05	4.18561
Integrin activation	4	0.000167	3.77649
Complement activation	9	0.000196	3.70837
Cellular component			
Collagen-containing extracellular matrix	28	2.95E-15	14.53055
Molecular function			
Extracellular matrix structural constituent	11	5.33E-07	6.27292
Growth factor binding	11	6.09E-07	6.21503
Insulin-like growth factor binding	5	1.18E-05	4.92792
Heparin binding	10	1.27E-05	4.89741
Integrin binding	9	2E-05	4.69961
Glycosaminoglycan binding	11	3.3E-05	4.48214
Fibronectin binding	5	0.000106	3.97509
Cell adhesion molecule binding	11	0.000308	3.51174
Extracellular matrix binding	5	0.000355	3.44919

3.3.1. ICAM-1 Subnetwork Analysis and Hub Protein Identification

Next, a list with proteins associated with wound healing and immune pathways (*Table 7*) was imported into Cytoscape (v3.10.3) to visualise the interactions between the involved proteins. The resulting subnetwork was screened for hub proteins using the cytoHubba (v0.1) plugin. Therefore, the top 10 proteins were computed based on MCC and DMNC and intersected using VENNY 2.1.0. (https://bioinfogp.cnb.csic.es/tools/venny/) (*SFigure 1*). This revealed seven overlapping hub proteins: collagen (I) alpha-1 and 2 chain (Col1a2, Col1a1), biglycan (Bgn), periostin (Postn), thrombospondin-1 (Thbs1), cellular communication network factor 2 (Ccn2) and complement factor I (Cfi).

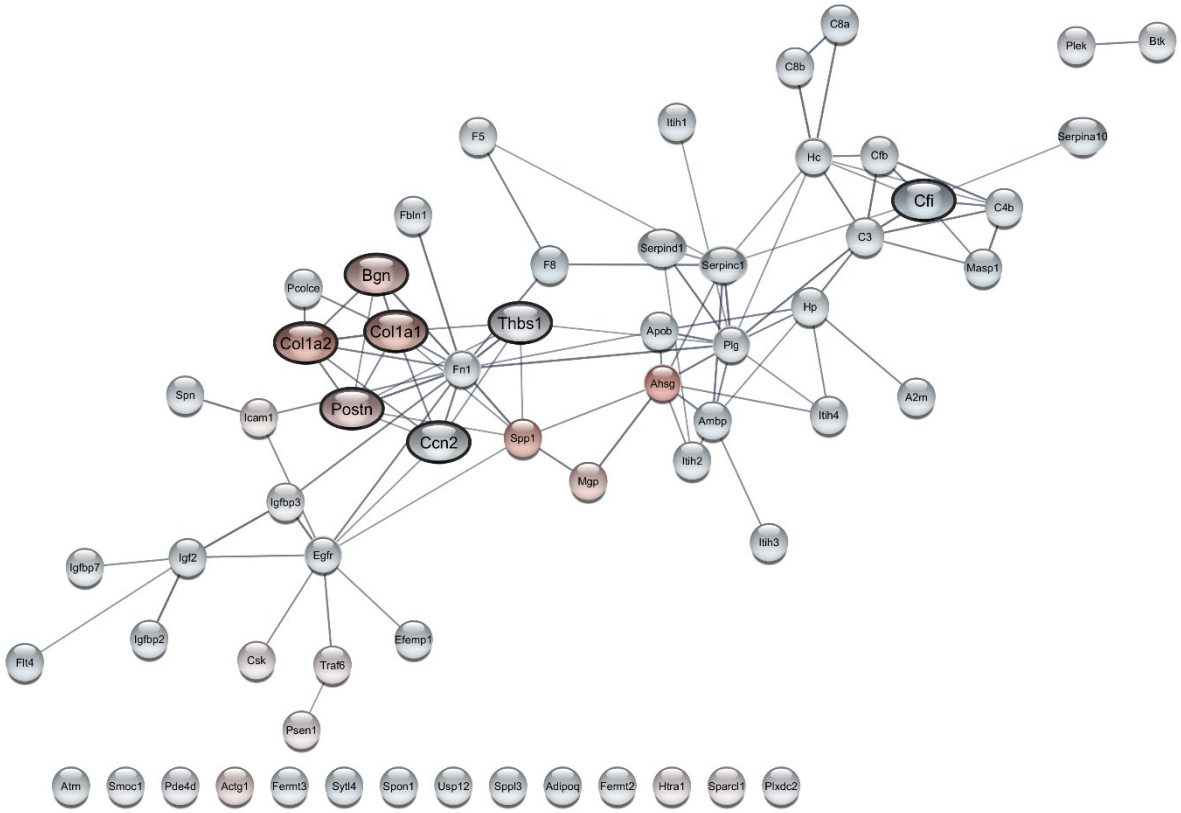

Figure 9: ICAM-1 subnetwork of proteins involved in coagulation and immune-related pathways. *It consists of 62 nodes (14 upregulated, 48 downregulated) and 97 edges. The seven hub proteins (Col1a1, Col1a2, Bgn, Postn, Ccn2, Thbs1, Cfi) are highlighted in a bigger font and oval shaped. (Created using Cytoscape - https://cytoscape.org/)*

The ICAM-1 PPI subnetwork (*Figure 9*) consists of 62 nodes and 97 edges. To distinguish between the 14 up- (red) and 48 downregulated DEPs (blue), node colours were continuously mapped based on $\log_2$ FC values. Hub proteins are displayed as oval-shaped nodes in a bigger font size. Whitin this subnetwork, there are a few smaller, but interconnected clusters, visualising the bidirectional link between the complement and coagulation cascade.[44] Overall, the abundance of coagulation and complement proteins was reduced, while several structural ECM and matricellular proteins were upregulated, indicating the onset of ECM remodelling and tissue repair.

Six hub proteins are organised in a small cluster, pointing to their connectivity and biological similarity. The proteins that contribute to the formation of collagen fibres are upregulated. Col1a1 and Col1a2 are the chains that make up collagen-I, which is an important structural component of the ECM. In their monomeric form, type I collagens bind to integrins, which are transmembrane receptors that facilitate the adhesion of cells to other cells or matrices, ECM formation and platelet aggregation.[46–48] Postn, a matricellular protein that regulates the formation of collagen fibrils, is often overexpressed at injured or inflamed areas.[49,50] Bgn is

another key component of the ECM that contributes to the assembly of collagen fibres and promotes inflammation by interacting with toll-like receptors (TLR, TLR4) on immune cells. It can also bind and regulate the activity of TGF-β (transforming growth factor-β) and TNF-α.[51,52]

The two downregulated matricellular proteins (Thbs1 and Ccn2) are integrin ligands associated with TGF-β signalling. Thbs1 can activate TGF-β, which in turn upregulates Ccn2.[53–55] The observed Thbs1 downregulation could result from cleavage by the upregulated high-temperature requirement A serine protease 1 (Htra1).[56] As a consequence, reduced levels of Thbs1 could fail to induce TGF-β signalling and subsequently Ccn2 expression.

Outside this cluster, the serine-protease Cfi was also identified as a hub protein. Cfi is an essential inhibitor of complement activation, responsible for the cleavage and inactivation of the complement component 3b (C3b) in the presence of cofactors.[57] Its downregulation aligns with the overall reduced abundance of complement-related proteins observed in this subnetwork.

Taken together, these findings indicate a shift towards early ECM remodelling, accompanied by reduced expression of coagulation- and complement-associated proteins. These alterations also suggest potential involvement of TLR2/4-mediated inflammatory signalling pathways.

3.4. IL-16 PPI Network and Functional Enrichment Analysis

After applying the p-value and $\log_2$ FC cutoffs as described in *Chapter 2.2.9*, a set of 394 DEPs was imported into Cytoscape (v3.10.3) and a PPI network was created using the stringApp (v2.2.0). The full network (*SFigure 5*) contains 310 nodes (169 singletons) and 378 edges, with 114 upregulated and 196 downregulated proteins. To explore dysregulated pathways following IL-16 stimulation. GO analysis and visualisation were carried out on the SRplot website (https://www.bioinformatics.com.cn/srplot). *Figure 10* depicts the most significantly enriched GO-BP, CC and MF terms, ordered by decreasing enrichment score.

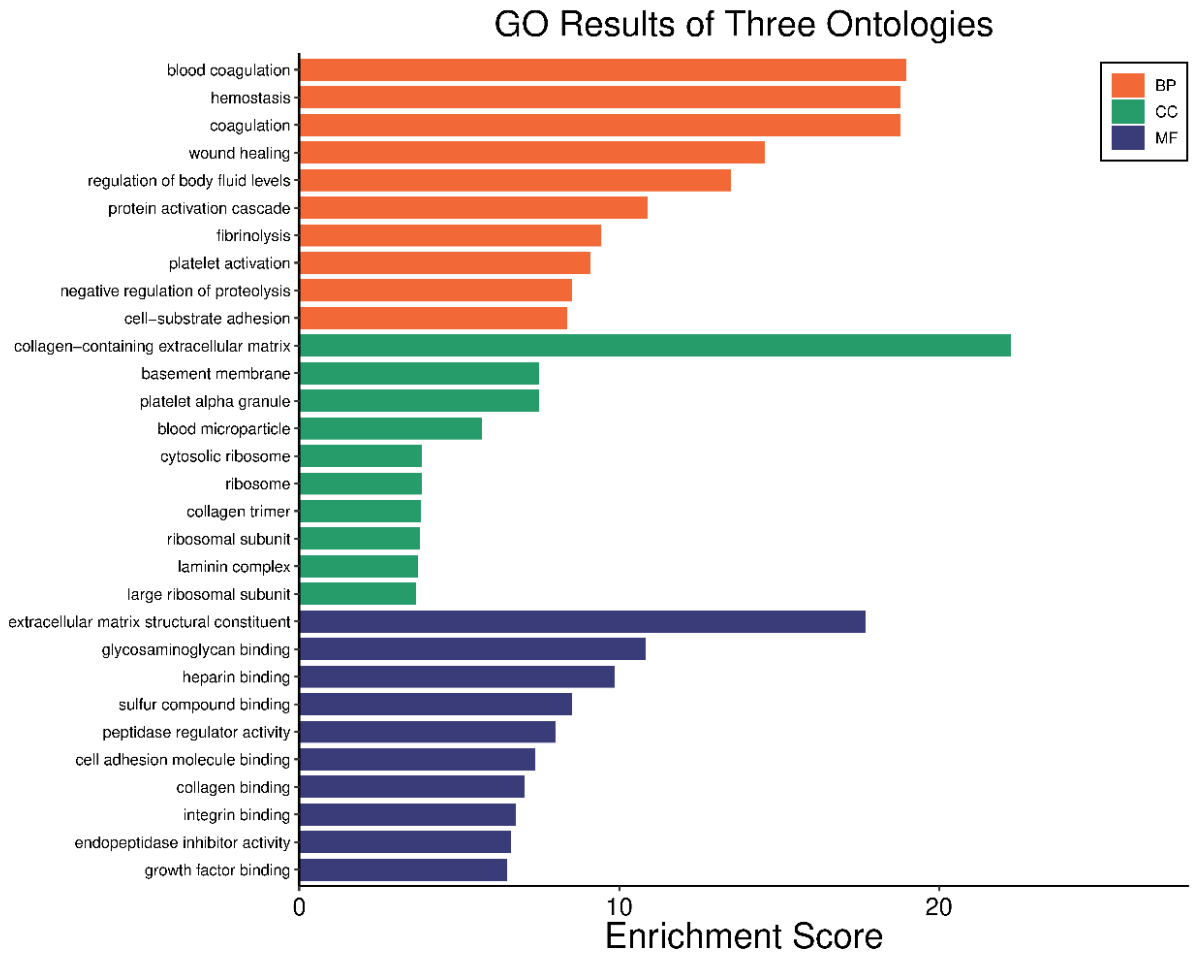

Figure 10: IL-16 – gene ontology of three categories: *biological process (BP in orange), cellular component (CC in green), molecular function (MF in blue). The 10 most significantly enriched GO terms of each category are arranged according to enrichment score, the most enriched term first. (Created with SRplot https://www.bioinformatics.com.cn/srplot)*

GO-BP analysis revealed significant enrichment in terms related to haemostasis, blood coagulation, wound healing, fibrinolysis and platelet activation. The DEPs were also enriched in the collagen-containing ECM and mainly concerned with the binding of molecules such as glycosaminoglycans, heparin, collagens, integrins and growth factors. Those are critical molecular functions related to coagulation.

As described in *Chapter 3.3*, the list of all significantly enriched GO terms was examined for coagulation- and immune system-related terms. *Table 8* lists the top 10 BP, one CC and 9 MF terms that were selected, including the number of associated DEPs, their p-values and enrichment scores.

Table 8: IL-16 group – coagulation- and immune system-related GO terms

Gene Ontology Term	*Number of DEPs*	*p-value*	*Enrichment Score*
Biological processes			
Blood coagulation	23	1.04E-19	18.98296
Haemostasis	23	1.56E-19	18.80721
Coagulation	23	1.56E-19	18.80721
Wound healing	26	2.81E-15	14.55154
Fibrinolysis	7	3.56E-10	9.44851
Platelet activation	11	8.03E-10	9.09512
Platelet aggregation	8	3.29E-08	7.48263
Response to oxidative stress	18	1.26E-07	6.90088
Integrin activation	6	2.04E-07	6.69089
Cellular component			
Collagen-containing matrix	35	5.64E-23	22.24849
Molecular function			
Extracellular matrix structural constituent	21	1.98E-18	17.70421
Glycosaminoglycan binding	18	1.52E-11	10.81880
Heparin binding	15	1.41E-10	9.85005
Cell adhesion molecule binding	16	4.32E-08	7.36438
Collagen binding	9	9.34E-08	7.029576
Integrin binding	11	1.7E-07	6.768385
Growth factor binding	11	3.18E-07	6.498046
Extracellular matrix binding	7	1.59E-06	5.798289
Fibronectin binding	6	4.99E-06	5.301736

3.4.1. IL-16 Subnetwork Analysis and Hub Protein Identification

A list of proteins involved in wound healing and immune pathways was imported into Cytoscape (v3.10.3) to construct the IL-16 PPI subnetwork. Five hub proteins were identified as previously described in *Chapter 3.3.1* and shown by *SFigure 2*. The resulting network (*Figure 11*) consists of 82 nodes (18 upregulated in red, 64 downregulated in blue) and 146 edges. Within this subnetwork, a module of coagulation- and complement-related proteins is visible, displaying an up- and downregulation pattern similar to the ICAM-1 network.

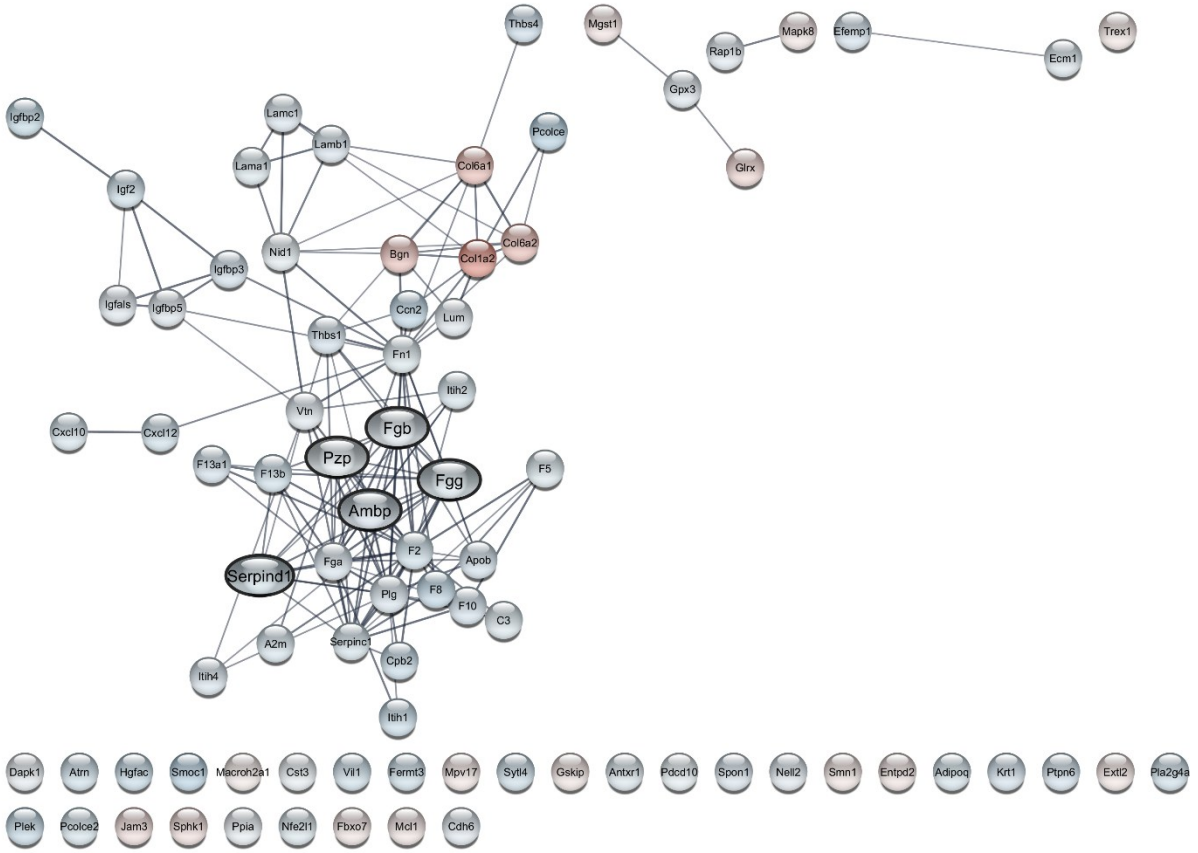

Figure 11: IL-16 subnetwork of proteins involved in coagulation and immune-related pathways. *It consists of 82 nodes (18 upregulated in red, 64 downregulated in blue) and 146 edges. The ovel shaped proteins are the five down-regulated hub proteins Fgb, Fgg, Pzp, Ambp, Serpind1. (Created using Cytoscape - https://cytoscape.org/)*

The five hub proteins, fibrinogen beta and gamma chain (Fgb, Fgg), the alpha-1 microglobulin/ bikunin precursor Ambp, pregnancy zone protein (Pzp) and heparin cofactor 2 (Serpind1) were all downregulated (larger font, oval shaped nodes). These proteins are functionally interconnected and form a coherent cluster within the subnetwork. Fibrinogen, an acute-phase protein that is typically upregulated during the early inflammatory phase of wound healing,[58] showed reduced abundance, consistent with the broader downregulation of coagulation-related proteins. At the same time, lower levels of serine protease inhibitors (Ambp, Pzp, Serpind1), that normally regulate proteolytic activity of serine proteases, were observed. Combined with the overexpression of collagen chains (Col1a2, Col6a1) and biglycan, this may reflect a shift towards matrix deposition at the onset of ECM remodelling.[59]

3.5. ICAM-1 vs IL-16 Stimulation

Roughly the same number of proteins were dysregulated in both groups, with a similar up- and downregulation profile following ICAM-1 (313 DEPs: 112 up- and 201 downregulated) and IL-16 treatment (310 DEPs: 114 up- and 196 downregulated). This quantitative comparison indicates that both inflammatory markers provoke a similar level of proteome alterations. The predominance of downregulated proteins (approximately 64% in the ICAM-1 and 63% in the IL-16 group) suggests that both treatments suppress the expression of proteins rather than promote it.

Functional enrichment analysis revealed that dysregulated proteins in both study groups participate in wound healing and immune-related pathways. The subnetworks exhibited a similar pattern, characterised by the downregulation of coagulation and complement proteins and the upregulation of many structural ECM and matricellular proteins, indicating a shift to ECM remodelling. Several proteins (e.g. Col1a2, Bgn, Thbs1 and Ccn2) appeared in both the ICAM-1 and IL-16 network, suggesting a potential overlap in the mechanisms underlying these pathway alterations.

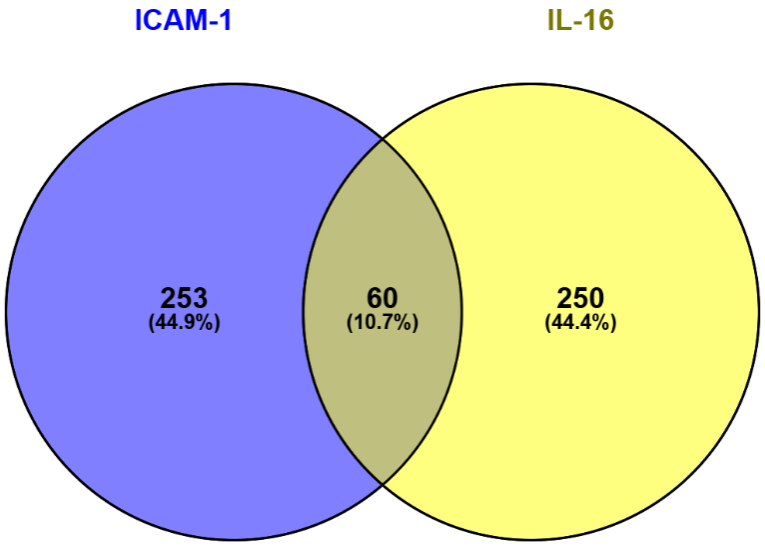

Figure 12: Venn Diagram identifying shared proteins: *intersecting 313 DEPs in ICAM-1 and 310 in IL-16 group reveals 60 shared proteins (10.7%). (Created with VENNY https://bioinfogp.cnb.csic.es/tools/venny/).*

To compare the two cohorts, the 313 DEPs from the ICAM-1 PPI network and the 310 IL-16-induced DEPs were intersected using VENNY 2.1. (https://bioinfogp.cnb.csic.es/tools/venny/). The Venn diagram (*Figure 12*) shows 60 shared proteins, which translates to an overlap of 10.7%. This relatively small intersection indicates that, despite similar trends in coagulation and immune-related pathways, each treatment exhibits a specific proteomic response. The shared and unique DEPs were assessed further to gain insight into the similarities and differences between the two treatments.

After merging the ICAM-1 and IL-16 DEP lists in RStudio (version 2024.12.1, build 563), three subnetworks were constructed in Cytoscape (v3.10.3) to distinguish shared from specific proteins. GO-BP analysis was performed on each subnetwork to explore functional differences. Subsequently, the biological processes associated with ICAM-1- and IL-16-specific DEPs were compared via Venn diagram, and manually to highlight shared and unique pathways between the two conditions.

3.5.1. ICAM-1- and IL-16-shared Proteins and Pathways

The Venn diagram (*Figure 12*) revealed that 60 proteins (10.7%) were shared between both study groups. The corresponding PPI network (*Figure 13*) revealed a similar up- and downregulation profile, suggesting that both treatments share some biological functions. Among the shared proteins, four were upregulated (red) and 53 downregulated (blue). Only three non-interacting proteins (green) are differently regulated in the ICAM-1 and IL-16 group. The shared proteins that were identified as hub proteins in either group are highlighted as enlarged oval nodes.

GO-BP analysis (*Figure 14*) confirmed that the overlapping proteins are associated with wound healing and complement activation via the alternative pathway. These results indicate that dysregulation of complement and coagulation pathways represent a shared response, rather than a treatment-specific effect. Following tissue injury, these interconnected systems are activated, both contributing to inflammatory responses.[60] The downregulation of these components, together with the upregulation of Col1a2 and Bgn, aligns with previous findings, suggesting a collagen-high ECM remodelling programme in both treatment groups.

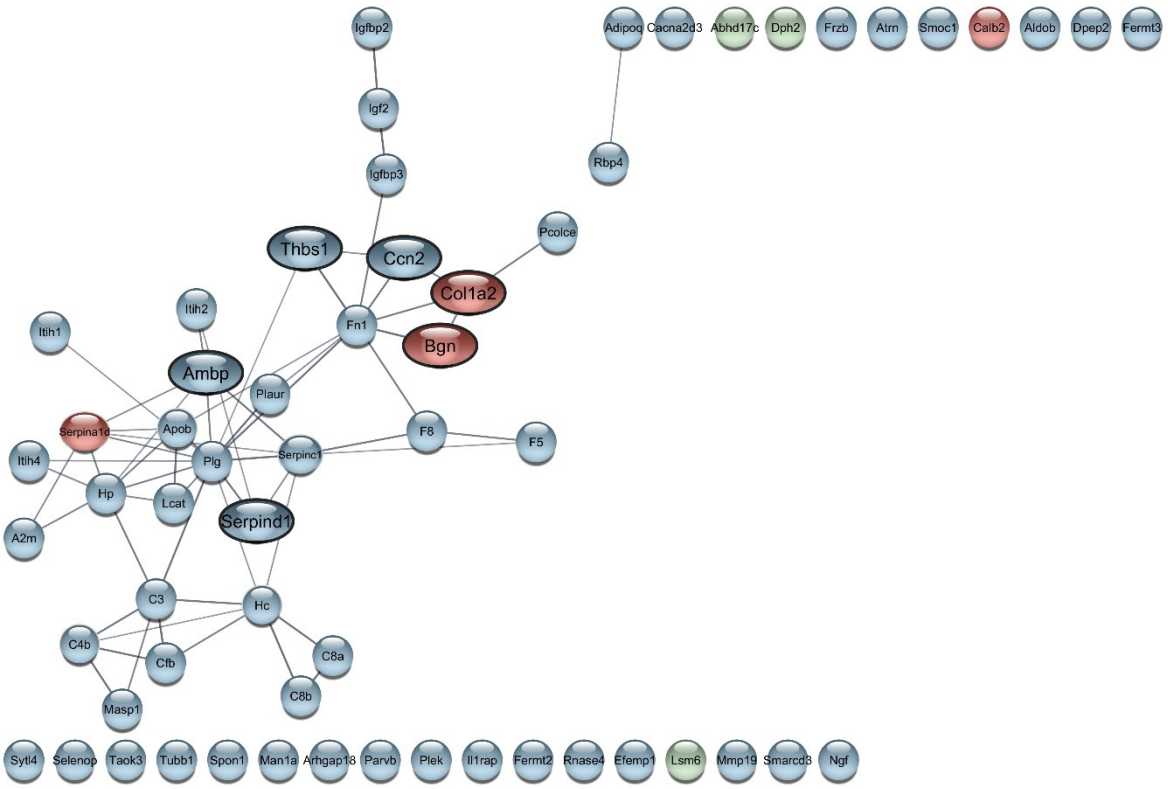

Figure 13: PPI subnetwork of proteins shared between ICAM-1 and IL-16 group. *Network consists of 60 nodes and 60 edges. The proteins exhibit a similar up and down-regulation pattern. 4 proteins (red) are up- and 53 (blue) downregulated. Only 3 nodes (green) are differently regulated in the ICAM-1 and IL-16 group. The shared proteins, previously identified as hub proteins are highlighted as oval nodes in a bigger font size (Bgn, Col1a2, Ccn2, Thbs1 – ICAM-1 group and Ambp, Serpind1 – IL-16 group) Figure was created using Cytoscape - https://cytoscape.org/*

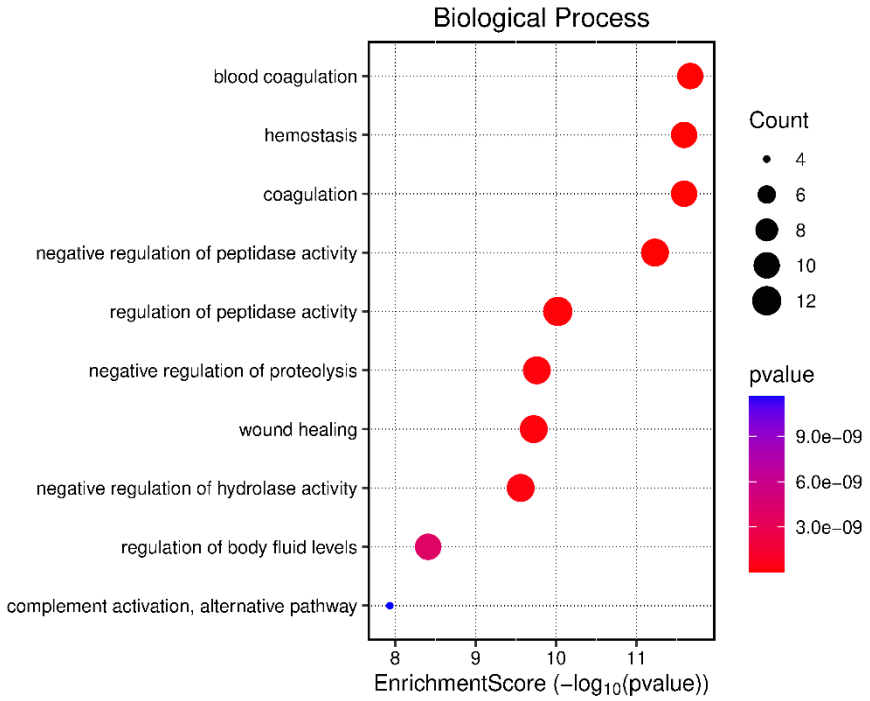

Figure 14: ICAM-1 and IL-16 shared pathways (BPs): *(A) The dot plot lists the most significantly enriched pathways first, starting with the highest significance in red and lowest in blue as indicated by the p-value on the y-axis. The x-axis shows the enrichment score; dots with the highest enrichment score are on the right. The dot size corresponds to the number of genes associated with each term. (Created with SRplot https://www.bioinformatics.com.cn/srplot)*

3.5.2. ICAM-1- and IL-16-specific DEPs

To determine whether the treatment-specific DEPs would be associated with distinct or overlapping biological pathways, GO-BP analysis was conducted on the SRplot website (https://www.bioinformatics.com.cn/srplot) for ICAM-1- and IL-16-specific proteins. The resulting lists of all significantly enriched terms (1015 for ICAM-1 and 489 for IL-16) were intersected using VENNY 2.1.0 (https://bioinfogp.cnb.csic.es/tools/venny/). The Venn diagram (*Figure 15*) reveals 151 shared GO-BP terms, corresponding to a partial functional overlap of 11.2% between both treatments.

To facilitate interpretation, the shared and treatment-specific GO-BP terms were grouped into the following categories and compared: (i) response to stimulus (including response to wounding), (ii) cell communication (e.g. signal transduction) and (iii) synthesis/ secretion of molecules. Within each category, terms associated with the same DEPs were put into subcategories. It should be noted that individual DEPs were not linked to all specific GO terms within a subcategory, but rather to the broader biological process it represents. Since several GO terms in the "overlapping" and "specific" categories were similar, manual comparison was also performed to identify overlapping subcategories between ICAM-1- and IL-16-sepcific pathways.

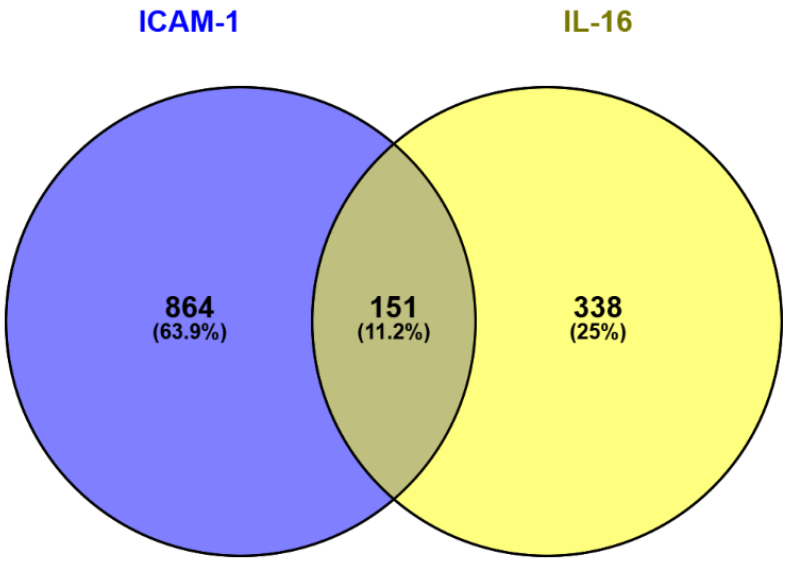

Figure 15: Overlapping and treatment-specific pathways: *The significantly enriched GO-BP terms of ICAM-1 specific (1015 terms) and IL-16 specific proteins (489 terms) were intersected using a Venn diagram. There are 864 ICAM-1 specific, 338 IL-16 specific and 151 overlapping (11.2%) GO-BP terms. (Created with VENNY https://bioinfogp.cnb.csic.es/tools/venny/)*

Both, ICAM-1 and IL-16-specific proteins, are involved in the response to various stimuli including ROS, oxidative and chemical stress, calcium, cyclic adenosine monophosphate (cAMP) and platelet activation. They also regulate the production and release of molecules that are associated with nociception, such as neurotransmitters and hormones.

Regarding cell communication, both treatments share overlapping functions in MAPK-related pathways, such as the stress activated MAPK and ERK1/2 cascade, as well as small guanosine triphosphatase (GTPase)-mediated signal transduction. Furthermore, both are associated with NF-κB regulation via the two major pathways. However, ICAM-1-specific DEPs are specifically linked to IκB kinase (IKK) signalling, whereas IL-16-specific proteins are connected to NF-κB-inducing kinase (NIK)-dependent mechanisms. The IKK complex serves as a central component in the canonical NF-κB cascade, in contrast to the noncanonical (alternative) pathway, where NIK plays a key role.[61,62]

3.5.2.1. ICAM-1-specific DEPs and Pathways

The PPI subnetwork of ICAM-1-specific DEPs (*Figure 16*) contains 107 interacting nodes, connected by 136 edges. The nodes were continuously mapped to reflect their $\log_2$ FC values, with the 48 upregulated proteins depicted in red and the 59 downregulated proteins in blue. The 146 singletons were excluded from this figure, however functional enrichment analysis was performed on all 253 DEPs (107 up- and 146 downregulated, *SFigure 4*). The interacting proteins that are involved in ICAM-1-specific pathways are highlighted, to visualise their interactions and interconnectedness of related biological processes.

GO-BP analysis (*Figure 17*) revealed that ICAM-1 treatment-specific DEPs are mostly involved in protein autophosphorylation, peptidyl-tyrosine phosphorylation and modification and regulation of ERK1/2. To determine whether these pathways are group specific, GO terms of ICAM-1 and IL-16-specific DEPs were intersected, as previously described (*Chapter 3.5.2*). This comparison revealed that most significantly enriched GO terms are not treatment-specific, but shared functions between both cohorts.

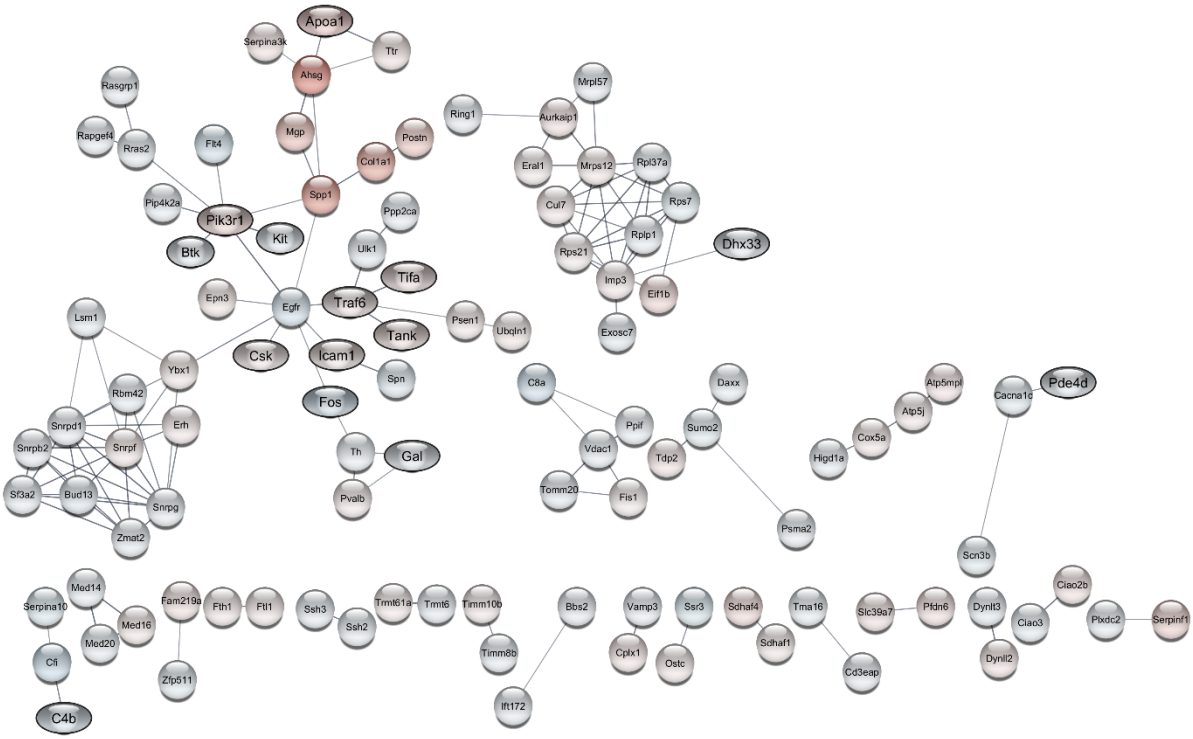

Figure 16: PPI subnetwork of ICAM-1-specific DEPs: *the network consists of 107 nodes (DEPs) and 134 edges (interactions). Red nodes (48) represent upregulated and blue nodes (59) down-regulated proteins. Singletons are not included in this figure. The interacting proteins involved in ICAM-1-specific pathways are highlighted. (Created using Cytoscape - https://cytoscape.org/)*

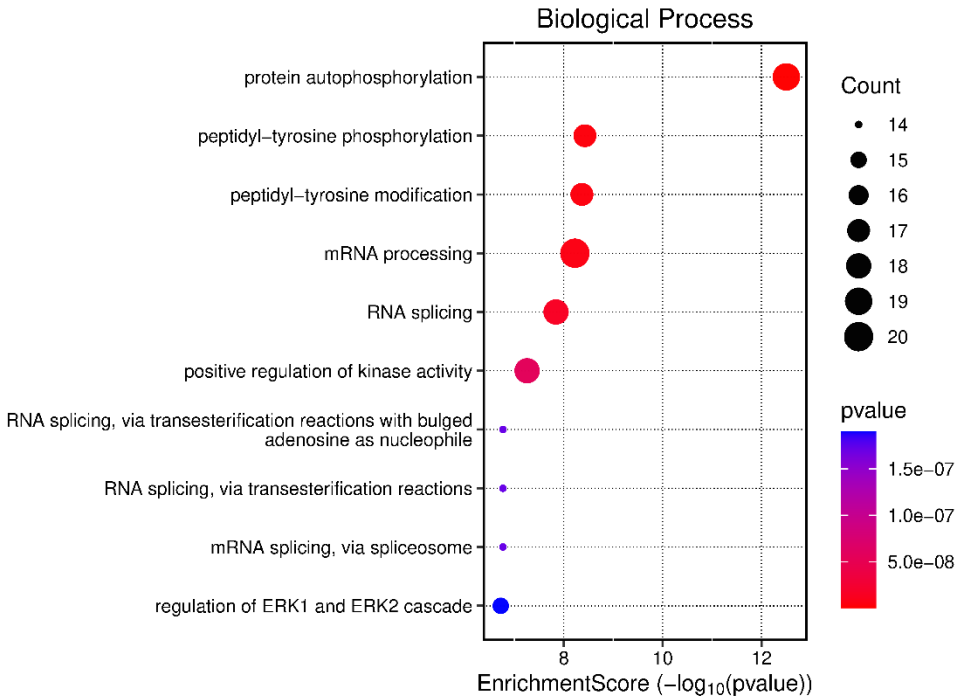

Figure 17: pathways (BPs) of ICAM-1-specific DEPs: *(A) The dot plot lists the most significantly enriched pathways first, starting with the highest significance in red and lowest in blue as indicated by the p-value on the y-axis. The x-axis shows the enrichment score; dots with the highest enrichment score are on the right. The dot size corresponds to the number of genes associated with each term. (Created with SRplot https://www.bioinformatics.com.cn/srplot)*

Manual comparison of the GO-BP terms revealed that ICAM-1-specific DEPs respond to several chemical stimuli, including growth factors such as TGF-β, platelet-derived growth factor (PDGF), fibroblast growth factor (FGF), as well as IL-7, insulin, monoamines (catecholamines), peptides and hormones. They also respond to physical stimuli such as mechanical stress or light. Moreover, these proteins are involved in a plethora of signalling cascades, including the canonical IKK-NF-κB pathway, TGF-β receptor, JAK-STAT and LPS-mediated signalling. In addition, they regulate the production of cytokines (IL-1β, IL-2, IL-17, type I IFN) and glucocorticoids/ steroids.

Next, the proteins involved in canonical NF-κB-, TGF-β receptor-, JAK-STAT- and LPS-mediated signalling as well as cytokine and glucocorticoid production were further analysed to predict whether these pathways could be activated following ICAM-1 stimulation.

The proteins significantly enriched in the canonical NF-κB pathway included Icam-1, the tyrosine protein kinase Fyn, TNF receptor-associated factor 6 (Traf6), TRAF-interacting protein with FHA domain-containing protein A (Tifa), period circadian protein homolog 1 (Per1) and TRAF family member-associated NF-kappa-B activator (Tank). The upregulation of Icam1, Fyn, Tifa and Traf6, all of which positively regulate IKK-NF-κB signalling, points to the activation of this pathway. This is further supported by the downregulation of the negative regulator Per1. In contrast, the overexpression of the inhibitor Tank points to a feedback mechanism aimed to limit excessive NF-κB signalling. All in all, these results indicate IKK-dependent NF-κB activation, self-limited through negative feedback by Tank.

TGF-β receptor signalling can be Smad protein-dependent (canonical) or -independent. In the Smad-independent pathway, TGF-β activates e.g. the ERK1/2 pathway.[63,64] Upon ICAM-1 stimulation, the serine-protease Htra1, which inhibits TGF-β signalling was upregulated. Together with the low expression of Smad proteins (Smad1, Smad5), these results suggest that after 2 hours of stimulation the canonical TGF-β receptor pathway is inactive. This is consistent with the downregulation of Thbs1 and Ccn2, which may be a result of Htra1-mediated reduction of TGF-β signalling.[56] The upregulated proto-oncogene tyrosine-protein kinase Src and dual specificity protein phosphatase 15 (Dusp15), which are involved in the ERK1/2 cascade, were also annotated to this pathway. This could be explained by the possible TGF-β-dependent activation of ERK1/2. However, since TGF-β itself was not overexpressed among the data, these results point to a TGF-β receptor-independent activation of ERK1/2.

The JAK-STAT signalling pathway was also enriched among ICAM-1-specific DEPs. The overexpressed fibroblast growth factor receptor 3 (Fgfr3), Ras-related protein Rac1 and the tyrosine protein kinases Fyn and Lyn facilitate STAT phosphorylation. However, the mast/stem cell growth factor receptor Kit, a JAK-STAT signalling activator, was downregulated, making the activation of the canonical JAK-STAT pathway unlikely.

GO-BP analysis showed that ICAM-1-specific proteins are involved in the LPS-mediated signalling pathway. Lipopolysaccharides are recognised by pattern recognition receptors (e.g. TLR2, TLR4). Although LPS were not introduced in this study, the upregulated proteins Lyn, Traf6 and protein kinase C alpha type (Prkca) are positive regulators of this pathway and associated with TLR2/4 signalling. This implies that following ICAM-1 stimulation, TLR-signalling is activated in the absence of LPS.[65] This is further supported by the increased expression oof Bgn, which may act as a DAMP (danger-associated molecular pattern) that interacts with TLR2/4.[52]

Finally, ICAM-1-specific proteins were significantly enriched in processes related to cytokine- (IL-1β, IL-2, IL-17, IFN) and glucocorticoid production. The upregulation of the inhibitor apolipoprotein A-I (Apoa1), which inhibits IL-1β synthesis, and arginase-2 (Arg2) along with the downregulation of the inducer glycoprotein hormone beta-5 (Gpb5), points to a suppression of IL-1β synthesis. The IFN pathway may also be attenuated, since all positive regulators, including ATP-dependent RNA helicase Dhx33, DNA-directed RNA polymerase III subunit RPC6 (Polr3f) and Zinc finger and BTB domain-containing protein 20 (Zbtb20), were downregulated. Dysregulation of the IL-17 synthesis suppressors Arg2 (upregulated) and OTU domain-containing protein 5 (Otud5, downregulated) implies that IL-17 production is unlikely to be activated. For IL-2, the inducers were both up- (Traf6) and downregulated (3',5'-cyclic-AMP phosphodiesterase 4D, Pde4d). A similar trend was observed for glucocorticoids: Apoa1 upregulated, galanin (Gal) downregulated. Therefore, the effects on IL-2 and glucocorticoid synthesis remain inconclusive, whereas the pattern suggests that IL-1β, IL-17 and IFN production may be reduced.

Considering the dysregulation of the proteins involved in the above-mentioned processes, the canonical NF-κB and toll-like receptor (TLR2/4)-mediated pathway are likely activated following ICAM-1 stimulation. In contrast, the activation of the TGF-β receptor and JAK-STAT signalling pathway appears attenuated. Moreover, there is no strong proteomic evidence that the synthesis of cytokines and glucocorticoids is favoured after two hours. On the contrary, IL-1β, IL-17 and IFN production is likely suppressed.

3.5.2.2. IL-16-specific DEPs and Pathways

The PPI subnetwork of IL-16 stimulation-specific DEPs (*Figure 18*) comprises 96 interacting DEPs (nodes) with 213 interactions (edges). To highlight the 49 upregulated (red) and 47 downregulated DEPs (blue), the nodes were continuously mapped based on their $\log_2$ FC values. The 154 singletons were hidden from this figure, however all 250 DEPs (108 upregulated, 142 downregulated, *SFigure 6*) were included in the functional enrichment analysis. The enlarged oval nodes represent the DEPs participating in pathways unique to IL-16 stimulation.

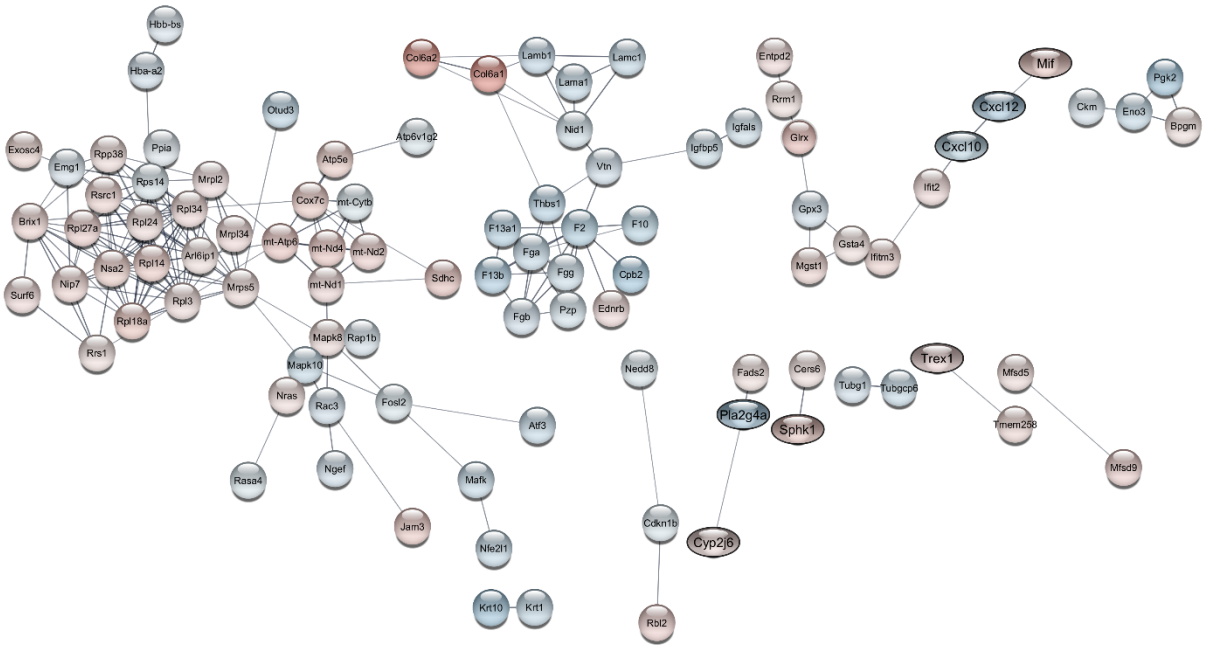

Figure 18: PPI subnetwork of IL-16-specific DEPs: *the network consists of 96 nodes (DEPs) and 213 edges (interactions). Red nodes (49) represent upregulated and blue nodes (47) down-regulated proteins. Singletons are not included in this figure. The interacting proteins participating in unique IL-16 pathways are highlighted. (Created using Cytoscape - https://cytoscape.org/)*

GO-BP analysis (*Figure 19*) showed that IL-16 treatment-specific DEPs were significantly enriched wound healing-related processes, including blood coagulation, fibrinolysis, platelet activation and aggregation, as well as responses to oxidative stress. Comparison of treatment-specific GO terms revealed that, unlike the ICAM-1 cohort, IL-16-associated proteins are closely linked to wounding responses. This suggests that while both treatments influence these pathways, IL-16 may have a more direct impact on their dysregulation.

IL-16-specific signalling processes include the noncanonical NF-κB- as well as cytokine-mediated pathway. The proteins also respond to pain, temperature stimuli and IFN and influence the synthesis of prostaglandins, cell adhesion molecules, IL-6, arachidonic acid (AA) and fatty acids. In addition, they regulate the secretion of dopamine, arachidonic acid, hormones and prostaglandins.

Subsequently, the proteins involved in the noncanonical NF-κB and cytokine-mediated signalling as well as the production/ secretion of cytokines, AA and PGs were examined, to anticipate whether these pathways would be activated following IL-16 stimulation.

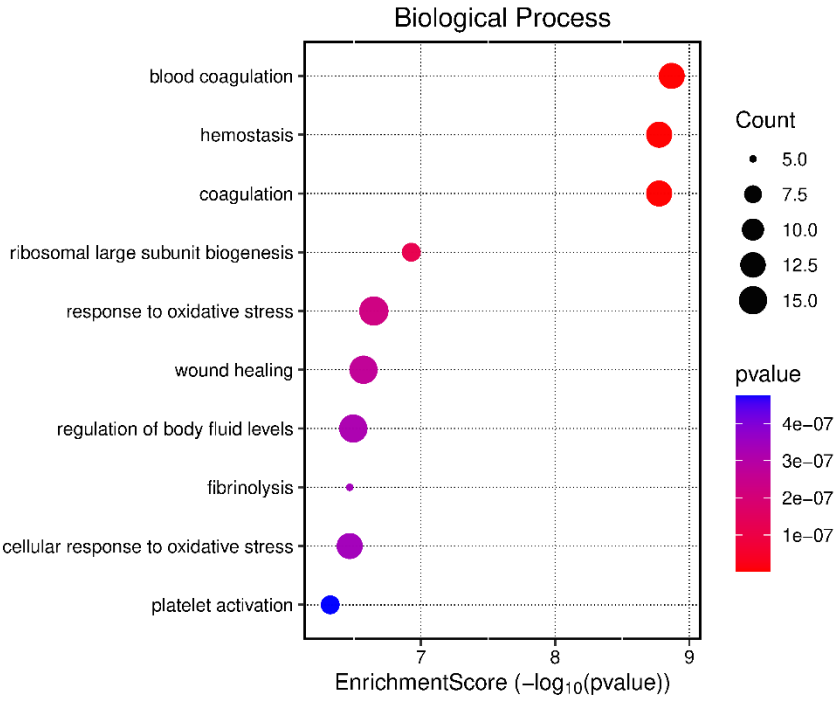

Figure 19: pathways (BPs) of IL-16-specific DEPs: *(A) The dot plot lists the most significantly enriched pathways first, starting with the highest significance in red and lowest in blue as indicated by the p-value on the y-axis. The x-axis shows the enrichment score; dots with the highest enrichment score are on the right. The dot size corresponds to the number of genes associated with each term. (Created with SRplot https://www.bioinformatics.com.cn/srplot)*

Compared to ICAM-1, IL-16 stimulation-specific proteins were associated with the activation of the noncanonical/ alternative NIK-NF-κB pathway. The complement C1q tumour necrosis factor-related protein 3 (C1qtnf3), a negative regulator of this pathway, was downregulated. Conversely, glutaredoxin (Glrx), an activator of NF-κB under oxidative stress conditions,[66] and sphingosine kinase 1 (Sphk1), which is a positive regulator of the non-canonical NF-κB pathway, were upregulated. Taking into consideration that the activators of this pathway are upregulated and the suppressors downregulated, these data suggest that two hours of IL-16 stimulation may activate the noncanonical NIK-NF-κB pathway.

GO-BP analysis annotated proteins unique to IL-16 stimulation to cytokine-mediated signalling pathways. The C-X-C motif chemokine 10 (Cxcl10) and stromal cell-derived factor 1 (Cxcl12) were downregulated, indicating a potential decrease in chemokine signalling. Both, the IFN signalling activator interferon-induced transmembrane protein 3 (Ifitm3) and suppressor three-prime repair exonuclease 1 (Trex1) were upregulated. This suggests partial activation, with negative feedback to limit overactive IFN signalling. As previously mentioned, the upregulated Sphk1 is associated with non-canonical NF-κB signalling. In addition, Sphk1 also regulates TNF-mediated signalling, suggesting that cytokine-mediated responses are primarily driven by TNF. Conversely, the cytokine signalling pathway inhibitor extracellular matrix protein 1 (Ecm1) and the tyrosine-protein phosphatase non-receptor type 6 (Ptpn6), which attenuates ERK activation and inflammatory responses to wounding, were both downregulated. Taken together, this pattern suggests a TNF-mediated activation of inflammatory pathways upon IL-16 stimulation, while limiting chemokine and IFN signalling.

Finally, the possible involvement of IL-16-specific DEPs in the synthesis of cytokines (TNF, IL-6), prostaglandins and arachidonic acid was examined. The proteins cytochrome P450 2J6 (Cyp2j6), macrophage migration inhibitory factor (Mif) and Trex1, which promote TNF production were upregulated, while the inhibitors Ilrun and Ptpn6 were downregulated. This points to the promotion of TNF synthesis. Similarly, the negative regulators of IL-6 synthesis C1qtnf3, Ptpn6 and proteoglycan 4 (Prg4) were also under-expressed, implying that IL-6 production is likely favoured under these conditions. On the other hand, the phospholipase A2 group IVA (Pla2g4a), which is essential for the release of arachidonic acid and subsequent production of prostaglandins, was downregulated.[67] This indicates that these biological processes are not favoured, despite the upregulation of positive regulators (Mif and Sphk1).

Summarising the observed patterns, the data suggest that noncanonical NF-κB and TNF-mediated signalling pathways are activated following 2 hours of IL-16 treatment. The synthesis of the cytokines TNF and IL-6 is supported, whereas the secretion of arachidonic acid and production of prostaglandins are not expected at this timepoint.

4. Discussion

This study investigated ICAM-1- and IL-16-induced proteomic alterations in murine DRGs to identify pathways that may contribute to TRPA1 sensitisation during the development of postsurgical pain. PPI network and functional enrichment analysis revealed that both treatments affected coagulation and complement cascades and were associated with early ECM remodelling. Overlapping and treatment-specific DEPs were subsequently examined to determine their pathway involvement and activation or suppression potential.

The findings suggest that proteins unique to ICAM-1 treatment may promote the activation of the canonical IKK-NF-κB and LPS-mediated signalling pathway via TLR2/4 engagement, while inhibiting TGF-β receptor and JAK-STAT signalling and suppressing the production of IL-1β, IL-17 and IFN. In contrast, IL-16-specific DEPs appear to drive noncanonical NF-κB signalling and TNF-mediated inflammatory pathways and promote the synthesis of TNF and IL-6, while AA and PG synthesis and secretion were not yet evident after two hours of stimulation.

4.1. ICAM-1- and IL-16-induced Onset of ECM Remodelling

The coagulation and complement cascades are essential defence systems that mediate immune response and haemostasis. They consist of various proteins that become active through proteolytic cleavage (e.g. following tissue injury), often followed by their degradation.[60,68,69] After two hours of ICAM-1 or IL-16 stimulation, coagulation- and complement-related proteins were downregulated. This reduced abundance likely reflects post-translational activation and consumption during cascade initiation, rather than reduced synthesis. Additionally, most acute-phase proteins, such as complement factors, fibronectin (Fn1) and plasminogen (Plg), are predominantly synthesised in the liver rather than locally within DRGs, which could further explain their lower detection levels.[70] Combined with the

upregulated structural ECM proteins (Col1a2, Bgn, Postn), these observations indicate a shift from coagulation-related processes to ECM remodelling and early tissue repair. The extracellular matrix is essential for regulating the physiological functions of primary afferent nociceptors, for instance, by engaging integrins or toll-like receptors (TLR2/4). Dysregulation of ECM proteins has been postulated to contribute to the chronification of pain. Inhibition of integrin signalling, in turn, can attenuate cytokine-induced mechanical hyperalgesia.[71,72]

As mentioned in *Chapter 1.2.1*, ICAM-1 has been identified as a protective factor in SCI repair, where it modulates inflammation and promotes tissue regeneration. It has been linked to NF-κB signalling, cell adhesion, ECM-receptor interactions and the response to LPS.[24] In the present study, ICAM-1 stimulation induced the overexpression of biglycan, which may function as an endogenous DAMP. Soluble Bgn can engage TLR2/4, activating downstream NF-κB and MAPK (p38, ERK) pathways and subsequent cytokine expression. Bgn also regulates TGF-β and TNF-α activity, further inducing inflammatory signalling.[51,52,73] The downregulation of Thbs1 and Ccn2 likely reflects Htra1-mediated suppression of TGF-β signalling, thereby removing an anti-inflammatory, anti-nociceptive mechanism.[74] The upregulation of alpha-2-HS-glycoprotein (Ahsg), a negative acute phase ECM protein that further inhibits TGF-β signalling, supports the idea that after two hours, the TLR-NF-κB pathway is the main driver of inflammation.[75] Taken together, these results indicate that ICAM-1 stimulation couples ECM remodelling to TLR-NF-κB signalling, which has been shown to promote TRPA1 sensitisation in DRG neurons, potentially contributing to inflammatory and neuropathic pain.[76]

The hub proteins identified within the IL-16 subnetwork, Fgb, Fgg, Ambp, Pzp and Serpind1, were all downregulated. Fibrinogen, a liver-derived acute-phase protein, is typically elevated during the early stages of inflammation in wound healing.[58] Its decreased expression, consistent with the overall downregulation of coagulation-related proteins, likely reflects rapid activation and consumption during the two-hour stimulation period. Consistent with this, IL-16-specific DEPs are more directly associated with the dysregulation of wound healing-related processes. Serine protease inhibitors (Serpind1, Pzp) normally limit excessive proteolysis of ECM components. Their suppression alongside the overexpression of structural ECM proteins (Col1a2, Bgn) is consistent with the early onset of a collagen-rich ECM remodelling program. Ambp is the precursor of alpha-1 microglobulin, a protein involved in tissue repair that inhibits oxidation during acute inflammation. Its reduced abundance may

facilitate ROS-mediated activation of TRPA1 channels, thereby promoting nociceptor sensitisation.[77] Collectively, the protein changes point to IL-16-induced ECM remodelling and activation of inflammatory signalling pathways, potentially linking it to TRPA1 activation and nociceptor sensitisation.

4.2. ICAM-1-induced TLR2/4-IKK-NF-κB Signalling

Subnetwork and hub protein analysis indicated that TLR-NF-κB signalling may be the main driver of inflammation following ICAM-1 stimulation, whereas TGF-β signalling appears to be suppressed. This interpretation is further supported by the pathway investigation of proteins unique to ICAM-1 stimulation.

The canonical NF-κB pathway is a rapid signalling cascade essential for both acute and chronic inflammatory responses. It is triggered by ligands of IL-1, TNF and toll-like receptors, leading to the activation of the IKK complex and nuclear translocation of NF-κB dimers.[78] In the present dataset, overexpression of canonical NF-κB activators (Icam1, Fyn, Tifa and Traf6) together with downregulation of the suppressor Per1 suggests induction of this pathway. The simultaneous upregulation of the suppressor Tank indicates a built-in feedback mechanism to prevent excessive NF-κB activity. Activation of this pathway in primary afferent neurons has been shown to promote pain following axonal injury, which was confirmed by the antinociceptive effects observed after IKK-β deletion.[79] ICAM-1 itself is tightly linked to NF-κB signalling. While NF-κB induces ICAM-1 expression, the soluble form (sICAM-1) can, in turn, activate NF-κB, amplifying the inflammatory response.[19] Under inflammatory conditions IKK-β-dependent NF-κB signalling has been tied to the overexpression of ICAM-1 in glial cells, contributing to the development of neuropathic pain. However, direct evidence for ICAM-1-mediated NF-κB pathways in neural tissue remains limited.[22]

GO-BP analysis linked ICAM-1-specific proteins to LPS-mediated signalling pathways, which typically involve toll like receptor (TLR2/4). Although LPS were not added to the cell cultures, the increased abundance of Lyn, Traf6 and Prkca suggests that ICAM-1 stimulation may initiate TLR2/4 receptor signalling in absence of an infection.[65] The elevated expression of Bgn further supports this mechanism, as it can act as an endogenous DAMP that activates TLR2/4.[52] Engagement of TLR4 has been shown to induce the release of TNF-α and IL-1β as well as the sensitisation of TRPA1 and TRPV1 nociceptors, thereby promoting neuropathic and inflammatory pain.[76,80,81] Furthermore, TLR activation can trigger downstream NF-κB pathways, underscoring the functional link between these pathways.[52] In a plantar incision model of lumbar DRGs (rats), TLR4 and phosphorylated NF-κB (p-p65) were increased in neuronal as well as satellite glial cells two hours after surgery, demonstrating its role in postsurgical pain.[81]

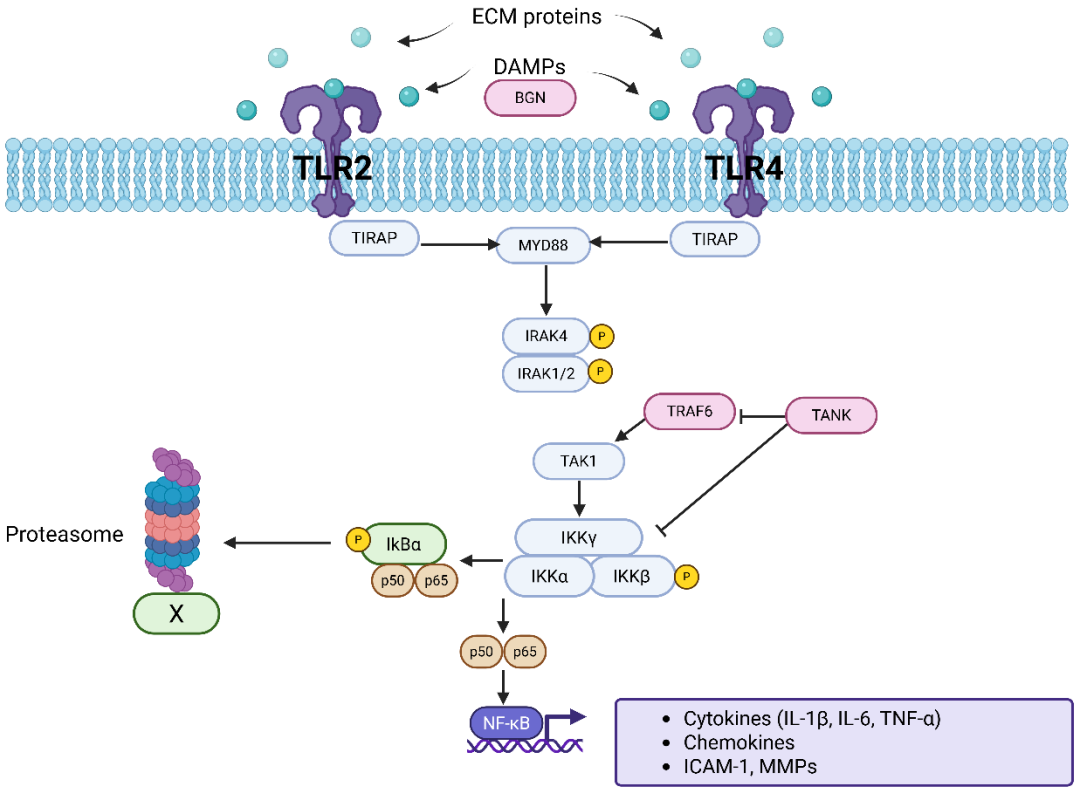

Figure 20: Proposed mechanism linking ECM remodelling to TLR2/4-IKK-NF-κB signalling following ICAM-1 stimulation. *Dysregulated extracellular matrix (ECM) components, particularly danger-associated molecular patterns (DAMPs) such as biglycan (BGN) bind toll-like receptors 2/4 (TLR2/4), activating Myeloid differentiation primary-response protein 88 (MyD88) signalling through TNF receptor associated factor 6 (TRAF6) and TGF-β-activated kinase 1 (TAK1). This triggers the IκB kinase (IKK) complex (IKKα, IKKβ, IKKγ), leading to IkBα degradation and NF-κB (p50/p65) translocation, which induces the transcription of pro-inflammatory genes (e.g. cytokines, chemokines, adhesion molecules). TRAF family member-associated NF-κB activator (TANK) can inhibit poly-ubiquitination of Traf6 and IKKγ, providing a negative feedback mechanism. Bgn, Traf6 and Tank were upregulated following ICAM-1 stimulation and are highlighted in red. (TIRAP = TIR domain-containing adaptor protein, IRAK1/2/4 = Interleukin-1 receptor-associated kinase 1) Figure adapted from Liu et al.[62], El − Zayat et al[83], Smith et al.[84] Yu et al[85]and Wang et al.[86] and created with BioRender https://www.biorender.com/)*

Dysregulation of ECM proteins at the onset of ECM remodelling creates an environment for pro-inflammatory signalling, as visualised by *Figure 20*. Various ECM-derived components, particularly DAMPs such as biglycan, can bind to TLR2/4 receptors and initiate signalling cascades that converge on the canonical IKK-NF-κB pathway. Both receptors signal through the myeloid differentiation primary-response protein 88 (MyD88) adaptor. The recruitment of MyD88 requires the TIR domain-containing adaptor protein (TIRAP).[82] Traf6, which was upregulated upon ICAM-1 stimulation, is essential for the activation of TGF-β-activated kinase 1 (TAK1).[83,84] Subsequently, the IKK complex, consisting of IKKα, IKKβ, IKKγ subunits, becomes activated, leading to IκBα phosphorylation and its ubiquitin-dependent proteasomal degradation.[85] This permits the nuclear translocation of NF-κB dimers (p50/p65), promoting the transcription of pro-inflammatory genes including cytokines (IL-1β, IL-6, TNF-α), chemokines and adhesion molecules (ICAM-1) and MMPs.[62] The transcription of MMPs further contributes to ECM remodelling by breaking down proteins and releasing ECM-bound growth factors.[59] The upregulated protein Tank can inhibit the polyubiquitination of Traf6 and IKKγ, likely providing a negative feedback mechanism to prevent excessive NF-κB signalling.[86]

ICAM-1-specific DEPs were also associated with TGF-β receptor-related pathways. The increased abundance of TGF-β signalling inhibitor Htra1 combined with the downregulation of Smad proteins (Smad1, Smad5) suggests that the canonical TGF-β receptor signalling pathway is likely suppressed.[63] This aligns with the reduced expression of Thbs1 and Ccn2, likely reflecting Htra1-mediated suppression of TGF-β signalling.[56] Although Src and Dusp15 can activate the Smad-independent TGF-β-mediated ERK1/2 cascades, the absence of TGF-β ligands among the DEPs implies that ERK activation occurs through a mechanism independent of TGF-β receptor engagement. Physiologically, TGF-β acts as an anti-inflammatory and anti-nociceptive cytokine. In the DRG, its secretion by macrophages promotes tissue repair and pain resolution, while excessive TGF-β can drive ECM deposition, scar formation and fibrosis.[74,87] Thus, suppression of this pathway may remove an anti-inflammatory brake, creating conditions that favour prolonged inflammation and nociceptor excitability. The concurrent activation of the ERK1/2 cascade (via Src and Dusp15) may promote chronic pain, as supported by the evidence that ERK1/2 activation in neurons of the dorsal horn drives central sensitisation in the spinal cord following peripheral inflammation.[88]

The JAK-STAT pathway is a major regulator of immune cell activation, migration and cytokine release and it plays an important role in neuroinflammation and pain modulation.[89] In glial cells, JAK-STAT signalling regulates ICAM-1 expression and supports the maintenance of neuropathic pain.[22] The upregulated ICAM-1-specific DEPs Fgfr3, Fyn/Lyn and Rac1 may promote STAT phosphorylation, suggesting potential regulation of JAK-STAT activity. However, the downregulation of Kit, a positive regulator of this cascade, indicates that canonical JAK-STAT signalling is likely attenuated.

Consistent with this interpretation, proteins uniquely regulated by ICAM-1 also modulate the production of cytokines (IL-1β, IL-2, IL-17, type I IFN) and glucocorticoids. Upregulation of the suppressors Apoa1 (IL-1β) and Arg2 (IL-1β, IL-17), together with the downregulation of the inducers Gpb5 (IL-1β) and Dhx33, Polr3f, Zbtb20 (IFN) as well as Otud5 (IL-17), suggests reduced synthesis of IFN, IL-1β and IL-17. In contrast, changes in IL-2 and glucocorticoid production remain uncertain, since the inducers were both up- and downregulated. Overall, this cytokine suppression pattern aligns with reduced JAK-STAT pathway activity likely limiting pro-inflammatory signalling.[89] Conversely, activation of TLR2/4-NF-κB signalling may still support the transcription of *pro*-IL-1β, enabling subsequent processing and release of active IL-1β, which can further increase the excitability of primary sensory neurons.[62,90]

Taken together, these findings suggest that TLR2/4- and IKK-NF-κB-mediated signalling are the principal drivers of inflammation after two hours of ICAM-1 stimulation, potentially promoting TRPA1 sensitisation. The upregulation of Bgn and the adaptor protein Traf6 highlights the functional link between structural ECM remodelling and inflammatory mechanisms. At the same time, elevated Tank levels indicate that this pathway is self-limited to dampen excessive NF-κB activation.[86] Suppression of anti-inflammatory TGF-β receptor signalling, together with activation of the ERK1/2 cascade, may facilitate the transition from acute to chronic pain.[74,88] In contrast, attenuated JAK-STAT activity combined with reduced IL-1β, IL-17 and IFN synthesis could provide a feedback mechanism to prevent excessive inflammation during the early phase of stimulation. Even though IL-1β synthesis is not predicted after two hours, NF-κB activation may still drive the transcription of pro-IL-1β and subsequent release of active IL-1β. In addition, upregulation of MMP transcripts may further drive ECM remodelling by cleaving structural ECM components and releasing growth factors, thereby establishing a bidirectional link between inflammatory signalling and ECM remodelling.[57,59]

4.3. IL-16-induced TNF/ NIK-NF-κB Signalling

While ICAM-1 is associated with the canonical NF-κB pathway, proteins unique to IL-16 stimulation are linked to noncanonical/ alternative NF-κB signalling, in which NIK plays a central role.[62] Unlike the rapid canonical response, the alternative NIK-NF-κB pathway is engaged more slowly (hours to days), because it requires *de novo* synthesis of proteins as well as processing of NF-κB precursors. It is activated by select members of the TNF receptor superfamily including the lymphotoxin-β receptor (LTβR), cluster of differentiation 40 (CD40), B-cell activating factor receptor (BAFFR) and receptor activator of NF-κB (RANK) (*Figure 21 B*). Ligand binding initiates the degradation of TRAF3, which under basal conditions mediates NIK turnover. Accumulating NIK then activates IKKα, which results in the phosphorylation, ubiquitination and processing of p100 to p52. The resulting nuclear translocation of NF-κB dimers (RelB/p52) promotes the transcription of a subset of immunoregulatory genes, especially those involved in lymphoid organ development and the survival of B-cells.[91] The elevated levels of Glrx, Sphk1, together with the reduced expression of the inhibitor C1qtnf3 suggest potential engagement of noncanonical NF-κB signalling in response to IL-16. However, since the ligands that typically activate this pathway were not increased, the mechanisms underlying pathway initiation remain uncertain. Given that Sphk1 generates Sphingosine-1-phosphate (S1P), a known cofactor for TRAF2 E3 ligase activity, it may modulate the TRAF2-TRA3 complex and promote TRAF3 degradation (*Chapter 5, Outlook*).[92]

GO-BP analysis linked IL-16-specific proteins to cytokine-mediated signalling. Reduced expression of chemokines (Cxcl10, Cxcl12) implies attenuated chemokine activity, while overexpression of Ifitm3 and Trex1 indicates potential activation of IFN-related pathways with built-in negative feedback activity. Notably, Sphk1, a regulator of noncanonical NF-κB signalling and enhancer of TNF-mediated responses, was also upregulated. This suggests that TNF-driven signalling may be a central axis following IL-16 stimulation. In addition, the downregulation of Ecm1 and Ptpn6, which normally dampen cytokine-mediated responses, further supports a shift towards a pro-inflammatory state. Overall, IL-16 treatment appears to favour TNF-mediated inflammatory pathways, while limiting chemokine and IFN signalling.

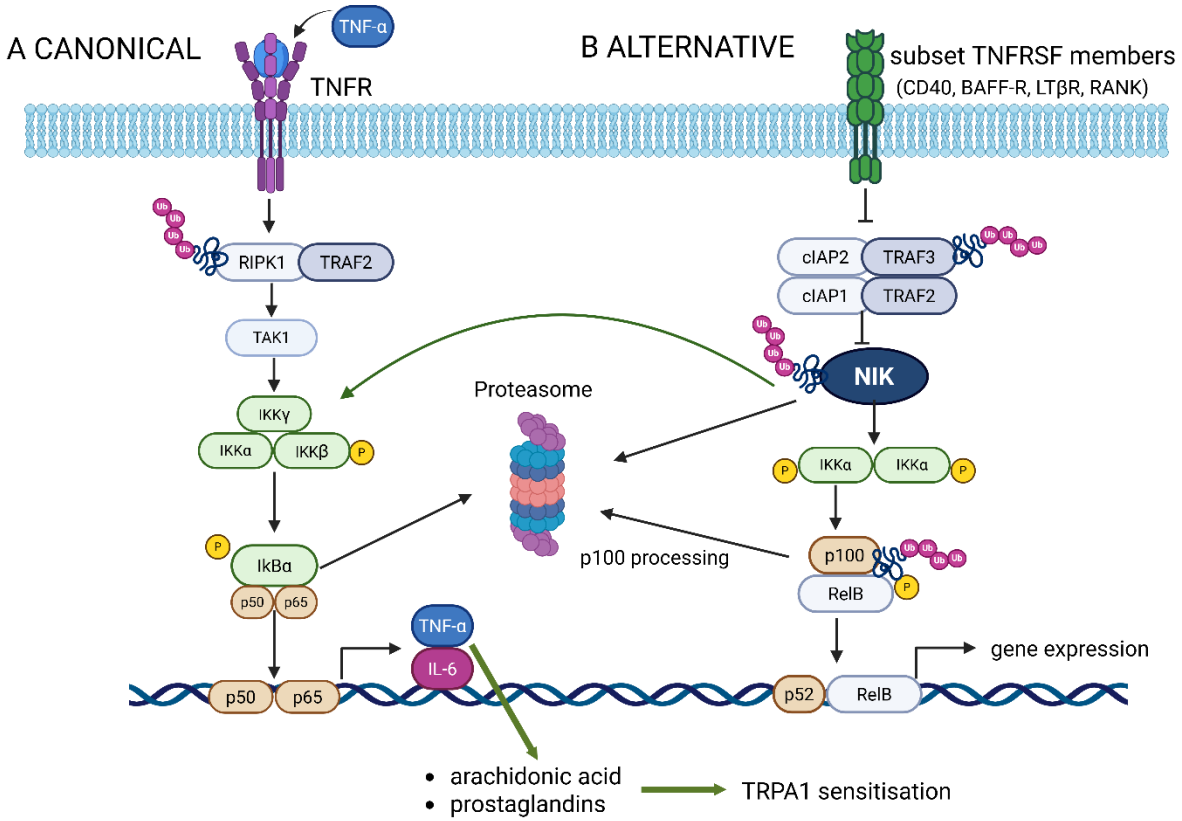

Figure 21: Proposed mechanism linking canonical (TNFR-mediated) and alternative NF-κB signalling following IL-16 stimulation. *(A) canonical NF-κB pathway initiated through TNFR engagement: autoubiquitination of TNF receptor associated factor 2 (TRAF2) activates and ubiquitinates receptor-interacting serine/threonine-protein kinase 1 (RIPK1), leading to TGF-β-activated kinase 1 (TAK1) activation. TAK1 stimulates the IκB kinase (IKK) complex (IKKα, IKKβ, IKKγ), resulting in IkBα degradation and NF-κB (p50/p65) translocation. This induces the transcription of pro-inflammatory genes, including TNF and IL-6 which drive the synthesis of arachidonic acid and prostaglandins, enhancing TRPA1 sensitisation. (B) alternative (non-canonical) NF-κB pathway: activation by a subset of TNF receptor superfamily ligands triggers ubiquitination and degradation of TRAF3, leading to nuclear factor-κ-B-inducing kinase (NIK) stabilisation and subsequent phosphorylation of IKKα. This drives processing of p100 to p52, enabling the formation of NF-κB dimers (p52/RelB), which translocate to the nucleus and drive transcription of immunoregulatory genes. NIK can also modulate IKK complex activity, highlighting potential crosstalk between the canonical and noncanonical pathway. (TNFRSF = TNF receptor superfamily, CD40 = cluster of differentiation 40, BAFFR = B-cell activating factor receptor, LTβR = lymphotoxin-β receptor, RANK = receptor activator of NF-κB, cIAP1/2 = cellular inhibitor of apoptosis 1/2) Figure adapted from Hofmann et al.[91] and Sun et al[13] and created with BioRender https://www.biorender.com/)*

Furthermore, IL-16 stimulation may promote the synthesis of the pro-inflammatory cytokines TNF and IL-6, as evidenced by the overexpression of TNF production inducers (Cyp2j6, Mif and Trex1) and the downregulation of suppressors (Ilrun, Ptpn6). A similar pattern was observed for IL-6 synthesis inhibitors (C1qtnf3, Prg4, Ptpn6). Notably, C1qtnf3 suppresses the phosphorylation and acetylation of the canonical NF-κB subunit p65, and thereby limits IL-6 and TNF-α expression.[93] Its downregulation therefore supports enhanced cytokine production. These findings are consistent with previous reports showing that IL-16 can promote IL-6 and TNF-α synthesis (*Chapter 1.2.2*).[32] In contrast, the downregulation of the cytosolic phospholipase Pla2g4a, which is required for the release of arachidonic acid and

following synthesis of prostaglandins, argues against the production of AA and PGs after 2 hours of IL-16 stimulation, despite positive regulators (Mif and Sphk1) being upregulated.[67]

As discussed in *Chapter 1.1.3*, neuroinflammation is characterised by the activation of glial cells in the spinal dorsal horn and the release of pro-inflammatory mediators, such as TNF-α and IL-6. These cytokines increase the excitability of neurons and sensitise nociceptors, thereby participating in the development of CPSP.[15,16] They mediate TRPA1 activation and TRPA1, in turn increases the expression of TNF-α and IL-6, creating a positive feedback loop.[13,94] Moreover, TNF-α and IL-6 stimulate the production of additional cytokines and prostaglandins, important mediators of peripheral sensitisation. Thus, although AA and PG synthesis is not favoured after 2 hours, their production may increase once TNF and IL-6 accumulate, further driving inflammation and promoting the transition to chronic pain.[32]

TNF binding to its receptors can activate the canonical NF-κB pathway, further enhancing TNF and IL-6 synthesis.[62,95] In addition, NIK can modulate components of the IKK complex, thereby influencing canonical NF-κB activation, highlighting the crosstalk between the two mechanism.[91] The interplay of canonical and non-canonical NF-κB pathways (*Figure 21*) may therefore amplify inflammatory responses and help sustain the neuroinflammatory environment underlying chronic pain.

Taken together, this pattern suggests that the TNF-NF-κB axis is the dominant mechanism following IL-16 stimulation. This is supported by the favoured synthesis of the pro-inflammatory and pro-nociceptive mediators TNF and IL-6, which are known to increase the excitability of neurons and promote TRPA1 sensitisation.[15,16] While the non-canonical NF-κB cascade may be slowly activated, accumulating TNF can rapidly signal through the canonical pathway, further amplifying cytokine and chemokine production.[62,95] The potential synergistic activity of both pathways may sustain neuroinflammation. Even though the synthesis and secretion of arachidonic acid and prostaglandins are not favoured after two hours, elevated TNF and IL-6 levels may activate these pathways later. This would further enhance inflammatory and nociceptive signalling and contribute to the chronification of pain.[32] In contrast, suppressed IFN signalling may limit uncontrolled inflammation and supports the notion that the TNF-NF-κB axis is the dominant mechanism.

4.4. Limitations

This study has several limitations that should be acknowledged.

Analytical Considerations:

First, few proteins reached statistical significance after adjustment for multiple testing. Therefore, unadjusted p-values were used for analyses, meaning that false-positive findings cannot be excluded and the results should be interpreted with caution. Nevertheless, the findings still provide valuable insight into potentially biologically relevant mechanisms that warrant further validation. Additionally, a mild $|\log_2 FC|$ threshold of ≥ 0.2 was applied to include a broad range of differentially expressed proteins. However, there might still be a few relevant less up- or downregulated proteins that might affect nociceptive mechanisms, which may not have been captured in this study.

The unbiased functional enrichment analysis did not yield biologically interpretable results. Consequently, the interpretation focused on coagulation and immune pathways, which are established contributors to postsurgical and neuropathic pain.[96] While this targeted approach enabled further examination of how ICAM-1 and IL-16 contribute to the dysregulation of these pathways, it also introduces selection bias and other relevant biological processes may have been overlooked.

Experimental Design:

Only one cytokine concentration and a two-hour incubation period were tested, based on previous data indicating their potential to sensitise TRPA1 channels.[33] However, additional experiments are needed to better mirror time- and dose-dependent *in-vivo* release kinetics. Six biological replicates were included per condition. Although this number is sufficient in proteomics, increasing the number could enhance the statistical power and reliability of the results. Furthermore, DRG contain multiple cell types including neurons, SGCs, immune and endothelial cells.[7] Because a bulk proteomics approach was used, the detected protein changes cannot be assigned to specific cell populations.

Experimental Animals:

Only male mice were included, which limits translational relevance. Women experience chronic pain more frequently than men due to differences in hormones, immune response, anatomy, psychosocial factors and sex-specific gene expression in dorsal root ganglia.[97] Oestrogen metabolites can activate and sensitise TRPA1 and TRPV1 channels, enhancing nociceptor excitability and pain perception.[98] Moreover, oestrogen attenuates LPS-mediated inflammatory signalling, one of the key pathways identified in the ICAM-1 cohort.[99] Interspecies differences also need to be considered. Murine models do not completely replicate human pain mechanisms, and cannot be directly translated to humans without further *in-vivo* and clinical validation.[100]

A final limitation concerns potential batch effects. The mice used for the IL-16 group were bred in-house, whereas those used for the ICAM-1 cohort were obtained from Janvier Labs (Le Genest-Saint-Isle, France). Although each treatment group was only analysed against its respective control, factors such as transport stress or microbiome differences may introduce batch variability. The microbiome, in particular, modulates immune and neural signalling pathways and influences DRG transcriptomes.[101,102] Therefore, inter-group comparisons should be interpreted with caution.

5. Conclusion and Outlook

In summary, this study offers novel insights into the molecular mechanisms through which ICAM-1 and IL-16 stimulation of murine DRGs may contribute to TRPA1 sensitisation during postsurgical pain. Both mediators similarly affected coagulation, complement and ECM remodelling pathways, suggesting they alter the microenvironment to promote sustained nociceptor excitability. Despite the shared responses, IL-16-specific DEPs were more directly associated with alteration in wound healing-related pathways.

Future investigations should clarify whether the apparent downregulation of coagulation- and complement-related proteins reflects their rapid activation and degradation, reduced detectability of active fragments or genuinely reduced synthesis. Analyses at multiple timepoints beyond the two-hour stimulation period will be essential to capture temporal dynamics of coagulation, complement and ECM remodelling pathways. Such experiments will

help determine whether these processes become amplified long-term and thereby contribute to sustained neuroinflammation and nociceptor sensitisation.

ICAM-1 stimulation primarily engaged TLR2/4-dependent canonical NF-κB pathways, indicating an early pro-inflammatory response that may facilitate TRPA1 sensitisation. Within this pathway, biglycan and Traf6 were upregulated, underscoring the connection between structural ECM remodelling and inflammation. The upregulation of Tank suggests the presence of an intrinsic negative feedback mechanism that limits excessive NF-κB signalling.[86] Attenuated TGF-β receptor pathways, combined with activation of the ERK1/2 cascade may further promote the development of chronic pain.[74,88] In contrast, reduced JAK-STAT activity and IL-1β, IL-17 and IFN synthesis suggests a compensatory mechanism to restrain excessive inflammation. However, canonical NF-κB is known to induce the transcription of pro-IL-1β and MMPs, suggesting that later production of these mediators could further amplify both inflammatory responses and ECM remodelling.[57,59]

Given these findings, future studies should examine whether biglycan acts as a key upstream driver of ICAM-1 induced TLR-NF-κB pathways. This could be achieved by blocking or silencing Bgn and analysing whether subsequent signalling events, including Traf6 activation and nuclear translocation of NF-κB, are attenuated. It will also be important to examine how prolonged ICAM-1 stimulation or secondary mediators maintain this inflammatory state and contribute to prolonged TRPA1 sensitisation. Finally, assessing whether MMP expression is enhanced at later timepoints, will be essential to confirm the potential bidirectional link between ECM remodelling and inflammatory signalling in this system.

In contrast to ICAM-1, IL-16 stimulation was associated with TNF-NF-κB signalling. Elevated expression of Sphk1 and Glrx, together with reduced C1qtnf3 suggests partial engagement of the non-canonical NF-κB pathway, although classical upstream activators were not increased. The synthesis of TNF and IL-6 was also favoured, indicating a crosstalk between the canonical (TNFR-dependent) and non-canonical pathway. As NIK can modulate IKK activity, this interplay may amplify and prolong NF-κB signalling.[91] TNF and IL-6 may also induce the synthesis of arachidonic acid and prostaglandins at later stages, thereby increasing neuronal excitability

and TRPA1 sensitisation, linking acute inflammatory signalling to sustained postoperative pain.[32] Conversely, attenuated chemokine and IFN signalling may help prevent excessive inflammation and supports the notion that the TNF-NF-κB axis represents the dominant mechanisms following IL-16 stimulation.

In the canonical TNFR-driven NF-κB pathway, TRAF2 ubiquitination is essential for downstream signalling. Through its RING domain, TRAF2 exhibits E3 ubiquitin ligase activity, which drives autoubiquitination and activates adaptors and kinases such as RIP1, cIAP1/2, TAK1 and IKK subunits. The lipid kinase Sphk1 catalyses the formation of S1P, which acts as a cofactor that enhances TRAF2's E3 ligase activity and facilitates ubiquitination of RIPK1.[103] This interaction functionally links TNF-α stimulation to NF-κB activation, supported by the evidence that Sphk1 depletion reduced TNF-α-induced IKK phosphorylation.[92] In the noncanonical pathway, TRAF3 degradation is considered the key mechanism preceding NIK stabilisation. Both TRAF2- and TRAF3-deficiency have been shown to increase NIK levels, promote p100 processing and enhance nuclear translocation of RelB/p52.[104]

It remains to be investigated whether Sphk1 and subsequent S1P generation triggers TRAF2/3 autoubiquitination and subsequent degradation, similarly to the canonical pathway. However, autoubiquitination of TRAF2 could alternatively activate cIAP1/2, enhancing the degradation of NIK and inactivating the noncanonical NF-κB pathway.[104] Studying these possibilities will be necessary to understand how IL-16 influences canonical and noncanonical NF-κB signalling.

Together, these findings highlight ICAM-1 and IL-16 as upstream regulators of complementary inflammatory responses in DRGs. Although they engage distinct signalling mechanisms, both appear to converge on NF-κB activation, potentially promoting TRPA1 sensitisation. Exploring temporal dynamics of these pathways may provide deeper insight into how acute postsurgical inflammation progresses into persistent pain and help identify potential targets to prevent this transition.

References

(1) Chapman, C. R.; Vierck, C. J. The Transition of Acute Postoperative Pain to Chronic Pain: An Integrative Overview of Research on Mechanisms. *The Journal of Pain* **2017**, *18* (4), 359.e1-359.e38. https://doi.org/10.1016/j.jpain.2016.11.004.

(2) Echeverria-Villalobos, M.; Tortorici, V.; Brito, B. E.; Ryskamp, D.; Uribe, A.; Weaver, T. The Role of Neuroinflammation in the Transition of Acute to Chronic Pain and the Opioid-Induced Hyperalgesia and Tolerance. *Front Pharmacol* **2023**, *14*, 1297931. https://doi.org/10.3389/fphar.2023.1297931.

(3) Martinez, V.; Lehman, T.; Lavand'homme, P.; Harkouk, H.; Kalso, E.; Pogatzki-Zahn, E. M.; Komann, M.; Meissner, W.; Weinmann, C.; Fletcher, D. Chronic Postsurgical Pain. *Eur J Anaesthesiol* **2024**, *41* (5), 351–362. https://doi.org/10.1097/EJA.0000000000001974.

(4) Park, R.; Mohiuddin, M.; Arellano, R.; Pogatzki-Zahn, E.; Klar, G.; Gilron, I. Prevalence of Postoperative Pain after Hospital Discharge: Systematic Review and Meta-Analysis. *Pain Rep* **2023**, *8* (3), e1075. https://doi.org/10.1097/PR9.0000000000001075.

(5) Segelcke, D.; Burgt, M. van der; Kappert, C.; Garcia, D. S.; Sondermann, J. R.; Bigalke, S.; Pradier, B.; Gomez-Varela, D.; Zahn, P. K.; Schmidt, M.; Pogatzki-Zahn, E. M. Phenotype- and Species-Specific Skin Proteomic Signatures for Incision-Induced Pain in Humans and Mice. *British Journal of Anaesthesia* **2023**, *130* (3), 331–342. https://doi.org/10.1016/j.bja.2022.10.040.

(6) Pogatzki-Zahn, E. M.; Segelcke, D.; Schug, S. A. Postoperative Pain—from Mechanisms to Treatment. *Pain Rep* **2017**, *2* (2), e588. https://doi.org/10.1097/PR9.0000000000000588.

(7) Berta, T.; Qadri, Y.; Tan, P.-H.; Ji, R.-R. Targeting Dorsal Root Ganglia and Primary Sensory Neurons for the Treatment of Chronic Pain. *Expert Opin Ther Targets* **2017**, *21* (7), 695–703. https://doi.org/10.1080/14728222.2017.1328057.

(8) Pinho-Ribeiro, F. A.; Verri, W. A.; Chiu, I. M. Nociceptor Sensory Neuron-Immune Interactions in Pain and Inflammation. *Trends Immunol* **2017**, *38* (1), 5–19. https://doi.org/10.1016/j.it.2016.10.001.

(9) Wang, J. Transition from Acute to Chronic Pain:Evaluating Risk for Chronic Postsurgical Pain. *Pain Phys* **2019**, *5* (22;5), 479–488. https://doi.org/10.36076/ppj/2019.22.479.

(10) Chen, O.; Donnelly, C. R.; Ji, R.-R. Regulation of Pain by Neuro-Immune Interactions between Macrophages and Nociceptor Sensory Neurons. *Curr Opin Neurobiol* **2020**, *62*, 17–25. https://doi.org/10.1016/j.conb.2019.11.006.

(11) Fülöp, B.; Borbély, É.; Helyes, Z. How Does Chronic Psychosocial Distress Induce Pain? Focus on Neuroinflammation and Neuroplasticity Changes. *Brain Behav Immun Health* **2025**, *44*, 100964. https://doi.org/10.1016/j.bbih.2025.100964.

(12) Song, C. Neuroinflammation and Synaptic Plasticity: New Insights into Postoperative Pain Mechanism. **2025**, *8*.

(13) Sun, J.; Ramnath, R. D.; Zhi, L.; Tamizhselvi, R.; Bhatia, M. Substance P Enhances NF-κB Transactivation and Chemokine Response in Murine Macrophages via ERK1/2 and P38 MAPK Signaling Pathways. *American Journal of Physiology-Cell Physiology* **2008**, *294* (6), C1586–C1596. https://doi.org/10.1152/ajpcell.00129.2008.

(14) Shutov, L. P.; Warwick, C. A.; Shi, X.; Gnanasekaran, A.; Shepherd, A. J.; Mohapatra, D. P.; Woodruff, T. M.; Clark, J. D.; Usachev, Y. M. The Complement System Component C5a Produces

Thermal Hyperalgesia via Macrophage-to-Nociceptor Signaling That Requires NGF and TRPV1. *J Neurosci* **2016**, *36* (18), 5055–5070. https://doi.org/10.1523/JNEUROSCI.3249-15.2016.

(15) Yang, J.-X.; Wang, H.-F.; Chen, J.-Z.; Li, H.-Y.; Hu, J.-C.; Yu, A.-A.; Wen, J.-J.; Chen, S.-J.; Lai, W.-D.; Wang, S.; Jin, Y.; Yu, J. Potential Neuroimmune Interaction in Chronic Pain: A Review on Immune Cells in Peripheral and Central Sensitization. *Front Pain Res (Lausanne)* **2022**, *3*, 946846. https://doi.org/10.3389/fpain.2022.946846.

(16) Hanani, M.; Spray, D. C. Emerging Importance of Satellite Glia in Nervous System Function and Dysfunction. *Nat Rev Neurosci* **2020**, *21* (9), 485–498. https://doi.org/10.1038/s41583-020-0333-z.

(17) DiSabato, D.; Quan, N.; Godbout, J. P. Neuroinflammation: The Devil Is in the Details. *J Neurochem* **2016**, *139* (Suppl 2), 136–153. https://doi.org/10.1111/jnc.13607.

(18) Dietrich, J.-B. The Adhesion Molecule ICAM-1 and Its Regulation in Relation with the Blood–Brain Barrier. *Journal of Neuroimmunology* **2002**, *128* (1), 58–68. https://doi.org/10.1016/S0165-5728(02)00114-5.

(19) Bui, T. M.; Wiesolek, H. L.; Sumagin, R. ICAM-1: A Master Regulator of Cellular Responses in Inflammation, Injury Resolution, and Tumorigenesis. *J Leukoc Biol* **2020**, *108* (3), 787–799. https://doi.org/10.1002/JLB.2MR0220-549R.

(20) McPeek, M. K.; Gomez, J. C.; Martin, J. R.; Iannone, M. A.; Dang, H.; Doerschuk, C. M. Leukocyte Kinetics and Bacterial Clearance during Streptococcus Pneumoniae Pneumonia and Contributions of ICAM-1. *American Journal of Physiology-Lung Cellular and Molecular Physiology* **2025**, *328* (1), L41–L59. https://doi.org/10.1152/ajplung.00039.2024.

(21) Miller, M. R.; Landis, H. E.; Miller, R. E.; Tizabi, Y. Intercellular Adhesion Molecule 1 (ICAM-1): An Inflammatory Regulator with Potential Implications in Ferroptosis and Parkinson's Disease. *Cells* **2024**, *13* (18), 1554. https://doi.org/10.3390/cells13181554.

(22) Chaudhari, A.; Padmar, J.; Awathale, S.; Goyal, S.; Nakhate, K.; Sherikar, A. From Glial Cells to Pain Pathways: ICAM-1 as a Central Player in Neuroinflammation and Neuropathy. *Discov. Neurosci.* **2025**, *20* (1), 5. https://doi.org/10.1186/s13064-025-00201-0.

(23) Greenwood, J.; Etienne-Manneville, S.; Adamson, P.; Couraud, P.-O. Lymphocyte Migration into the Central Nervous System: Implication of ICAM-1 Signalling at the Blood–Brain Barrier. *Vascular Pharmacology* **2002**, *38* (6), 315–322. https://doi.org/10.1016/S1537-1891(02)00199-4.

(24) Yuan, X.; Zhang, M.; Wang, F.; Wang, X.; Cui, L.; Tang, B.; Song, X.; Wang, X.; Zhang, L.; Wang, Z.; Yang, L.; Wang, T. Key Targets in Subacute Spinal Cord Injury Identified by Bioinformatics and Mendelian Randomization. *World Neurosurgery* **2025**, *198*, 123966. https://doi.org/10.1016/j.wneu.2025.123966.

(25) Ahsan, F.; Santoso, B.; Rahmawati, N. Y.; Alditia, F. N.; Mufid, A. F.; Sa'adi, A.; Dwiningsih, S. R.; Tunjungseto, A.; Widyanugraha, M. Y. A. Soluble Adhesion Molecules in Serum and Peritoneal Fluid Are Associated with Pelvic Pain in Endometriosis. *International Journal of Gynecology & Obstetrics* **2025**, *169* (1), 138–147. https://doi.org/10.1002/ijgo.16004.

(26) Luchting, B.; Hinske, L. C. G.; Rachinger-Adam, B.; Celi, L. A.; Kreth, S.; Azad, S. C. Soluble Intercellular Adhesion Molecule-1: A Potential Biomarker for Pain Intensity in Chronic Pain Patients. *Biomark Med* **2017**, *11* (3), 265–276. https://doi.org/10.2217/bmm-2016-0246.

(27) Ferraz-Amaro, I.; Ibrahim-Achi, Z.; de Vera-González, A.; González-Delgado, A.; Renuncio-García, M.; Vicente-Rabaneda, E. F.; Ocejo-Vinyals, J. G.; Castañeda, S.; González-Gay, M. Á. Associations Between Soluble Cell Adhesion Molecules and Cardiovascular Comorbidities in Systemic

Sclerosis: Implications for Insulin Resistance. *J Clin Med* **2025**, *14* (5), 1467. https://doi.org/10.3390/jcm14051467.

(28) Skundric, D. S.; Cai, J.; Cruikshank, W. W.; Gveric, D. Production of IL-16 Correlates with CD4+ Th1 Inflammation and Phosphorylation of Axonal Cytoskeleton in Multiple Sclerosis Lesions. *J Neuroinflammation* **2006**, *3*, 13. https://doi.org/10.1186/1742-2094-3-13.

(29) Hridi, S. U.; Barbour, M.; Wilson, C.; Franssen, A. J.; Harte, T.; Bushell, T. J.; Jiang, H.-R. Increased Levels of IL-16 in the Central Nervous System during Neuroinflammation Are Associated with Infiltrating Immune Cells and Resident Glial Cells. *Biology (Basel)* **2021**, *10* (6), 472. https://doi.org/10.3390/biology10060472.

(30) Niewold, T. B.; Lehman, J. S.; Gunnarsson, I.; Meves, A.; Oke, V. Role of Interleukin-16 in Human Diseases: A Novel Potential Therapeutic Target. *Front Immunol* **2025**, *16*, 1524026. https://doi.org/10.3389/fimmu.2025.1524026.

(31) Richmond, J.; Tuzova, M.; Cruikshank, W.; Center, D. Regulation of Cellular Processes by Interleukin-16 in Homeostasis and Cancer. *Journal of Cellular Physiology* **2014**, *229* (2), 139–147. https://doi.org/10.1002/jcp.24441.

(32) González-Rodríguez, S.; Sordo-Bahamonde, C.; Álvarez-Artime, A.; Baamonde, A.; Menéndez, L. Hyperalgesic Effect Evoked by Il-16 and Its Participation in Inflammatory Hypernociception in Mice. *J Neuroimmune Pharmacol* **2024**, *19* (1), 44. https://doi.org/10.1007/s11481-024-10145-7.

(33) Weiß, L. *The Impact of the Inflammatory Components ICAM-1, IL-16, and TREM-1 in Postoperative Pain in Mice*; 2023.

(34) Hughes, C. S.; Moggridge, S.; Müller, T.; Sorensen, P. H.; Morin, G. B.; Krijgsveld, J. Single-Pot, Solid-Phase-Enhanced Sample Preparation for Proteomics Experiments. *Nat Protoc* **2019**, *14* (1), 68–85. https://doi.org/10.1038/s41596-018-0082-x.

(35) Gao, Y.; Wang, M.; Wang, L.; Jia, X.; Hu, C.; Liu, P.; Liu, B.; Tan, M.; Zhai, L. The Impact of Different Alkylation Quenching Methods on Tryptic Activity and Protein Identification in Proteomics Sample Preparation. *Journal of Mass Spectrometry* **2025**, *60* (6), e5141. https://doi.org/10.1002/jms.5141.

(36) Xian, F.; Sondermann, J. R.; Gomez Varela, D.; Schmidt, M. Deep Proteome Profiling Reveals Signatures of Age and Sex Differences in Paw Skin and Sciatic Nerve of Naïve Mice. *eLife 11*, e81431. https://doi.org/10.7554/eLife.81431.

(37) Grundtner, S.; Sondermann, J. R.; Xian, F.; Malzl, D.; Segelcke, D.; Pogatzki-Zahn, E. M.; Menche, J.; Gómez-Varela, D.; Schmidt, M. Deep Proteomics and Network Pharmacology Reveal Sex- and Age-Shared Neuropathic Pain Signatures in Mouse Dorsal Root Ganglia. *Pharmacological Research* **2025**, *211*, 107552. https://doi.org/10.1016/j.phrs.2024.107552.

(38) Xiao, L.; Yang, Z.; Lin, S. Identification of Hub Genes and Transcription Factors in Patients with Rheumatoid Arthritis Complicated with Atherosclerosis. *Sci Rep* **2022**, *12* (1), 4677. https://doi.org/10.1038/s41598-022-08274-1.

(39) Chin, C.-H.; Chen, S.-H.; Wu, H.-H.; Ho, C.-W.; Ko, M.-T.; Lin, C.-Y. cytoHubba: Identifying Hub Objects and Sub-Networks from Complex Interactome. *BMC Syst Biol* **2014**, *8* (Suppl 4), S11. https://doi.org/10.1186/1752-0509-8-S4-S11.

(40) Tang, D.; Chen, M.; Huang, X.; Zhang, G.; Zeng, L.; Zhang, G.; Wu, S.; Wang, Y. SRplot: A Free Online Platform for Data Visualization and Graphing. *PLOS ONE* **2023**, *18* (11), e0294236. https://doi.org/10.1371/journal.pone.0294236.

(41) Manon-Jensen, T.; Kjeld, N. G.; Karsdal, M. A. Collagen-mediated Hemostasis. *Journal of Thrombosis and Haemostasis* **2016**, *14* (3), 438–448. https://doi.org/10.1111/jth.13249.

(42) Amirrah, I. N.; Lokanathan, Y.; Zulkiflee, I.; Wee, M. F. M. R.; Motta, A.; Fauzi, M. B. A Comprehensive Review on Collagen Type I Development of Biomaterials for Tissue Engineering: From Biosynthesis to Bioscaffold. *Biomedicines* **2022**, *10* (9), 2307. https://doi.org/10.3390/biomedicines10092307.

(43) Campbell, P. G.; Durham, S. K.; Hayes, J. D.; Suwanichkul, A.; Powell, D. R. Insulin-like Growth Factor-Binding Protein-3 Binds Fibrinogen and Fibrin*. *Journal of Biological Chemistry* **1999**, *274* (42), 30215–30221. https://doi.org/10.1074/jbc.274.42.30215.

(44) Mayger, K.; Young, J.; Leite, R.; Parmar, K.; Hunt, B. J. Investigation of the Impact of Antithrombin Deficiency on the Inflammatory Response: Results from a Single Centre Cohort Study. *Thrombosis Research* **2025**, *249*. https://doi.org/10.1016/j.thromres.2025.109315.

(45) Obaha, A.; Novinec, M. Regulation of Peptidase Activity beyond the Active Site in Human Health and Disease. *Int J Mol Sci* **2023**, *24* (23), 17120. https://doi.org/10.3390/ijms242317120.

(46) Lin, P.; Tian, P.; Pang, J.; Lai, L.; He, G.; Song, Y.; Zheng, Y. Clinical Significance of COL1A1 and COL1A2 Expression Levels in Hypopharyngeal Squamous Cell Carcinoma. *Oncol Lett* **2020**, *20* (1), 803–809. https://doi.org/10.3892/ol.2020.11594.

(47) Jokinen, J.; Dadu, E.; Nykvist, P.; Käpylä, J.; White, D. J.; Ivaska, J.; Vehviläinen, P.; Reunanen, H.; Larjava, H.; Häkkinen, L.; Heino, J. Integrin-Mediated Cell Adhesion to Type I Collagen Fibrils*. *Journal of Biological Chemistry* **2004**, *279* (30), 31956–31963. https://doi.org/10.1074/jbc.M401409200.

(48) Danen, E. H. J. Integrins: An Overview of Structural and Functional Aspects. In *Madame Curie Bioscience Database [Internet]*; Landes Bioscience, 2013.

(49) Liu, A. Y.; Zheng, H.; Ouyang, G. Periostin, a Multifunctional Matricellular Protein in Inflammatory and Tumor Microenvironments. *Matrix Biology* **2014**, *37*, 150–156. https://doi.org/10.1016/j.matbio.2014.04.007.

(50) Norris, R. A.; Damon, B.; Mironov, V.; Kasyanov, V.; Ramamurthi, A.; Moreno-Rodriguez, R.; Trusk, T.; Potts, J. D.; Goodwin, R. L.; Davis, J.; Hoffman, S.; Wen, X.; Sugi, Y.; Kern, C. B.; Mjaatvedt, C. H.; Turner, D. K.; Oka, T.; Conway, S. J.; Molkentin, J. D.; Forgacs, G.; Markwald, R. R. Periostin Regulates Collagen Fibrillogenesis and the Biomechanical Properties of Connective Tissues. *J Cell Biochem* **2007**, *101* (3), 695–711. https://doi.org/10.1002/jcb.21224.

(51) Schaefer, L.; Babelova, A.; Kiss, E.; Hausser, H.-J.; Baliova, M.; Krzyzankova, M.; Marsche, G.; Young, M. F.; Mihalik, D.; Götte, M.; Malle, E.; Schaefer, R. M.; Gröne, H.-J. The Matrix Component Biglycan Is Proinflammatory and Signals through Toll-like Receptors 4 and 2 in Macrophages. *J Clin Invest* **2005**, *115* (8), 2223–2233. https://doi.org/10.1172/JCI23755.

(52) Appunni, S.; Rubens, M.; Ramamoorthy, V.; Anand, V.; Khandelwal, M.; Sharma, A. Biglycan: An Emerging Small Leucine-Rich Proteoglycan (SLRP) Marker and Its Clinicopathological Significance. *Mol Cell Biochem* **2021**, *476* (11), 3935–3950. https://doi.org/10.1007/s11010-021-04216-z.

(53) Chen, C.; Melo, E.; Jakob, P.; Friedlein, A.; Elsässer, B.; Goettig, P.; Kueppers, V.; Delobel, F.; Stucki, C.; Dunkley, T.; Fauser, S.; Schilling, O.; Iacone, R. N-Terminomics Identifies HtrA1 Cleavage of Thrombospondin-1 with Generation of a Proangiogenic Fragment in the Polarized Retinal Pigment Epithelial Cell Model of Age-Related Macular Degeneration. *Matrix Biology* **2018**, *70*, 84–101. https://doi.org/10.1016/j.matbio.2018.03.013.

(54) Rebolledo, D. L.; Lipson, K. E.; Brandan, E. Driving Fibrosis in Neuromuscular Diseases: Role and Regulation of Connective Tissue Growth Factor (CCN2/CTGF). *Matrix Biology Plus* **2021**, *11*, 100059. https://doi.org/10.1016/j.mbplus.2021.100059.

(55) LI, Q.; CHEN, J.; CHEN, Y.; CONG, X.; CHEN, Z. Chronic Sciatic Nerve Compression Induces Fibrosis in Dorsal Root Ganglia. *Mol Med Rep* **2016**, *13* (3), 2393–2400. https://doi.org/10.3892/mmr.2016.4810.

(56) Lin, M. K.; Yang, J.; Hsu, C. W.; Gore, A.; Bassuk, A. G.; Brown, L. M.; Colligan, R.; Sengillo, J. D.; Mahajan, V. B.; Tsang, S. H. HTRA1, an Age-related Macular Degeneration Protease, Processes Extracellular Matrix Proteins EFEMP1 and TSP1. *Aging Cell* **2018**, *17* (4), e12710. https://doi.org/10.1111/acel.12710.

(57) Liu, Y.; Lv, Z.; Xiao, T.; Zhang, X.; Ding, C.; Qin, B.; Xu, B.; Liu, Q. Functional and Expressional Analyses Reveal the Distinct Role of Complement Factor I in Regulating Complement System Activation during GCRV Infection in Ctenopharyngodon Idella. *Int J Mol Sci* **2022**, *23* (19), 11369. https://doi.org/10.3390/ijms231911369.

(58) Laurens, N.; Koolwijk, P.; Maat, M. P. M. D. Fibrin Structure and Wound Healing. *Journal of Thrombosis and Haemostasis* **2006**, *4* (5), 932–939. https://doi.org/10.1111/j.1538-7836.2006.01861.x.

(59) Bonnans, C.; Chou, J.; Werb, Z. Remodelling the Extracellular Matrix in Development and Disease. *Nat Rev Mol Cell Biol* **2014**, *15* (12), 786–801. https://doi.org/10.1038/nrm3904.

(60) Satyam, A.; Graef, E. R.; Lapchak, P. H.; Tsokos, M. G.; Lucca, J. J. D.; Tsokos, G. C. Complement and Coagulation Cascades in Trauma. *Acute Medicine & Surgery* **2019**, *6* (4), 329. https://doi.org/10.1002/ams2.426.

(61) Pflug, K. M.; Sitcheran, R. Targeting NF-κB-Inducing Kinase (NIK) in Immunity, Inflammation, and Cancer. *Int J Mol Sci* **2020**, *21* (22), 8470. https://doi.org/10.3390/ijms21228470.

(62) Liu, T.; Zhang, L.; Joo, D.; Sun, S.-C. NF-κB Signaling in Inflammation. *Sig Transduct Target Ther* **2017**, *2* (1), 17023. https://doi.org/10.1038/sigtrans.2017.23.

(63) Kamato, D.; Do, B. H.; Osman, N.; Ross, B. P.; Mohamed, R.; Xu, S.; Little, P. J. Smad Linker Region Phosphorylation Is a Signalling Pathway in Its Own Right and Not Only a Modulator of Canonical TGF-β Signalling. *Cell Mol Life Sci* **2019**, *77* (2), 243–251. https://doi.org/10.1007/s00018-019-03266-3.

(64) Zhang, Y. E. Non-Smad Pathways in TGF-β Signaling. *Cell Res* **2009**, *19* (1), 128–139. https://doi.org/10.1038/cr.2008.328.

(65) Loegering, D. J.; Lennartz, M. R. Protein Kinase C and Toll-Like Receptor Signaling. *Enzyme Res* **2011**, *2011*, 537821. https://doi.org/10.4061/2011/537821.

(66) Quatrana, A.; Petrillo, S.; Torda, C.; De Santis, E.; Bertini, E.; Piemonte, F. Redox Homeostasis and Inflammation in Fibroblasts of Patients with Friedreich Ataxia: A Possible Cross Talk. *Front Mol Neurosci* **2025**, *18*, 1571402. https://doi.org/10.3389/fnmol.2025.1571402.

(67) *PLA2G4A phospholipase A2 group IVA [Homo sapiens (human)] - Gene - NCBI*. https://www.ncbi.nlm.nih.gov/gene/5321 (accessed 2025-10-13).

(68) Heurich, M.; McCluskey, G. Complement and Coagulation Crosstalk – Factor H in the Spotlight. *Immunobiology* **2023**, *228* (6), 152707. https://doi.org/10.1016/j.imbio.2023.152707.

(69) Yurashevich, M.; Devinney, M.; Foster, M. W.; Myers, R.; O'Grady, N.; Ji, R.-R.; Habib, A. S.; Berger, M. Cerebrospinal Fluid Proteome of Patients with Persistent Pain and/or Postpartum

Depression after Elective Cesarean Delivery: An Exploratory Prospective Cohort Study. *Journal of Clinical Anesthesia* **2025**, *104*, 111855. https://doi.org/10.1016/j.jclinane.2025.111855.

(70) Heurich, M.; Föcking, M.; Mongan, D.; Cagney, G.; Cotter, D. R. Dysregulation of Complement and Coagulation Pathways: Emerging Mechanisms in the Development of Psychosis. *Mol Psychiatry* **2022**, *27* (1), 127–140. https://doi.org/10.1038/s41380-021-01197-9.

(71) Reichling, D. B.; Green, P. G.; Levine, J. D. The Fundamental Unit of Pain Is the Cell. *Pain* **2013**, *154 Suppl 1*, 10.1016/j.pain.2013.05.037. https://doi.org/10.1016/j.pain.2013.05.037.

(72) Soles, A.; Selimovic, A.; Sbrocco, K.; Ghannoum, F.; Hamel, K.; Moncada, E. L.; Gilliat, S.; Cvetanovic, M. Extracellular Matrix Regulation in Physiology and in Brain Disease. *Int J Mol Sci* **2023**, *24* (8), 7049. https://doi.org/10.3390/ijms24087049.

(73) Frey, H.; Schroeder, N.; Manon-Jensen, T.; Iozzo, R. V.; Schaefer, L. Biological Interplay between Proteoglycans and Their Innate Immune Receptors in Inflammation. *FEBS J* **2013**, *280* (10), 2165–2179. https://doi.org/10.1111/febs.12145.

(74) Fang, X.-X.; Zhai, M.-N.; Zhu, M.; He, C.; Wang, H.; Wang, J.; Zhang, Z.-J. Inflammation in Pathogenesis of Chronic Pain: Foe and Friend. *Mol Pain* **2023**, *19*, 17448069231178176. https://doi.org/10.1177/17448069231178176.

(75) Mancuso, E.; Spiga, R.; Rubino, M.; Averta, C.; Rotundo, S.; Segura-Garcìa, C.; Mannino, G. C.; Sesti, G.; Andreozzi, F. Effects of Alpha-2-HS-Glycoprotein on Cognitive and Emotional Assessment in Prediabetic and Diabetic Subjects. *Journal of Affective Disorders* **2021**, *282*, 700–706. https://doi.org/10.1016/j.jad.2020.12.135.

(76) Liu, X.; Gong, R.; Peng, L.; Zhao, J. Toll-like Receptor 4 Signaling Pathway in Sensory Neurons Mediates Remifentanil-Induced Postoperative Hyperalgesia via Transient Receptor Potential Ankyrin 1. *Mol Pain* **2023**, *19*, 17448069231158290. https://doi.org/10.1177/17448069231158290.

(77) Kunka, Á.; Lisztes, E.; Bohács, J.; Racskó, M.; Kelemen, B.; Kovalecz, G.; Tóth, E. D.; Hegedűs, C.; Bágyi, K.; Marincsák, R.; Tóth, B. I. TRPA1 Up-Regulation Mediates Oxidative Stress in a Pulpitis Model in Vitro. *British Journal of Pharmacology* **2024**, *181* (17), 3246–3262. https://doi.org/10.1111/bph.16386.

(78) Shih, R.-H.; Wang, C.-Y.; Yang, C.-M. NF-kappaB Signaling Pathways in Neurological Inflammation: A Mini Review. *Front Mol Neurosci* **2015**, *8*, 77. https://doi.org/10.3389/fnmol.2015.00077.

(79) Kanngiesser, M.; Häussler, A.; Myrczek, T.; Küsener, N.; Lim, H.-Y.; Geisslinger, G.; Niederberger, E.; Tegeder, I. Inhibitor Kappa B Kinase Beta Dependent Cytokine Upregulation in Nociceptive Neurons Contributes to Nociceptive Hypersensitivity After Sciatic Nerve Injury. *The Journal of Pain* **2012**, *13* (5), 485–497. https://doi.org/10.1016/j.jpain.2012.02.010.

(80) Michot, B.; Casey, S. M.; Lee, C. S.; Erdogan, O.; Basu, H.; Chiu, I.; Gibbs, J. L. Lipopolysaccharide-Induced TRPA1 Upregulation in Trigeminal Neurons Is Dependent on TLR4 and Vesicular Exocytosis. *J. Neurosci.* **2023**, *43* (40), 6731–6744. https://doi.org/10.1523/JNEUROSCI.0162-23.2023.

(81) Xing, F.; Zhang, W.; Wen, J.; Bai, L.; Gu, H.; Li, Z.; Zhang, J.; Tao, Y.-X.; Xu, J.-T. TLR4/NF-κB Signaling Activation in Plantar Tissue and Dorsal Root Ganglion Involves in the Development of Postoperative Pain. *Mol Pain* **2018**, *14*, 1744806918807050. https://doi.org/10.1177/1744806918807050.

(82) Troutman, T. D.; Bazan, J. F.; Pasare, C. Toll-like Receptors, Signaling Adapters and Regulation of the pro-Inflammatory Response by PI3K. *Cell Cycle* **2012**, *11* (19), 3559–3567. https://doi.org/10.4161/cc.21572.

(83) El-Zayat, S. R.; Sibaii, H.; Mannaa, F. A. Toll-like Receptors Activation, Signaling, and Targeting: An Overview. *Bulletin of the National Research Centre* **2019**, *43* (1), 187. https://doi.org/10.1186/s42269-019-0227-2.

(84) Smith, S. F.; Hosgood, S. A.; Nicholson, M. L. Ischemia-Reperfusion Injury in Renal Transplantation: 3 Key Signaling Pathways in Tubular Epithelial Cells. *Kidney International* **2019**, *95* (1), 50–56. https://doi.org/10.1016/j.kint.2018.10.009.

(85) Yu, H.; Lin, L.; Zhang, Z.; Zhang, H.; Hu, H. Targeting NF-κB Pathway for the Therapy of Diseases: Mechanism and Clinical Study. *Sig Transduct Target Ther* **2020**, *5* (1), 209. https://doi.org/10.1038/s41392-020-00312-6.

(86) Wang, W.; Huang, X.; Xin, H.-B.; Fu, M.; Xue, A.; Wu, Z.-H. TRAF Family Member-Associated NF-κB Activator (TANK) Inhibits Genotoxic Nuclear Factor κB Activation by Facilitating Deubiquitinase USP10-Dependent Deubiquitination of TRAF6 Ligase. *J Biol Chem* **2015**, *290* (21), 13372–13385. https://doi.org/10.1074/jbc.M115.643767.

(87) Deng, Z.; Fan, T.; Xiao, C.; Tian, H.; Zheng, Y.; Li, C.; He, J. TGF-β Signaling in Health, Disease and Therapeutics. *Sig Transduct Target Ther* **2024**, *9* (1), 61. https://doi.org/10.1038/s41392-024-01764-w.

(88) Lai, H. H.; Qiu, C.-S.; Crock, L. W.; Morales, M. E. P.; Ness, T. J.; Gereau, R. W. Activation of Spinal Extracellular Signal-Regulated Kinases (ERK) 1/2 Is Associated with the Development of Visceral Hyperalgesia of the Bladder. *PAIN* **2011**, *152* (9), 2117–2124. https://doi.org/10.1016/j.pain.2011.05.017.

(89) Kraev, K.; Geneva-Popova, M.; Hristov, B.; Uchikov, P.; Popova, S.; Kraeva, M.; Basheva-Kraeva, Y.; Sheytanov, I.; Petranova, T.; Stoyanova, N.; Atanassov, M. Exploring the Novel Dimension of Immune Interactions in Pain: JAK Inhibitors' Pleiotropic Potential. *Life (Basel)* **2023**, *13* (10), 1994. https://doi.org/10.3390/life13101994.

(90) Binshtok, A. M.; Wang, H.; Zimmermann, K.; Amaya, F.; Vardeh, D.; Shi, L.; Brenner, G. J.; Ji, R.-R.; Bean, B. P.; Woolf, C. J.; Samad, T. A. Nociceptors Are Interleukin-1β Sensors. *J Neurosci* **2008**, *28* (52), 14062–14073. https://doi.org/10.1523/JNEUROSCI.3795-08.2008.

(91) Hoffmann, A.; Cheng, G.; Baltimore, D. NF-κB: Master Regulator of Cellular Responses in Health and Disease. *Immun. Inflamm.* **2025**, *1* (1), 2. https://doi.org/10.1007/s44466-025-00014-0.

(92) Alvarez, S. E.; Harikumar, K. B.; Hait, N. C.; Allegood, J.; Strub, G. M.; Kim, E.; Maceyka, M.; Jiang, H.; Luo, C.; Kordula, T.; Milstien, S.; Spiegel, S. SPHINGOSINE-1-PHOSPHATE: A MISSING COFACTOR FOR THE E3 UBIQUITIN LIGASE TRAF2. *Nature* **2010**, *465* (7301), 1084–1088. https://doi.org/10.1038/nature09128.

(93) Yu, H.; Zhang, Z.; Li, G.; Feng, Y.; Xian, L.; Bakhsh, F.; Xu, D.; Xu, C.; Vong, T.; Wu, B.; Selaru, F. M.; Wan, F.; Donowitz, M.; Wong, G. W. Adipokine C1q/Tumor Necrosis Factor- Related Protein 3 (CTRP3) Attenuates Intestinal Inflammation Via Sirtuin 1/NF-κB Signaling. *Cell Mol Gastroenterol Hepatol* **2022**, *15* (4), 1000–1015. https://doi.org/10.1016/j.jcmgh.2022.12.013.

(94) Yao, K.; Dou, B.; Zhang, Y.; Chen, Z.; Li, Y.; Fan, Z.; Ma, Y.; Du, S.; Wang, J.; Xu, Z.; Liu, Y.; Lin, X.; Wang, S.; Guo, Y. Inflammation—the Role of TRPA1 Channel. *Front Physiol* **2023**, *14*, 1093925. https://doi.org/10.3389/fphys.2023.1093925.

(95) Shih, R.-H.; Wang, C.-Y.; Yang, C.-M. NF-kappaB Signaling Pathways in Neurological Inflammation: A Mini Review. *Front. Mol. Neurosci.* **2015**, *8*. https://doi.org/10.3389/fnmol.2015.00077.

(96) Fritzinger, D. C.; Benjamin, D. E. The Complement System in Neuropathic and Postoperative Pain. *Open Pain J* **2016**, *9*, 26–37. https://doi.org/10.2174/1876386301609010026.

(97) Franco-Enzástiga, Ú.; Inturi, N. N.; Natarajan, K.; Mwirigi, J. M.; Mazhar, K.; Schlachetzki, J. C. M.; Schumacher, M.; Price, T. J. Epigenomic Landscape of the Human Dorsal Root Ganglion: Sex Differences and Transcriptional Regulation of Nociceptive Genes. *bioRxiv* **2024**, 2024.03.27.587047. https://doi.org/10.1101/2024.03.27.587047.

(98) Xie, Z.; Feng, J.; Cai, T.; McCarthy, R.; Eschbach, M. D.; Wang, Y.; Zhao, Y.; Yi, Z.; Zang, K.; Yuan, Y.; Hu, X.; Li, F.; Liu, Q.; Das, A.; England, S. K.; Hu, H. Estrogen Metabolites Increase Nociceptor Hyperactivity in a Mouse Model of Uterine Pain. *JCI Insight 7* (10), e149107. https://doi.org/10.1172/jci.insight.149107.

(99) Gregus, A. M.; Levine, I. S.; Eddinger, K. A.; Yaksh, T. L.; Buczynski, M. W. Sex Differences in Neuroimmune and Glial Mechanisms of Pain. *Pain* **2021**, *162* (8), 2186–2200. https://doi.org/10.1097/j.pain.0000000000002215.

(100) Rostock, C.; Schrenk-Siemens, K.; Pohle, J.; Siemens, J. Human vs. Mouse Nociceptors – Similarities and Differences. *Neuroscience* **2018**, *387*, 13–27. https://doi.org/10.1016/j.neuroscience.2017.11.047.

(101) Lin, B.; Wang, Y.; Zhang, P.; Yuan, Y.; Zhang, Y.; Chen, G. Gut Microbiota Regulates Neuropathic Pain: Potential Mechanisms and Therapeutic Strategy. *J Headache Pain* **2020**, *21* (1), 103. https://doi.org/10.1186/s10194-020-01170-x.

(102) Cescon, M.; Gambarotta, G.; Calabrò, S.; Cicconetti, C.; Anselmi, F.; Kankowski, S.; Lang, L.; Basic, M.; Bleich, A.; Bolsega, S.; Steglich, M.; Oliviero, S.; Raimondo, S.; Bizzotto, D.; Haastert-Talini, K.; Ronchi, G. Gut Microbiota Depletion Delays Somatic Peripheral Nerve Development and Impairs Neuromuscular Junction Maturation. *Gut Microbes* **2024**, *16* (1), 2363015. https://doi.org/10.1080/19490976.2024.2363015.

(103) Park, E.-S.; Choi, S.; Shin, B.; Yu, J.; Yu, J.; Hwang, J.-M.; Yun, H.; Chung, Y.-H.; Choi, J.-S.; Choi, Y.; Rho, J. Tumor Necrosis Factor (TNF) Receptor-Associated Factor (TRAF)-Interacting Protein (TRIP) Negatively Regulates the TRAF2 Ubiquitin-Dependent Pathway by Suppressing the TRAF2-Sphingosine 1-Phosphate (S1P) Interaction*. *Journal of Biological Chemistry* **2015**, *290* (15), 9660–9673. https://doi.org/10.1074/jbc.M114.609685.

(104) Vallabhapurapu, S.; Matsuzawa, A.; Zhang, W.; Tseng, P.-H.; Keats, J. J.; Wang, H.; Vignali, D. A. A.; Bergsagel, P. L.; Karin, M. Non-Redundant and Complementary Functions of Adaptor Proteins TRAF2 and TRAF3 in a Ubiquitination Cascade That Activates NIK-Dependent Alternative NF-κB Signaling. *Nat Immunol* **2008**, *9* (12), 1364–1370. https://doi.org/10.1038/ni.1678.

Appendix

Supplementary Figures and Tables

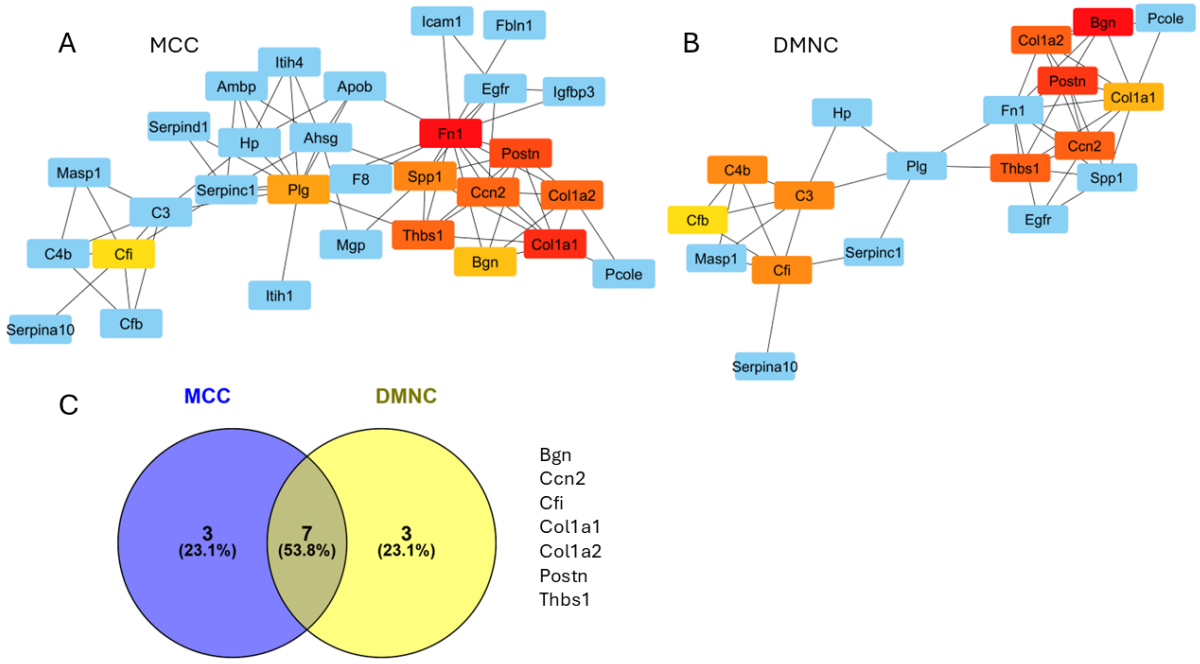

SFigure 1: Identifying ICAM-1 hub proteins. *The top 10 hub proteins were obtained using cytoHubba (v0.1) (A) MCC and (B) DMNC algorithm. (C) The results were then intersected in a Venn Diagram. Therefore, Bgn, Ccn2, Cfi, Col1a1, Col1a2, Postn and Thbs1 are referred to as hub proteins (Created using cytoHubba (v0.1) in Cytoscape (v3.10.3) https://cytoscape.org/ and VENNY 2.1.0 https://bioinfogp.cnb.csic.es/tools/venny/).*

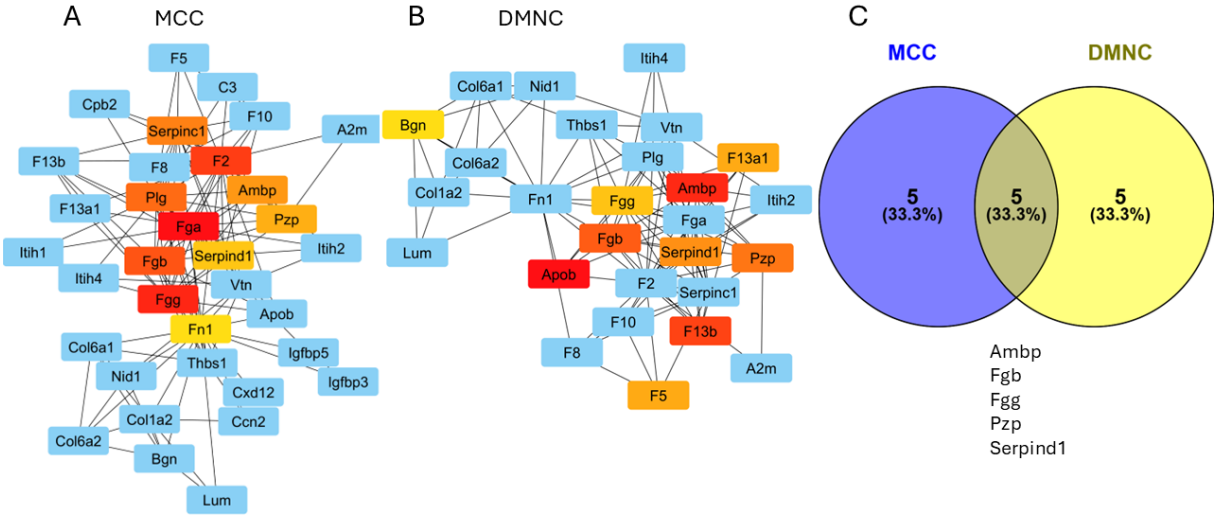

SFigure 2: Identifying IL-16 hub proteins. *The top 10 hub proteins were obtained using the cytoHubba (v0.1) (A) MCC and (B) DMNC algorithm. (C) The results were then intersected in a Venn Diagram. Ambp, Fgb, Fgg, Pzp and Serpind1 are referred to as hub proteins (Created using cytoHubba (v0.1) in Cytoscape (v3.10.3) https://cytoscape.org/ and VENNY 2.1.0 https://bioinfogp.cnb.csic.es/tools/venny/).*

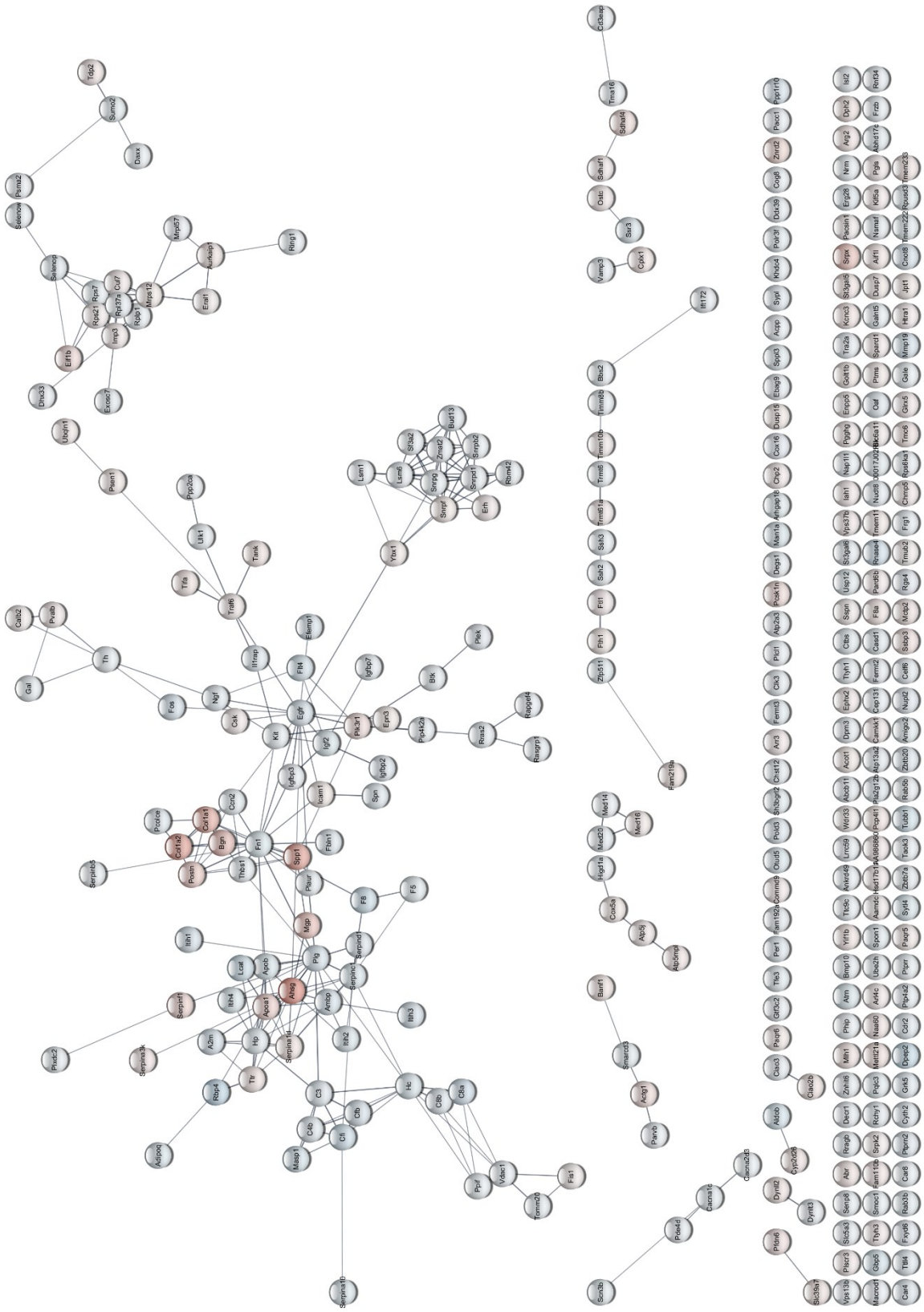

SFigure 3: complete ICAM-1 PPI network. *The network comprises 313 nodes (DEPs) with 281 edges (interactions). The nodes were continuously mapped based on log2 FC value to highlight the 112 upregulated (red) and 201 downregulated DEPs (blue). 156 DEPs are non-interacting singletons. All 313 DEPs were included in the functional enrichment analysis. (Created with Cytoscape (v3.10.3) https://cytoscape.org/)*

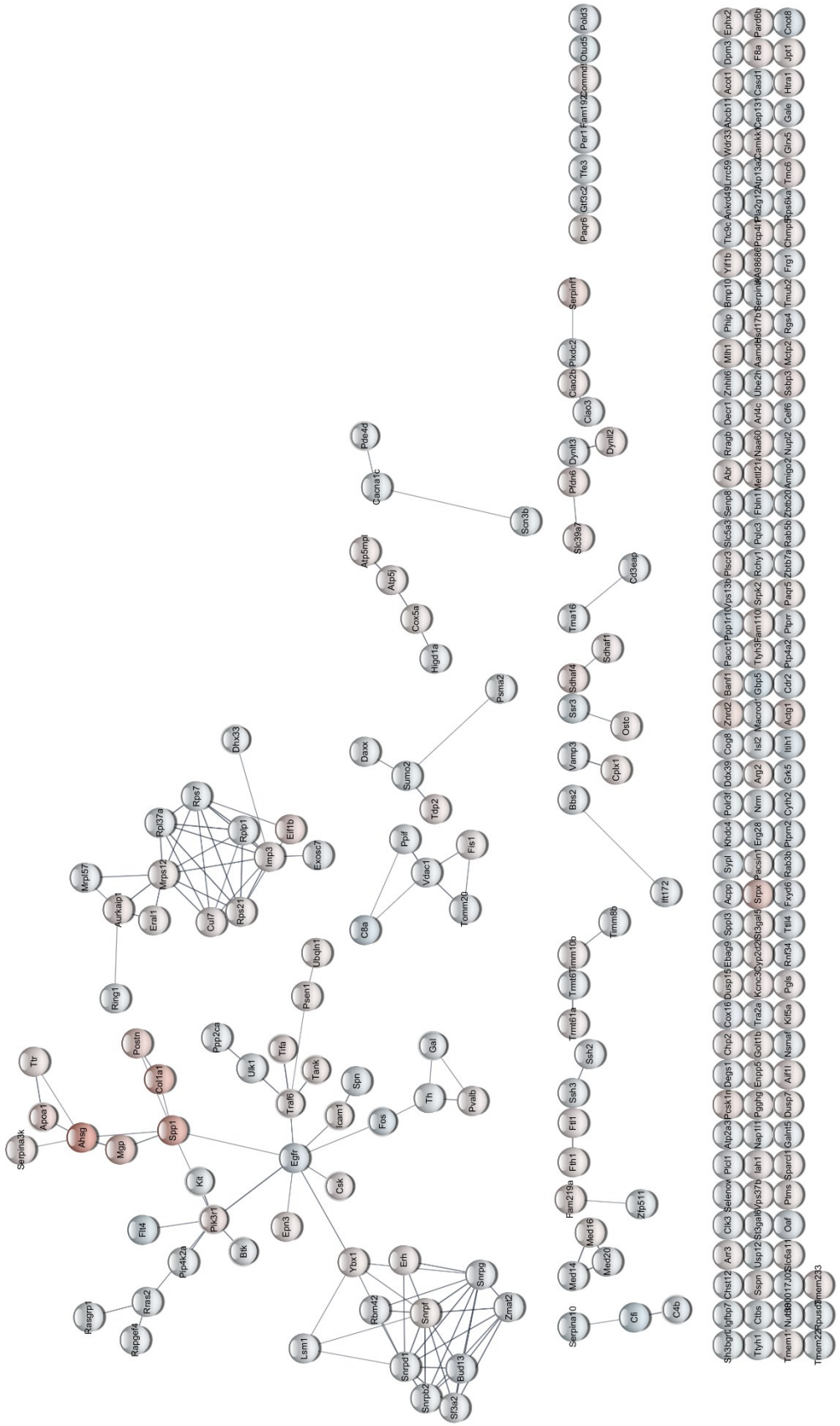

SFigure 4: complete PPI subnetwork ICAM-1-specific DEPs. *The network consists of 253 ICAM-1 specific DEPs (nodes) connected by 136 edges (interactions). The nodes were continuously mapped based on log2 FC value to highlight the 107 upregulated (red) and 146 downregulated DEPs (blue). 146 DEPs are non-interacting singletons. All 253 DEPs were included in the functional enrichment analysis. (Created with Cytoscape (v3.10.3) https://cytoscape.org/)*

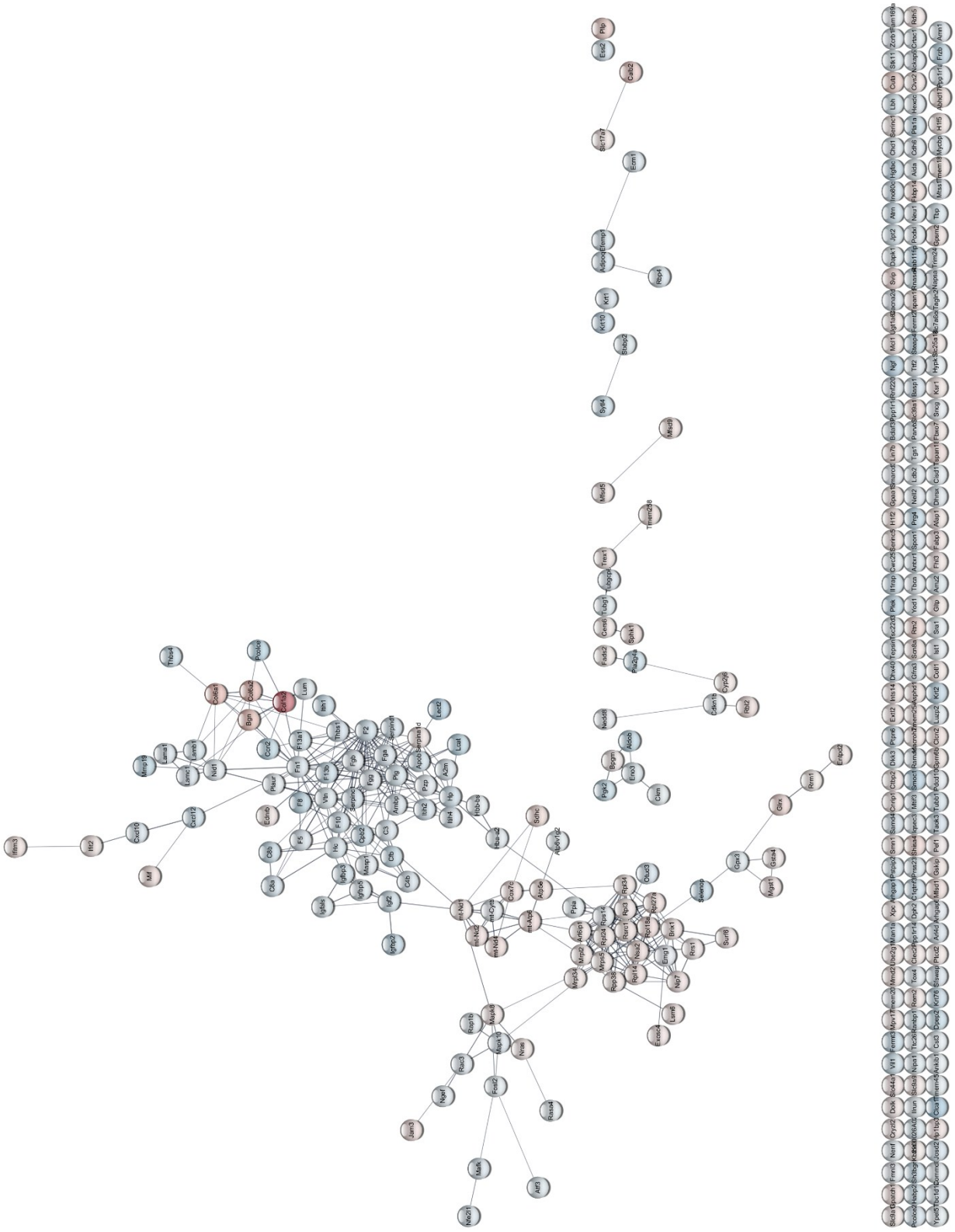

SFigure 5: complete IL-16 PPI network. *The network comprises 310 nodes (DEPs) and 378 edges (interactions). The nodes were continuously mapped based on log2 FC value to highlight the 114 upregulated (red) and 196 downregulated DEPs (blue). 169 DEPs are non-interacting singletons. All 310 DEPs were included in the functional enrichment analysis. (Created with Cytoscape (v3.10.3) https://cytoscape.org/)*

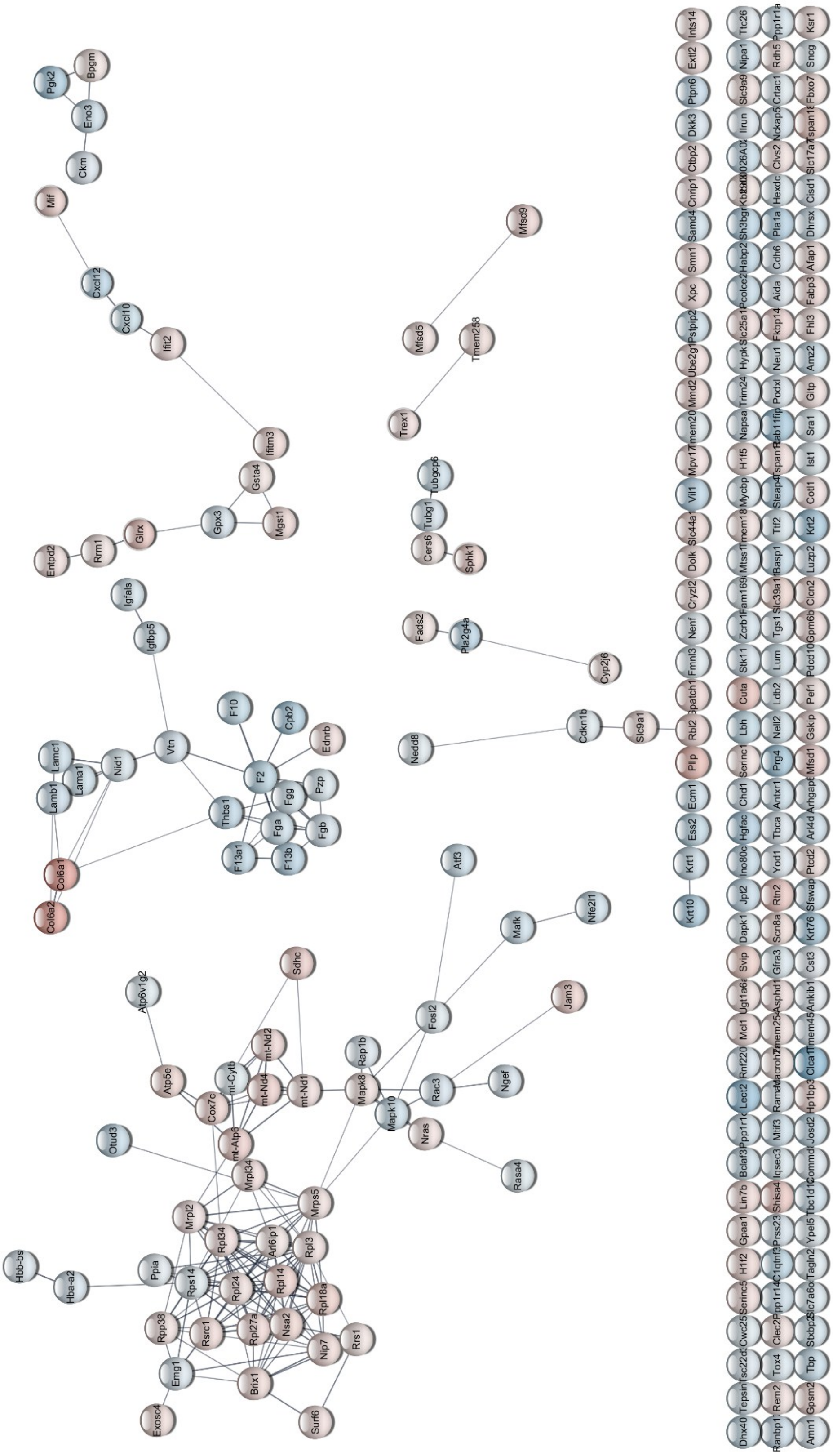

SFigure 6: complete PPI subnetwork IL-16-specific DEPs. *The network comprises 250 IL-16 specific DEPs (nodes) and 213 edges (interactions). To highlight the 108 upregulated (red) and 142 downregulated DEPs (blue), the nodes were continuously mapped based on log2 FC value. 154 DEPs are non-interacting singletons. All 250 DEPs were included in the functional enrichment analysis. (Created with Cytoscape (v3.10.3) https://cytoscape.org/)*

STable 1: ICAM-1 DEPs filtered

DEPs	logFC	AveExpr	t	P.Value	adj.P.Val	B
Dnajb6;Dnajb7	0.564145940421843	15.8423555417914	8.58619802833213	2.16775908375082e-05	0.124886585894138	2.3658748984433
Postn	0.886048702841734	15.1551880702409	7.85123311713671	4.21638864285728e-05	0.124886585894138	1.9417539769533
C5	-0.515650927214946	16.7083458288503	-7.49705014501748	5.91444602496545e-05	0.124886585894138	1.71547021396362
Ahsg	2.27500610111288	19.8538396230245	7.43282854397785	6.29706723278146e-05	0.124886585894138	1.67279361747829
Cplx1	0.324634134269235	18.0685738210603	7.10215588337055	8.75438668772962e-05	0.138897099187518	1.44465459243421
Klc1;Klc2;Klc4	-0.312346840630319	17.6741843957118	-6.56087033191548	0.00015400548706673	0.171965713398367	1.03897649557619
Lcat	-0.749390366358334	16.4682958240709	-6.30113240343375	0.00020438412852671	0.180153254622489	0.829086508837857
Gbp5	-0.645427385471999	13.1469256361452	-8.17793439246914	0.00014579785832364	0.171965713398367	0.824628054809414
Camk2a;Camk2b; Camk2d	-0.635062665127602	18.3890305819858	-6.02073823760012	0.00027998680944461	0.22211353593241	0.590713676543496
Pvalb	0.266864547689913	19.2294521351336	5.89525311425122	0.00032337276934905	0.233210561749642	0.479925103539816
Ppp1cb;Ppp1cc	-0.748659815328697	15.9649569150816	-9.4334181252953	0.00017341808990129	0.171965713398367	0.418916176369605
Lmnb1;Lmnb2	-0.439937013777079	14.8800299543831	-6.07537068581736	0.00043934686014041	0.288066796790719	0.215909563736813
Frg1	-0.279592818532986	15.2692495747853	-5.57388805459074	0.00047206206457574	0.288066796790719	0.184185495529297
Actb;Actbl2;Actg1	-0.449042016620464	21.4068313330767	-5.3719581005489	0.00060299525491184	0.320653564376559	-0.0107429968252779
Pcolce	-0.400409603630052	15.4062454591026	-5.28685417477466	0.00066965411828108	0.320653564376559	-0.0950520149039331
Decr1	-0.244237775019048	18.7473253944489	-5.18327358290949	0.00076184428587279	0.320653564376559	-0.199413864872722
Sytl4	-0.514680304139928	15.4571874749734	-6.09091926402242	0.00076553336015944	0.320653564376559	-0.24141794387617
Pfdn6	0.445662759094001	15.6319062475919	5.08892196218107	0.00085795170223662	0.320653564376559	-0.296162946125721
Pcsk1n	0.544924866620882	17.5117324832456	5.06205724291768	0.00088767582909054	0.320653564376559	-0.324006127781265
Tuba1a;Tuba1b; Tuba3a;Tuba4a	-0.718755854074804	20.5569701451212	-5.34936310166685	0.00095042303209101	0.320653564376559	-0.373949660495644
Tubb1;Tubb2a;Tubb2b; Tubb4b;Tubb5;Tubb6	-0.337114536387482	21.1214612769579	-4.95997118118551	0.00101127946867575	0.320653564376559	-0.431012949239324
Prkca;Prkcg	0.282501238390857	17.4256615107239	4.93356631908551	0.00104621541522793	0.320653564376559	-0.459001602861988
Sf3a2	-0.213156708428873	16.391865162664	-4.88129386454016	0.00111930829768699	0.320653564376559	-0.514787788556098
Smarcd3	-0.348049195649319	14.0851758777082	-4.87360817622307	0.00113051523395065	0.320653564376559	-0.523032566600871
Rps6ka1;Rps6ka2; Rps6ka3;Rps6ka6	0.557797592441048	15.2068678383979	5.66547203601555	0.00113203905554352	0.320653564376559	-0.525785768384822

F8	-0.763017087221177	15.0961942450231	-5.66142276047509	0.00113637695162599	0.320653564376559	-0.528623152283588
Eci2;Eci3	0.336644875821037	18.5822660495362	4.84573912876495	0.00117218623054585	0.320653564376559	-0.553020359544504
Tln1;Tln2	-0.240620727878419	18.5816381225256	-4.76952806629091	0.00129489775265046	0.328797050398335	-0.635758445414195
Aldob	-0.576614441403981	16.540980194451	-4.68843001012212	0.0014409565291983	0.328797050398335	-0.72498359085425
Atp2a3	-0.271810701357071	14.2698702495837	-4.68657748585176	0.00144449494131341	0.328797050398335	-0.72703601389923
Mat1a;Mat2a	-0.610153783016973	17.6645545402801	-5.37964409490505	0.00149017486010872	0.328797050398335	-0.732432250778829
Wdr33	0.242243590261653	14.9108442907275	4.67312656395721	0.00147047094398362	0.328797050398335	-0.741957474867905
Ambp	-0.563940065704099	20.9960981892996	-4.66213014537209	0.00149208292125804	0.328797050398335	-0.754181040560887
Hbb-b1;Hbb-b2;Hbb-y	-0.626102671068793	20.3742134109864	-4.92033400979567	0.00154928945378356	0.330003417111618	-0.764669859642319
Snrpg	-0.292027182809093	17.1012085133881	-4.60776281435339	0.00160411097038087	0.330003417111618	-0.814945387718758
Col1a2	1.89324388453312	21.0055837307324	4.59929988949396	0.00162235387209796	0.330003417111618	-0.824453450670444
F8a1	0.351193399813578	14.571933434245	4.82579475016875	0.00173140291059227	0.335005348529963	-0.855225816107878
C4b	-0.431208971052815	20.3291315617107	-4.55628561991001	0.00171861319962774	0.335005348529963	-0.872985378793837
Cpne2;Cpne3;Cpne4; Cpne5;Cpne6;Cpne7; Cpne8;Cpne9	0.454181553254543	20.123480166318	4.78020019859463	0.0018275707757541	0.34519330866803	-0.899486752206841
Aurkaip1	0.419970638206376	14.7299763104266	5.1100396633262	0.00194954426866287	0.352987429939426	-0.939611572305589
Dmd;Drp2	-0.377974494524556	16.2913085252764	-5.18285516446311	0.00114543939473071	0.320653564376559	-0.954734398353846
Fgfr1;Fgfr2;Fgfr3;Fgfr4	0.588235246244935	14.1266675148925	5.64352854915714	0.00207125412764433	0.352987429939426	-1.01216542961696
Fbln1	-0.429721433069977	15.154205082033	-4.65836852683776	0.00211467335824825	0.352987429939426	-1.01964479920883
Ppp2r1a;Ppp2r1b	-0.297590092866209	19.2731422499937	-4.42008657349663	0.00206642701793953	0.352987429939426	-1.02891934937217
Tubb4a;Tubb4b;Tubb5	-0.593039045103652	18.8569384017964	-4.3958917342124	0.00213581200517994	0.352987429939426	-1.05697925829801
Fam219a	0.387416486319831	14.4473905038075	5.54306716017705	0.00224946379569022	0.353021418491719	-1.07076587563284
Srpx	1.1532026747691	13.4931604979439	7.07960665709296	0.00071074107115231	0.320653564376559	-1.09628516800224
Col1a1	1.58722772610803	20.5893377098793	4.35157116057309	0.00226951876252082	0.353021418491719	-1.10866027931871
Krt1;Krt2;Krt5;Krt6a; Krt6b;Krt75;Krt77; Krt79;Krt8	-0.909517200809454	17.9811251787016	-4.53584728489286	0.00245424798169078	0.36894602678963	-1.14327665614716
Tmem222	-0.32683876473577	14.2148198630479	-4.27081775041841	0.00253690759299462	0.372690517319007	-1.20375423104085
Serpina3k	0.379059237846821	14.5112253977932	4.78264509703647	0.00273698366577571	0.38375045486388	-1.20807655493665
Plscr3	0.250935255329471	15.9310464856782	4.2148754443033	0.00274193790225552	0.38375045486388	-1.27033158778264

Dpep2	-0.856592152993965	12.7394341236059	-5.18813186851894	0.00303901890181355	0.38375045486388	-1.28983558427659
Cdr2	-0.407254208665968	13.6653392975889	-4.67351925503753	0.0030747407826455	0.38375045486388	-1.301831694903
Nap1l1	-0.200025071315885	19.4959054543461	-4.18689231706849	0.00285112354369971	0.38375045486388	-1.3038485763991
Cul7;Cul9	0.274048279170447	14.5336093890858	4.66991233939103	0.00308667796651078	0.38375045486388	-1.30496780290662
Serpina10	-0.455950647911925	16.2737261575673	-6.32546961261431	0.00121649654660278	0.321682236806663	-1.31405083465944
Cacna1c	-0.322823194502698	13.9326870669534	-4.36020373745261	0.00305008310178212	0.38375045486388	-1.32543691655124
Serpinf1	0.73347906235297	18.0344274560332	4.14881414967174	0.0030072680354574	0.38375045486388	-1.3496852312076
Sypl1	-0.402105797070405	16.6935995121546	-4.12574933360234	0.00310629717456868	0.38375045486388	-1.3775770441699
Fermt3	-0.328157839761943	16.4743899211473	-4.11710566600861	0.00314430600859098	0.38375045486388	-1.38805435976846
Apoa1	0.822282806550103	16.6967387458724	4.07913948042716	0.00331726616363382	0.388909245577286	-1.43423358500163
Spp1	1.87615942511339	17.1790784636084	4.07565419143657	0.00333364788847289	0.388909245577286	-1.43848577636835
Tuba1a;Tuba1b; Tuba1c;Tuba3a	-0.227430683209064	23.141188281719	-4.03952819775069	0.00350865201005665	0.403393281098252	-1.48268864445452
Sdhaf4	0.567652076719355	14.0420611522373	4.45443788678215	0.00390381192522404	0.430124166705588	-1.49669933616754
Rac1;Rac2	0.361316616644366	18.2111406264505	4.00511876129036	0.00368452240918768	0.417561661029797	-1.52500688892818
Ngf	-0.419394980885439	19.5073357569342	-3.98808038424918	0.00377508204705913	0.421798956046761	-1.54603893834816
Snrpa;Snrpb2	-0.299585518094034	17.0565942412331	-4.11768781587284	0.0041488124915045	0.439776779369679	-1.58652532676018
Wnk1;Wnk2;Wnk4	0.687727132757905	13.5700334600194	5.55379689476145	0.00222960160660189	0.353021418491719	-1.59375785560282
Rapgef3;Rapgef4	0.352331176184348	14.3688042779086	4.33250120397068	0.00447205757757515	0.441126963646278	-1.60906779001305
Htra1	0.239245160948901	18.5889595250427	3.93660562225684	0.00406344538454301	0.439776779369679	-1.60988872888725
Ssbp3	0.441464255281932	13.0237419358398	4.70507597983118	0.00469119223079356	0.441126963646278	-1.62040365979481
Bgn	1.27683633191426	16.4973892805451	3.92061928543981	0.00415772828094365	0.439776779369679	-1.62981248699949
Serpina1a;Serpina1b; Serpina1c;Serpina1d	0.612202884482738	15.6949149945232	5.43331701575491	0.0024649110575886	0.36894602678963	-1.64364954690578
Krt2;Krt4;Krt5;Krt6a; Krt6b;Krt73;Krt75; Krt76;Nefh	-0.298643667097839	19.8304353035365	-3.89301673865346	0.00432606909159937	0.441126963646278	-1.6643178134639
Zbtb20	-0.361170504502024	13.1569486187104	-4.24743633609517	0.00492316778287834	0.441126963646278	-1.68913499459344
Rap1a;Rap1b	-0.200590936073905	19.7681356347146	-3.85941079010497	0.00454091260907523	0.441126963646278	-1.7065050633311
Rab5b	-0.230544227159214	17.8852678669006	-3.8573336336514	0.00455456057054632	0.441126963646278	-1.70911897448741
Grk5	-0.409817438044501	14.1067954698458	-4.58123293889384	0.00526926474217677	0.444692310634982	-1.71160453445731

Prpsap1;Prpsap2	0.222815002765902	17.8547724498333	3.85099687989159	0.00459646746517119	0.441126963646278	-1.71709775081591
Lrrc59	-0.252870298741136	20.5384356919997	-3.84736339674775	0.00462068229962346	0.441126963646278	-1.72167585635974
Arr3	0.273393761029833	16.209553592617	4.20975704808541	0.0051390371639463	0.441126963646278	-1.72504376969561
Plcl1	-0.214697634964168	14.9478280176337	-3.84199449451796	0.0046567121302225	0.441126963646278	-1.7284446666213
Dmxl1;Dmxl2	0.523162853384729	14.5757277304818	5.15219840146027	0.00313560690470736	0.38375045486388	-1.7674773574064
Tubb2a;Tubb2b;Tubb4a Tubb4b;Tubb5	-0.402010973006085	19.8554236368326	-3.79763905836283	0.00496609581076789	0.441126963646278	-1.78455241816476
Serpina1d	0.382857618543834	13.4950030410741	4.48218147168054	0.0057911951107231	0.449730993530606	-1.78653313966402
Apob	-0.493740767135115	18.258807035865	-3.77385751492023	0.00514093579105959	0.441126963646278	-1.81477140929272
Efemp1	-0.557344985560306	15.7859648890809	-3.76980055583584	0.00517141152390065	0.441126963646278	-1.81993598396588
Snap23;Snap25	0.295459313137783	19.9053589222488	3.74762358278977	0.00534144060341604	0.44603840323052	-1.84821596765272
Gal	-0.250164355332675	15.4459040280168	-4.03147653387095	0.00631424625988458	0.449730993530606	-1.89865598832091
Rab3b	-0.336544674928424	15.065651055636	-3.69476776317421	0.00577113913047512	0.449730993530606	-1.91594408142357
Iah1	0.256045210788116	16.5665390396345	3.69468238937423	0.00577186221528594	0.449730993530606	-1.91605384619766
Plek	-0.3587643645448	19.8849181402567	-3.67272979128233	0.00596102789906265	0.449730993530606	-1.94431734697674
Arhgap18	-0.375733373272976	15.8347627199237	-3.96371648358586	0.00683697472516454	0.449730993530606	-1.96625255774626
Golt1b	0.307153881295207	17.7232110326017	3.7766110734091	0.00649091514864793	0.449730993530606	-1.97236237762311
Thbs1	-0.268778708058406	18.2057665743179	-3.64935216570283	0.00616973698287571	0.449730993530606	-1.97450074490019
Dph2	0.389098480518008	15.5059962827833	4.68689126914147	0.00477130760840455	0.441126963646278	-1.99742802498946
Srpk2	0.20028136132775	15.7168215709406	3.62745224113102	0.0063723031025658	0.449730993530606	-2.00285525928461
Ostc	0.27055180971302	18.0309592898714	3.6217022774148	0.00642665011269605	0.449730993530606	-2.01031249500299
Glrx5	0.251832151365704	16.9674750161204	3.61956489841437	0.0064469772254511	0.449730993530606	-2.01308583000634
Man1a1	-0.528632998269931	14.5468471502186	-4.63031833760944	0.00503083084622077	0.441126963646278	-2.02768767819701
Exosc7	-0.318900574885111	15.1319524569521	-3.59585808540704	0.0066770659849008	0.449730993530606	-2.04389441564517
Degs1	-0.292912284812431	18.3704345150587	-3.59196406485621	0.00671568520424933	0.449730993530606	-2.04896334591381
Dynlt3	-0.321623813347351	17.826490753037	-3.59030680740102	0.00673219295481666	0.449730993530606	-2.05112134860687
Igfbp3	-0.2027031549102	17.4152192754973	-3.58406373225664	0.00679476683570291	0.449730993530606	-2.05925461379861
Tfe3	-0.342399477251146	14.3395175743409	-3.86096513493476	0.00772368766898904	0.449730993530606	-2.07045016361231
Tmc6	0.419966333436701	12.4874418439399	4.12670412510797	0.00822113150279032	0.449730993530606	-2.0704520264649
Ptms	0.292101834960125	19.391137626456	3.57252259874562	0.0069120717546292	0.449730993530606	-2.07430588353109
Fos	-0.598190651578633	12.9079595205777	-4.11731771287102	0.00829960315810582	0.449730993530606	-2.0782747418669

Hsd17b11	0.213000843873751	19.6857492219341	3.56881271842879	0.00695023357783295	0.449730993530606	-2.07914845317569
Efr3a;Efr3b	-0.26455481863275	13.8701992320911	-3.56468976643867	0.00699290654666419	0.449730993530606	-2.08453269384079
Cnot8	-0.605113967162863	14.085837823043	-4.51245973047179	0.00562557915062456	0.449730993530606	-2.09243059306305
Map1a;Map1b	0.927323135804613	19.8087862945574	3.5489124444359	0.00715878431480003	0.449730993530606	-2.10516062926933
Eno1;Eno2	-0.207259801694516	21.2885390860629	-3.54860061389331	0.0071621044994919	0.449730993530606	-2.10556871241381
Slc5a3	-0.273370999129661	14.347959262355	-3.65678763083913	0.00762736220736666	0.449730993530606	-2.11295764784801
Med16	0.280287826199329	13.9482134425439	3.81900390011748	0.0081218394937157	0.449730993530606	-2.11358831432095
Epn3	0.285311501888334	14.1552371000292	3.53873648540287	0.0072679779234768	0.449730993530606	-2.11848522177637
Myh1;Myh10;Myh11; Myh14;Myh3;Myh4; Myh6;Myh7;Myh7b; Myh8;Myh9	-0.536497164067764	15.9039437892418	-3.81248091145691	0.0081857488025484	0.449730993530606	-2.12032473443016
Nrm	-0.283529403352148	16.262480554061	-4.00140880290909	0.00654051374837643	0.449730993530606	-2.12939072662458
Mmp19	-0.588427552832236	17.9985912650735	-3.51955430921485	0.00747863598333452	0.449730993530606	-2.14364528818689
Fth1	0.279276726737145	18.3879009687541	3.49642244742947	0.0077412953504697	0.449730993530606	-2.17405920786807
Epb41l1;Epb41l2; Epb41l3	-0.255406745906832	15.3145723450018	-3.99832079938765	0.00937248711329111	0.449730993530606	-2.17893194153754
Selenow	-0.234347919658205	14.8673442114473	-3.74758276987329	0.00885278118871925	0.449730993530606	-2.18779203431607
Znhit6	-0.296973666184426	13.5206206115445	-3.74043702347749	0.00892982325490648	0.449730993530606	-2.19527007740004
F5	-0.334796557384884	19.3966136633167	-3.47670259391024	0.0079729149106898	0.449730993530606	-2.20004956144845
Ppp1ca;Ppp1cc	-0.569237250592797	15.9401781971348	-3.72008299856336	0.00915335813724887	0.449730993530606	-2.21662421767032
Macrod1	-0.20369288942905	17.5390963660183	-3.46094118461883	0.00816330375308599	0.449730993530606	-2.22086371290642
Dysf;Myof	-0.334151288105117	15.0461403739618	-3.87775595151728	0.00757046133326151	0.449730993530606	-2.22884500247013
Abhd16a;Abhd16b	-0.293948574589978	15.1347546461188	-3.7059511454736	0.00931218987045429	0.449730993530606	-2.2314970631071
Rpl37a	-0.256515243483619	19.3235074495418	-3.43472367465397	0.00849070905949579	0.449730993530606	-2.2555655441816
Atp13a2	-0.320457291478368	15.2806413567538	-3.43449754490265	0.0084935925334548	0.449730993530606	-2.25586528113343
Dusp15	0.275357608800951	14.5339331530317	3.41551941857081	0.00873931138735222	0.449730993530606	-2.28104683252344
Tubb2a;Tubb2b	-0.224372148555677	21.3608137388991	-3.40755945990916	0.00884459463766342	0.449730993530606	-2.29162381794097
Igf2	-0.522608630739366	17.4374975460528	-3.50734847220108	0.00935473203526341	0.449730993530606	-2.29183522932657
Dynll2	0.375726114897585	19.3411600260163	3.40603631004288	0.00886489274933944	0.449730993530606	-2.29364875294857
Tubb1	-0.614864569940522	17.9177574260952	-3.50550917620307	0.00937845278315176	0.449730993530606	-2.29406066105725

Commd9	0.2162690779033	15.3086319563079	3.40428511140305	0.00888829064500806	0.449730993530606	-2.29597726611888
Usp15;Usp4	-0.295333093283094	16.8403080217619	-3.50057937811868	0.00944235005394738	0.449730993530606	-2.30002821092566
Selenop	-0.395053022948733	18.0353306478786	-3.39975820130391	0.00894907723677233	0.449730993530606	-2.30199853962179
Msn;Rdx	-0.447679802381387	20.0536425067674	-3.39747584866664	0.00897989031634886	0.449730993530606	-2.30503539553925
Paqr6	0.285037902935354	14.5886918829751	3.63652690530271	0.0101379183465973	0.454373481602013	-2.30511437866749
Snrpb2	-0.207140729494149	17.1030929055396	-3.38608299875645	0.00913538144712983	0.449730993530606	-2.3202053246937
Sumo2	-0.343546880464135	16.3006523726557	-3.38601806039092	0.00913627582324813	0.449730993530606	-2.32029184360488
Aamdc	0.203944290224543	15.6747578146178	3.38439001715654	0.00915872853947788	0.449730993530606	-2.32246111402028
Acp3	-0.214143715393963	17.7540440223386	-3.37087435328291	0.00934738584924314	0.449730993530606	-2.34048399779601
Igfbp2	-0.470703490826352	15.0564038012796	-3.36965774941157	0.00936456737004593	0.449730993530606	-2.34210754333692
Fn1	-0.449313316299069	19.4234461848478	-3.36120401380844	0.00948487770534707	0.449730993530606	-2.3533945335488
Pgls	0.271058963364919	16.6710389856628	3.36098468841602	0.00948802063559815	0.449730993530606	-2.35368749465192
Rbm42	-0.257039328297783	14.868457862941	-3.35847133539254	0.00952411533003173	0.449730993530606	-2.35704513915269
Sspn	0.244124736537724	15.5291132052616	3.45190818288032	0.0100989020807547	0.454373481602013	-2.35916287033421
Serpinc1	-0.459368749704492	21.3907133561243	-3.35017200684952	0.00964433363853186	0.450049992673372	-2.36813845876441
Rasgrp1	-0.245606515358876	13.616932438676	-3.57307278995877	0.0109635973563509	0.463720865247261	-2.37319996469416
Celf1;Celf2	-0.700524442920148	14.1308250966723	-3.68077870551955	0.00960269590445641	0.450049992673372	-2.39361104594119
Abhd17c	-0.323236026831932	13.7515311077114	-3.72934268249835	0.0124344613891291	0.471150163358832	-2.41672253084995
Kcnc3	0.328144659226766	14.0267284991181	3.71800513481521	0.012586587224012	0.471150163358832	-2.42706120683566
Atp12a;Atp1a1;Atp1a2;Atp1a3;Atp1a4	-0.365331755874767	21.310946404351	-3.28698123156981	0.0106136890302397	0.463720865247261	-2.4529018966807
Nudt8	-0.294497926871827	13.9080788308469	-3.37439061793331	0.0112478019940316	0.466907013967062	-2.45414822471843
Rufy1;Rufy2;Rufy3	0.208149059485098	19.5800298531208	3.28326283556175	0.010673829197879	0.463720865247261	-2.45790586498649
Myh10;Myh14	0.420881281260518	15.9951153370653	3.28149649841927	0.0107025226375862	0.463720865247261	-2.46028349996476
Sec23a;Sec23b	-0.223542818391319	16.9109157735243	-3.59470975909716	0.0106740210400758	0.463720865247261	-2.46806219756083
Dock7;Dock8	0.325632160095735	14.5160618850347	3.65354911142699	0.0134926263536374	0.472486756973814	-2.48632613100128
Itih1	-0.589597910642382	19.8455557935817	-3.26136193733866	0.0110353823249057	0.463720865247261	-2.48741413428517
C8b	-0.421884165916962	15.4361244605307	-3.34277720948863	0.0117558570160324	0.469201648979715	-2.49316210953403
Tifa	0.42276612912797	13.7585340190505	3.64515179451163	0.0136160191950871	0.472486756973814	-2.49410825047131
Sh3bgrl2	-0.32528315638397	15.7415656783955	-3.23926017727293	0.0114133011053526	0.469128070822602	-2.51725369469242
Ca8	-0.228784271825754	13.8818014911322	-3.43426894258798	0.0130396306778097	0.471150163358832	-2.52475877164895

Atrn	-0.517098782065549	16.6827415425689	-3.22822721940235	0.011607008603725	0.469201648979715	-2.53217168812591
Rchy1	-0.313061672826366	13.5926990759785	-3.60250710415008	0.0142627153200573	0.473104836165745	-2.53384618087955
Galnt5	-0.206010232766703	15.2348280301684	-3.22696590865251	0.0116293720994923	0.469201648979715	-2.53387808424961
Phip	-0.224660344686148	14.398734081188	-3.22169040368298	0.0117233991831016	0.469201648979715	-2.54101726273596
Parvb	-0.219017971165322	17.0373149700043	-3.2190813750647	0.0117701948085712	0.469201648979715	-2.54454921677746
Usp12	-0.33511787236692	13.9212292909875	-3.48172655758389	0.0122849335918161	0.471150163358832	-2.56806067924759
Itih2	-0.463599073699807	20.5284492320971	-3.19925691146999	0.0121322209097924	0.471150163358832	-2.57141291260915
Cep131	-0.237244181278516	14.4571325853976	-3.27906326389009	0.0128558765722618	0.471150163358832	-2.57226453851038
Serpina1a;Serpina1b; Serpina1c;Serpina1d; Serpina1e	0.430007107974321	15.2688871054692	3.27019364929401	0.0130175224616516	0.471150163358832	-2.58332563113348
Slc66a3	-0.325436760635428	14.5695774252535	-3.37301378555771	0.0140897641685098	0.473104836165745	-2.59276834088027
Tomm20	-0.317591272836857	17.8338875106811	-3.18235893203897	0.0124500052865509	0.471150163358832	-2.59434742014182
Ccn2	-0.32420778477228	18.6614465598705	-3.16873422901881	0.0127125694114601	0.471150163358832	-2.61286329738303
Rnase4	-0.661627802710637	16.7599921787551	-3.26755340852282	0.0130660577258216	0.471150163358832	-2.62675799843875
Ftl1	0.258739089791565	18.1943103899	3.15628088140195	0.0129576261201719	0.471150163358832	-2.62980573047787
Sparcl1	0.213534343256249	15.5267506068995	3.1547344515993	0.0129883995593376	0.471150163358832	-2.63191082012069
H2ac11;H2ac12;H2ac1 H2ac15;H2ac20;H2ac21; H2ac25;H2ac4;H2ac6; H2ac7;H2ac8;H2aj;H2ax; H2az1;H2az2;Hist1h2af; Hist1h2an;Hist1h2ao; Hist1h2ap;Hist2h2aa1	-0.208276953161707	23.9504756989794	-3.23121439495131	0.01375403753154	0.472486756973814	-2.63207534875449
Per1	-0.445053783191801	13.2603861354218	-3.48016657910794	0.0163193518205791	0.479636028744591	-2.64986240588997
Traf6	0.314022324652361	13.0138968058351	3.47815875991182	0.0163557903436227	0.479636028744591	-2.65179131105965
Cfi	-0.784147489461649	16.4095566340804	-3.38855580214486	0.0138148316006391	0.472486756973814	-2.65244836873505
Aldoa;Aldoc	-0.214255442769232	18.7513996999985	-3.13768867679018	0.0133327088411048	0.472486756973814	-2.65513208118553
Tppp2;Tppp3	-0.482216126245167	16.253815825678	-3.20308721515033	0.0143130165989889	0.473104836165745	-2.66739184247142
Frzb	-0.245525931959051	16.0175118626403	-3.12838556835741	0.013524631485708	0.472486756973814	-2.66781903233537
C3	-0.441011730331422	21.6784407235968	-3.12751350770101	0.0135427693063445	0.472486756973814	-2.66900877064619

Rab13;Rab3a;Rab3b;Rab3c;Rab3d;Rab8a;Rab8b	0.310756166145644	17.413028876572	3.12284230531527	0.0136403579300939	0.472486756973814	-2.6753830113162
Fyn;Hck;Lyn;Src;Yes1	0.209847050405067	15.8068080404362	3.44976510437724	0.0168810326476804	0.486547593667135	-2.67915479836976
Yif1b	0.320974236965117	14.96478494242	3.11842131112704	0.0137333954445276	0.472486756973814	-2.68141797783081
Dnm1;Dnm2	0.245645727662129	18.6116747676911	3.11443559574691	0.0138178403653	0.472486756973814	-2.68686054502319
Cfb	-0.590685067784005	19.2785578104133	-3.10364984675204	0.014049084178383	0.473104836165745	-2.70159710711448
Lsm6	-0.260364105717336	15.6381210085295	-3.10139213097635	0.0140979978453486	0.473104836165745	-2.70468336825031
Ptprn2	-0.425785676761745	14.2562677083943	-3.27132777741772	0.016042893196197	0.477624045768555	-2.70715010836418
Znf511	-0.337478141025565	13.0310057342559	-3.41927537570443	0.0174663189337378	0.486547593667135	-2.70871650419147
Arg2	0.322032167404199	14.1386249055853	3.1666542349851	0.015073245479662	0.477624045768555	-2.71330633502338
Psen1	0.275394828676024	14.0742801075431	3.2549173539988	0.0163848939606434	0.479636028744591	-2.72577967688556
Otud5	-0.45084577178476	13.2887671226749	-3.39577616845809	0.0179330205928083	0.486547593667135	-2.73162611085796
Uap1;Uap1l1	-0.563700751060168	14.5494352584974	-3.52670016396514	0.0154999768088065	0.477624045768555	-2.73311069185855
Tank	0.410709538026998	12.8542040436994	3.38673094818238	0.0181163884112855	0.486547593667135	-2.74047348370107
Adipoq	-0.519085976877193	17.7072828977132	-3.07523473110545	0.0146778196347291	0.476643949189522	-2.74047843079675
Camk1;Camk1d	0.217352832910532	16.1130761342607	3.07429818388335	0.0146990348087588	0.476643949189522	-2.74176133803178
Egfr	-0.608720391364134	13.7024151574191	-3.38527733868914	0.0181460527237083	0.486547593667135	-2.74189680511507
Nsmaf	-0.311641092924331	13.4111630864553	-3.3818115358065	0.018217001209651	0.486547593667135	-2.7452920756644
Cyp2d26	0.410687139086326	14.3726464185337	3.23569884633196	0.0167955408993055	0.486273817351061	-2.74765624863776
Acot1;Acot3;Acot4;Acot5;Acot6	0.200183875885021	15.3651938213684	3.13505902312747	0.0157672933785797	0.477624045768555	-2.75327513115314
Ephx2	0.216749166673779	14.4054643812183	3.06504321818539	0.0149104084796944	0.477377972306438	-2.75444374879451
Ttr	0.366191774925747	14.7442825731095	3.06469760469968	0.014918362964824	0.477377972306438	-2.75491752026924
Polr1g	-0.239389379269554	14.3040730602197	-3.2277056869713	0.0169696187903215	0.486547593667135	-2.75677361792124
Hpcal4;Vsnl1	0.282307139732533	15.9311618418722	3.06185209478346	0.0149840221127016	0.477382519759285	-2.75881863099234
Ca4	-0.421340939003247	14.4906804715993	-3.05589310646028	0.01512250018486	0.477624045768555	-2.76699080955356
Khdc4	-0.292819366434896	14.574319159992	-3.21454784308403	0.0172604639779062	0.486547593667135	-2.77180585978944
Sdhaf1	0.253782900023166	14.0643674295264	3.1130044298357	0.0162718202603995	0.479636028744591	-2.7812560329146
Snrpf	0.300354912503387	17.3239851037061	3.04323148155119	0.0154211771842119	0.477624045768555	-2.78436647712126
Slc39a7	0.423519397066205	16.3077243383634	3.03781518376716	0.0155508110242559	0.477624045768555	-2.79180401759287

Serpind1	-0.482689966062029	18.7218075726352	-3.02524194125846	0.0158561267403273	0.477624045768555	-2.80908000636884
Plg	-0.545968669280494	20.9446709293382	-3.02184352575737	0.0159397154782244	0.477624045768555	-2.81375206032816
Fis1	0.204867006689486	17.5533750281256	3.01636899585816	0.0160753334451285	0.477624045768555	-2.82128054495618
Afg3l1;Afg3l2	-0.310597853644872	16.9620740519307	-3.16030314641573	0.0185180034967637	0.487147391728858	-2.83408726248042
Ybx1	0.292304978173433	19.2308181086688	3.00003231713949	0.0164872054767145	0.480856621495501	-2.8437626927137
Pacsin1;Pacsin2	-0.275581362766935	18.8897139633162	-3.28057353912026	0.0204335609771033	0.498661181664939	-2.84551164093951
Znrd2	0.681854854273434	14.7071015098037	3.17607088518019	0.0181425077564525	0.486547593667135	-2.85130274165942
Oaf	-0.442657368715864	13.9916441606371	-3.27075132876406	0.0206642482443104	0.498661181664939	-2.85534171876574
Ptprn;Ptprn2	0.645316224543199	13.6827201881648	3.33725556719234	0.0191574361023804	0.488764383800416	-2.87824727778462
Tubb2a;Tubb2b;Tubb3; Tubb4a;Tubb4b;Tubb5; Tubb6	-0.271874260788351	21.6326926966079	-2.97375554911634	0.0171728130420935	0.486547593667135	-2.87997367267913
Gtf3c2	-0.200683597637903	14.9461854519237	-2.97199866132818	0.0172196954443712	0.486547593667135	-2.88239688980788
Pold3	-0.425769750799573	13.81519806111	-3.23793192698934	0.0214564774359301	0.498661181664939	-2.8883232595775
Flt4	-0.680978048355291	14.3063154289242	-3.02187608524477	0.0185451294973043	0.487147391728858	-2.89136508147762
H1-2;H1-3;H1-4;H1-6	0.227559442783768	22.2508364458843	2.96487244404669	0.0174112229447167	0.486547593667135	-2.89222850817954
Cog8	-0.205894835397832	16.0197564210682	-2.96033195969636	0.0175344056487414	0.486547593667135	-2.89849495323324
Tra2a	-0.238932429444453	17.2636231877	-2.95919829036616	0.0175653026223883	0.486547593667135	-2.90005982680965
Ppp2ca	-0.226208418382527	16.9995665057102	-3.11862637055929	0.0195517015880252	0.493960664642687	-2.90655523574636
Pde4d	-0.252410881166636	14.0142716253382	-3.01195352595357	0.0188122088351206	0.487489258226467	-2.9102773500918
Cox5a	0.282229947428313	19.7571887574414	2.94906483153332	0.0178439979229716	0.486547593667135	-2.91405233345592
Masp1	-0.619904006141152	15.1122059470308	-3.00791016950431	0.0189222034267001	0.487489258226467	-2.91546668753616
Ube2h	-0.293591519002335	15.763942831117	-2.94550282550271	0.017943046648185	0.486547593667135	-2.91897280585779
Tmub2	0.200151926449053	14.428422446446	2.94003645360142	0.0180961588457142	0.486547593667135	-2.92652589613118
Smad1;Smad5	-0.290465393937902	14.7615390865516	-3.07721075103404	0.0206411225227694	0.498661181664939	-2.93043348364245
Cpt1a;Cpt1b	0.300626048877202	17.0464761937529	2.93530647229535	0.0182297364396471	0.486547593667135	-2.93306339531441
Jpt1	0.280950516545719	15.498314959371	2.92547532784493	0.0185106492585643	0.487147391728858	-2.94665699826801
Ift172	-0.244341379902632	14.011443233465	-3.17149185954046	0.0231664946985426	0.50628044750286	-2.95572743427464
Ssr3	-0.516208929198697	18.4996721034218	-2.91806075749067	0.0187254718808254	0.487489258226467	-2.95691408696027
Vps13b	-0.200250159481921	16.111174564775	-2.91118972425796	0.0189268488004225	0.487489258226467	-2.96642295730789
Ttyh3	0.251358921846697	13.6157051894902	3.15447038755366	0.0236287350757231	0.509744568456766	-2.97313178784277

Med20	-0.250384949360598	14.0925766990081	-3.04016898076773	0.0216712364118621	0.498661181664939	-2.97374051266129
Fxyd6	-0.35417759614508	13.3533197384269	-3.03930931394338	0.0216957932289134	0.498661181664939	-2.9747481364314
Eif1b	0.661441008434243	15.6295562857623	3.21422177744028	0.0220499762824103	0.498661181664939	-2.97648146624745
Th	-0.214463340928502	14.2683460481314	-3.0371747606237	0.0217568978465653	0.498661181664939	-2.97725056353886
Rps6ka3;Rps6ka6	-0.456901304955899	14.9485442199603	-3.21279419604177	0.0220862925303274	0.498661181664939	-2.97763966259625
Aif1l	0.352337698997564	15.152079678399	2.90124911546487	0.0192221602774511	0.488764383800416	-2.98018600499224
Septin10;Septin14; Septin7	0.694974617693283	17.0220954624574	2.90122381125492	0.0192229180513019	0.488764383800416	-2.98022104855597
Slc6a11	0.241968483991428	16.9419358070376	2.89917373401235	0.0192844134790786	0.488764383800416	-2.98306033481125
Epb41;Epb41l3	-0.285599971879293	17.4197637504536	-3.14305937513728	0.0239443773363075	0.509959933402322	-2.98483028879068
Igfbp7	-0.336111410409924	13.02015472191	-3.02356674209684	0.0221508408935705	0.498661181664939	-2.99322040516835
Clk3	-0.243269598164879	13.6844053067981	-3.02316966319452	0.0221624510484375	0.498661181664939	-2.99368683060947
Smoc1	-0.237712594618319	14.8333181846477	-3.02025133649021	0.0222479814828241	0.498661181664939	-2.99711556266155
Rbp4	-1.0121354592137	16.9981672643944	-3.1875446195185	0.0227397961280158	0.502492486583702	-2.998194120396
Ttyh1	-0.274265686850001	13.3307776578144	-3.01733049430175	0.0223339423541595	0.498661181664939	-3.00054855944376
Ssh3	-0.293740995392429	15.0019345524314	-3.01594880864499	0.022374730373119	0.498661181664939	-3.00217297218289
Pcp4l1	0.346992351215661	17.4338205286633	2.88248238174626	0.0197927242277573	0.497974352131189	-3.0061883880583
Rpusd3	-0.306555502202841	13.2529514252455	-3.11136299737088	0.0248460892488306	0.514114079259985	-3.01745431589872
Rps21	0.205195317006446	19.8421307481611	2.87186975772335	0.0201230928922672	0.498223932312554	-3.02090359801981
Psme3ip1	-0.31009249394314	14.3470824545869	-2.99344925382067	0.0230503573786901	0.505133936699305	-3.02907629283473
Cdh2;Cdh4	-0.226715833823187	15.2326327349834	-2.91555165522174	0.0216284511306751	0.498661181664939	-3.03452437429877
Banf1	0.359594142329733	16.3669733085447	2.84995402618729	0.0208234539975543	0.498661181664939	-3.05131502514391
Il1rap	-0.411171359091416	17.96609311099	-2.84774347524109	0.0208954783434738	0.498661181664939	-3.05438421026959
C8a	-0.696280252059797	16.6292794402295	-2.89212107310161	0.0223778369687027	0.498661181664939	-3.06487981355336
Mlh1	0.418868668430964	13.9882129308961	3.10407958769979	0.0250585984280383	0.51499964075033	-3.06707238005769
Pip4k2a	-0.210344029157014	16.8810608840226	-2.83265619607044	0.0213939582311382	0.498661181664939	-3.07533980616414
Gale	-0.201913237079317	16.6088660878895	-2.83157366292428	0.021430192563831	0.498661181664939	-3.07684392773762
Icam1	0.290294941221967	14.4759537769178	2.85427838146782	0.0236462878094151	0.509744568456766	-3.07730820236294
Ighm	-0.30994092337577	13.5781877104009	-2.8515824468231	0.0237394841830048	0.509959933402322	-3.0803316334471
Mrpl57	-0.222472779521464	15.5864725249091	-3.0462719565163	0.026818862361087	0.521093007459065	-3.08503966169626
Hcn1;Hcn2;Hcn4	0.24301163875535	15.5914586368575	2.93644187736762	0.0248625824109355	0.514114079259985	-3.08580829967533

Ttc9c	-0.213139940043469	15.1407749563203	-3.04292675638158	0.0269248561866569	0.521093007459065	-3.08853425108743
H3-3a;H3-5;H3c1;H3c2	-0.214285086670287	22.6373797219089	-2.82180235280305	0.0217601292710904	0.498661181664939	-3.09042375163335
Ubqln1	0.297321828745481	16.3455199923919	2.82130115524908	0.0217771929772466	0.498661181664939	-3.0911204476868
Eral1	0.24554313879203	15.5365221770354	2.83973986062398	0.0241534554542154	0.509959933402322	-3.09362428398664
Rras2	-0.265401991199148	14.4655532268471	-2.818574675724	0.0218702598874064	0.498661181664939	-3.09491067677056
Nap1l1;Nap1l4	-0.391369341828931	19.1902807442473	-2.81797701541327	0.0218907153425471	0.498661181664939	-3.09574157374266
Senp8	-0.294514147327757	14.2102808415172	-3.03313104981581	0.02723792317762	0.521093007459065	-3.09877923206693
Psma2	-0.21714574418208	17.9798365325744	-2.81303591996395	0.0220605847726029	0.498661181664939	-3.10261170054282
Ring1	-0.286647023379944	14.2601631434537	-2.91954587015039	0.025428700775966	0.518575535361794	-3.10273165642474
Chst12	-0.2809816896426	13.8493203887407	-3.0256005540206	0.0274813445179711	0.521093007459065	-3.10666706176398
Atp12a;Atp1a1;Atp1a2; Atp1a3;Atp1a4;Atp4a	0.269237089465133	20.9800279804684	2.80665681673573	0.0222818990101997	0.498661181664939	-3.11148324784792
Ctnnd2;Pkp4	0.439659961532767	14.0553520437873	2.99840916826017	0.0283806148743657	0.522578322167593	-3.13523475263179
Dhx36;Dhx57	0.282927722193147	16.0471212600003	2.80076337095092	0.0255701224633986	0.519012246422512	-3.13750243703281
A2m	-0.587721593220785	19.5948103996598	-2.77692181717098	0.0233440332083501	0.508266078373444	-3.15286468235877
Rplp1	-0.223661437260589	20.0584777978606	-2.77578948601707	0.0233854933324476	0.508266078373444	-3.15444139821466
Spon1	-0.373310329535	14.6865566856315	-2.998080348737	0.0283916874895036	0.522578322167593	-3.15659656237462
Paqr5	0.307433742285673	13.867181896935	2.97782069737193	0.0290832373618517	0.522864341788283	-3.15695434281239
Trmt6	-0.285841707272551	14.1717381478238	-2.76455066354276	0.0238011228657771	0.509959933402322	-3.17009420990339
Pla2g12b	-0.447000236108648	14.0879201663912	-2.87354161336929	0.0270414462957978	0.521093007459065	-3.17111274662217
Naa60	0.377428193698927	12.9225058846659	2.87330144230743	0.0270501482708566	0.521093007459065	-3.17140010576603
Actg1	0.536928806382299	21.9644646224635	2.75472909206075	0.0241705451858405	0.509959933402322	-3.18377790359014
Fam110b	0.345483385843227	12.5885731324	2.94871490283913	0.0301096408718678	0.526122865719224	-3.18778877215743
Isl2	-0.221243296714626	16.1312447954431	-2.85531273155478	0.0277105294537208	0.521093007459065	-3.1929454671987
Mctp2	0.404250013766269	13.0529018342667	2.95430180217734	0.0299095507466491	0.525363787336501	-3.19423219595243
Snta1;Sntb1;Sntb2	0.474611100532776	16.289202948184	2.85296365326134	0.027798032965154	0.521093007459065	-3.19576222030112
Zmat2	-0.26057208786767	14.3571659999636	-2.93497064878231	0.0306082142149164	0.530507082073246	-3.20240161335533
Tfcp2;Ubp1	-0.372274009121082	13.9242758620883	-2.84390198418243	0.0281383633519403	0.522377847939514	-3.20663487801135
Gstm1;Gstm2; Gstm4;Gstm7	-0.308266129818833	18.5991438539218	-2.7391229979235	0.0279904409847033	0.522377847939514	-3.20728164482714
Casd1	-0.342637479881846	14.5680016257013	-2.73614073536564	0.0248858951765831	0.514114079259985	-3.2096871313624

Scn3b	-0.377704873780679	13.9376891472774	-2.83537008706339	0.0284628755235152	0.522675906314921	-3.21688185704007
Hp	-0.377676275085957	22.7802293571066	-2.72320666405717	0.0253964154131743	0.518575535361794	-3.22772338380262
Mettl21A	0.496525509588949	13.602502984606	2.8216574641258	0.0289928547151552	0.522864341788283	-3.23337103312058
Btk	-0.284618191615401	13.35902905706	-2.81641761684881	0.0291981474110941	0.522864341788283	-3.23967831506038
Vamp3	-0.231305795477287	16.3052996925796	-2.71412604703295	0.0257612326257869	0.52000981786353	-3.24038981788859
Klc1;Klc4	0.489393921914752	16.0114668901211	2.75445953096911	0.0273667348263261	0.521093007459065	-3.24431932364767
Bud13	-0.484606804563798	13.4229941707254	-2.89189403258205	0.0322309140323347	0.546341540637845	-3.24854174911954
Tmem233	0.321600739197386	15.4568902324989	2.70623467325713	0.0260826253648879	0.521093007459065	-3.25139974647416
Ciao2b	0.37322036736068	14.7394707312915	2.77019224971431	0.0310779479438936	0.535959480519364	-3.25440430673151
Mgp	1.12159920845944	17.680883148752	2.70315884777436	0.026209003068183	0.521093007459065	-3.2556916611467
Crmp1;Dpysl2	0.238045498673443	20.3763054712679	2.69432284658575	0.0265755458034817	0.521093007459065	-3.26802284830248
Timm10b	0.269404989354713	14.0395318662717	2.69368066886412	0.026602388599092	0.521093007459065	-3.2689191423451
Plxdc2	-0.278317034443267	13.5672782144508	-2.85922136703944	0.0335250690094506	0.554161983530045	-3.28352911832553
Atp5mpl	0.331958141684364	18.8190377220821	2.71475192373505	0.0290122016826275	0.522864341788283	-3.29638412090357
Arl4c	0.211617563979399	14.5470562456935	2.84482663832874	0.0341133351949665	0.555857820135612	-3.29905708275291
Higd1a	-0.223824044681965	18.1935899775075	-2.67093461633223	0.0275712498404081	0.521093007459065	-3.30067372387355
Sec61a1;Sec61a2	-0.202474070331188	19.1263808775043	-2.66929176797765	0.0276426066064932	0.521093007459065	-3.30296775977833
Dhx33	-0.213457319459531	13.8260373502915	-2.83802629142299	0.0343951911527758	0.555857820135612	-3.30640493079514
Rnf34	-0.2588611435116	13.4928810683623	-2.82945157129511	0.0347542517064494	0.555857820135612	-3.31568104807311
St3gal5	0.319874996739923	17.9264622498236	2.69974421032677	0.0296606443856455	0.523003327133612	-3.31609323319595
Ssh2	-0.252802057868646	13.3228077723829	-2.7519054147271	0.0318568785689189	0.544232344017065	-3.31761649850579
Ica	-0.373739238965424	16.8629448936588	-2.69352522743357	0.0299337491335054	0.525363787336501	-3.32426512066237
Ces1;Ces1f	-0.242859314976421	21.8025844126737	-2.64819020446198	0.0285760807722127	0.522864341788283	-3.33243914331483
Nmt1;Nmt2	-0.212738914483502	17.7529451290312	-2.64476528388384	0.0287305942679709	0.522864341788283	-3.33722344242284
Ctbs	-0.331897974867601	14.1514474830899	-2.68053311798761	0.0305127582513694	0.530507082073246	-3.34134567917047
Rgs4	-0.353131570160615	14.5103804089563	-2.61390282349321	0.033670247833289	0.554161983530045	-3.35035090357897
Csnk1g2;Csnk1g3	0.345675419871846	14.5578348680255	2.72368724939857	0.0330999095072823	0.553716587633862	-3.35186602438693
Tuba1a;Tuba1c;	-0.234308709844996	20.7516587706798	-2.63175048195097	0.029325555315386	0.523003327133612	-3.35540590864778
Med14	-0.206993556239704	13.9138815055149	-2.78888399223018	0.0365098394391706	0.560257069583158	-3.35973206285633
Timm8b	-0.210463119509168	13.8773633563885	-2.71183266539424	0.0336374143796787	0.554161983530045	-3.36628194499259
Vps37b	0.253630351730346	14.3173744613699	2.59336347584899	0.0347103435369972	0.555857820135612	-3.37396778259349

Bbs2	-0.251227309528325	14.4621578003115	-2.64717443447978	0.036736928643522	0.560528880117487	-3.38195081009572
Tubb1;Tubb3;Tubb6	0.470658381435165	18.0262945547011	2.60706222563027	0.0304888558582281	0.530507082073246	-3.38990401161008
Nck1;Nck2	0.338243077048174	14.8728849670064	2.68984046852714	0.034659293500665	0.555857820135612	-3.39306773650388
Kit	-0.25006682592802	14.0199226371354	-2.57561545400527	0.0356358065664232	0.556494226496549	-3.39440554238998
Aldh1l1;Aldh1l2	0.334438360912333	14.38547083109	2.72796091689536	0.0393320409690038	0.562554463818101	-3.3947953268111
Nup42	-0.360109551000138	14.2905605443908	-2.72030627956286	0.039703226471258	0.562554463818101	-3.40174805603782
Prkar2a;Prkar2b	-0.325202200534225	17.2843825341973	-2.62435069082154	0.0379021432615215	0.562554463818101	-3.40585342967783
Tmed4;Tmed9	-0.289270796372925	17.7521902902281	-2.62255819917057	0.037995296149354	0.562554463818101	-3.4077336549125
Sarg	0.251545504539028	13.6364905644284	2.67737315435917	0.0352531893841418	0.556494226496549	-3.40827615418666
Cacna1c;Cacna1d	-0.201084275154452	13.9198856893336	-2.6692377929448	0.0356465417505089	0.556494226496549	-3.41820919851788
Zbtb7a	-0.263733439352801	14.1420710752051	-2.55371940471291	0.0368127500997366	0.560528880117487	-3.41965708909916
Rragb	-0.278856756296628	15.7763892651737	-2.69938661820802	0.0407373537314389	0.562554463818101	-3.42080412827858
Kctd12;Kctd16	-0.30612403602937	15.2429491871793	-2.66533984583806	0.0358366579513062	0.556494226496549	-3.42297097096209
Trmt61a	0.224179175568649	14.3911687006589	2.66514312143966	0.0358462813235518	0.556494226496549	-3.4232113339979
Pacc1	-0.214040070911466	13.7551797040117	-2.72927540945394	0.0392686822641247	0.562554463818101	-3.42494206966172
Hk1;Hk2	0.287465230517547	18.8441645244134	2.57220243117119	0.0322118109862609	0.546341540637845	-3.43862506960854
Pja1;Pja2	-0.420926982207899	14.3413615776336	-2.67823201892187	0.0418131201295523	0.562554463818101	-3.44015494390838
Snx12;Snx3	0.431147013137902	17.6259759307634	2.56937709484438	0.0323557124122401	0.547287561975054	-3.4425740687046
Acot1	0.30494932053513	16.0218853169772	2.56168762160486	0.0327506670615909	0.551615799999152	-3.45332173626844
Krt6a;Krt6b	0.861103831812201	18.3345543655408	2.63855662961243	0.0371723729642494	0.562554463818101	-3.45573231654645
Rpl32-ps	0.356041114847045	14.8689286510267	2.5585204088694	0.0329147626703349	0.55320511072832	-3.45774857488018
Amigo2	-0.299275703494132	13.1508180283254	-2.69899688859256	0.0407568967715458	0.562554463818101	-3.45827930088391
Sppl3	-0.326538784989701	14.1419332155577	-2.6584892029772	0.0428451317285399	0.564154412664708	-3.45828678520366
Dpm3	-0.289891161278915	15.5368406930189	-2.58678107410197	0.0350506505850549	0.556494226496549	-3.46490726912866
Ptprr	-0.284713917166998	13.7349889622011	-2.68908469956942	0.041257406144023	0.562554463818101	-3.46922325137078
Chp2	0.208397037852668	14.0015099474687	2.6877417858419	0.0413257308271206	0.562554463818101	-3.47070709091572
Ulk1	-0.286558407674958	13.9037834596951	-2.50828969623202	0.0393840726000968	0.562554463818101	-3.47217040835459
Itih4	-0.457489862308933	17.7762162096975	-2.54639768210483	0.0335505852040948	0.554161983530045	-3.47469236036118
Dip2a;Dip2b	0.220852581033501	14.9347845955603	2.62132100341208	0.0380597324032518	0.562554463818101	-3.47685334031459
Rps7	-0.29996408497583	20.7697954195504	-2.53631841851133	0.0340886927461513	0.555857820135612	-3.48877948014076
Polr3f	-0.304925824044274	15.519505972144	-2.56631670599877	0.0361308146176584	0.5584015219975	-3.49193958974718

Ddx39a	-0.279138651450854	16.3820604492683	-2.56631061196949	0.0361311413411943	0.5584015219975	-3.4919476423604
Pgghg	0.2629520696982	13.8971336222084	2.66811161691974	0.0423387102014761	0.562792508267584	-3.49242807937934
Ciao3	-0.249327932903549	14.2480290260856	-2.60296501360907	0.0390294485674657	0.562554463818101	-3.49937905268224
Serpinb5	-0.243116783749343	13.9508359098027	-2.53374691228289	0.0429271664471834	0.564154412664708	-3.501414615077
Celf6	-0.23983893542707	16.6478862236684	-2.52645747272697	0.0346235978920982	0.555857820135612	-3.50256072110925
Rps6ka1	-0.226251835339678	14.1135822888282	-2.59397467218465	0.0395138833444736	0.562554463818101	-3.5104232383057
Abcb11	-0.316079325849733	15.261816372098	-2.65072818242422	0.0432584046388434	0.564304161422804	-3.51171065737638
Erg28	-0.421998702420737	16.5956272035421	-2.59646448757415	0.0462721818493299	0.579049982979367	-3.51569629047868
Acta2;Actc1;Actg2	-0.443143198675795	19.5245808800411	-2.51371201816526	0.0353275699823799	0.556494226496549	-3.52037171649169
Tdp2	0.316902160579451	13.1357697057703	2.58262876710908	0.0401343211966122	0.562554463818101	-3.52437172762894
Lsm1	-0.212153243492697	14.2639608463549	-2.63715767475815	0.043991514644964	0.566533580646915	-3.52679435641284
Septin11;Septin8	0.864929256918082	17.5981609027665	2.5078148936432	0.0356581646096379	0.556494226496549	-3.52861187215313
Pard6b	0.230527784091194	13.2778237338084	2.63041078718968	0.0443610267263873	0.569539940771134	-3.5343034309182
Imp3	0.251776872081999	13.8380477528341	2.56897053087629	0.04089486450202	0.562554463818101	-3.54117829224257
Tma16	-0.235993809638664	15.4944934853524	-2.49861249237385	0.0361803078667232	0.5584015219975	-3.54146947089017
Pygl;Pygm	-0.465799959227226	13.1979928614959	-2.56130453629416	0.0413283792552661	0.562554463818101	-3.5506185193535
Cox16	-0.354543503074368	13.0060222484664	-2.60611432018763	0.045719949348726	0.576548364451408	-3.56139813861679
Ankrd49	-0.216857436028498	13.9771561083676	-2.50260028934759	0.0397188569725208	0.562554463818101	-3.57620961973702
Ebag9	-0.217221792097675	16.5137659872437	-2.53901081239126	0.0426168202962813	0.564154412664708	-3.57810023119474
Ptp4a2	-0.24045052257045	15.6581975625469	-2.49969806899008	0.039890757780739	0.562554463818101	-3.58005112062093
Pitpna;Pitpnb	-0.331508851882951	17.1770239989548	-2.45690234946622	0.0386453498248361	0.562554463818101	-3.59972493876067
St3gal6	-0.2870911855833	14.224856515637	-2.52002718682819	0.0437472657601191	0.564304161422804	-3.60153342156534
Snrpd1	-0.254070320510799	18.2613101718014	-2.44251800499598	0.0395341182435429	0.562554463818101	-3.61980439801286
Tmem11	0.287705548274783	16.4501564233002	2.4418196064083	0.0395777898224109	0.562554463818101	-3.62077914093365
Daxx	-0.214136184028968	13.4157269456597	-2.54269088818187	0.0494851914237474	0.593897161217229	-3.63250760350531
Ppif	-0.209276742372637	16.4369270747561	-2.43063596462904	0.0402837556952217	0.562554463818101	-3.63638566200714
Cdk16;Cdk17	0.323235440153882	14.7439741584128	2.42996937658541	0.0403262312831266	0.562554463818101	-3.63731572943339
Mrps12	0.284766968435335	15.1949772224591	2.42718813334859	0.0405039404941132	0.562554463818101	-3.6411961245003
Pip4p1;Pip4p2	-0.363575271603706	14.7699951598556	-2.48704791082152	0.0457866468680685	0.576548364451408	-3.64230792778613
Plaur	-0.28855959886558	14.6963549363399	-2.41766871309817	0.0411181620385045	0.562554463818101	-3.65447538559471
Itih3	-0.60793749271998	16.4899125944428	-2.35136905831393	0.0497711876602726	0.595255766102535	-3.65455253325283

Calb2	0.206267555792067	14.7470023032859	2.41709188506595	0.0411556796976151	0.562554463818101	-3.655279925175
Snx5;Snx6	-0.320779481592179	16.9474742274611	-2.40972181641623	0.0416380722207087	0.562554463818101	-3.66555822770229
Tubb2a;Tubb2b;Tubb3; Tubb4b;Tubb5;Tubb6	-0.636877289984721	21.9541448720937	-2.40677015910242	0.0418328534713285	0.562554463818101	-3.66967396436711
Chmp5	0.212886157722089	16.5626506186227	2.37945373491045	0.0436793634982373	0.564304161422804	-3.70774439926656
Araf;Braf;Raf1	0.247813607071446	14.9654979285085	2.36569298406383	0.0446402248200972	0.569657485693383	-3.72690823170863
Taok3	-0.219329947095918	14.2870146923074	-2.3645101383078	0.0447237981798234	0.569657485693383	-3.72855503057599
Vapa;Vapb	0.218627325241663	20.4021091616479	2.35927374530564	0.0450956547702322	0.573307418737584	-3.73584436220827
Arf1;Arf3	-0.415592182960683	17.3469935317077	-2.36005056983292	0.0491294245427349	0.591416881483332	-3.76503830648927
Krt10;Krt14;Krt15; Krt16;Krt25;Krt27	-0.504658533767	20.7090598209789	-2.33593947944001	0.0467905963019233	0.579984063223684	-3.7683068872518
Atp5pf	0.257874621596482	18.7026900017643	2.3261270090454	0.0475221885684583	0.584715890353822	-3.78194755129609
Erh	0.2526174498025	17.7837826826738	2.32243746814002	0.0478002097471097	0.585061832081663	-3.78707482410728
Enpp5	0.205214153378336	15.179570049091	2.31268778689499	0.0485427046268617	0.586459462071838	-3.800619134505
Vdac1	-0.221941824769271	21.4962531555855	-2.29635433177592	0.049812391096419	0.595255766102535	-3.82329401057629

STable 2: IL-16 DEPs filtered

DEPs	logFC	AveExpr	t	P.Value	adj.P.Val	B
Ckb;Ckm	0.580502445854741	17.0302494538742	9.19624076473417	1.29484765493498e-05	0.0495271902708065	2.75879517657306
Pcolce	-0.796900728415858	15.4212717467767	-8.74494508749383	1.89345996020981e-05	0.0495271902708065	2.52610640854291
Ccn2	-0.722443118371192	18.3544001217037	-8.45421071694144	2.43976306752742e-05	0.0495271902708065	2.36574890454266
Calb2	0.692198566658828	14.4150253322148	11.4924325847429	1.96518331545713e-05	0.0495271902708065	1.8908715899152
Plek	-0.658377857020724	20.2201945252992	-7.5952039099944	5.38892339883576e-05	0.0875161159970927	1.83861941662692
Ngf	-0.757669655624579	19.0837134499423	-6.67260947545495	0.00013691285017218	0.173490308242993	1.17068707222309
Pstpip2	-0.381600707727637	14.1908172086023	-6.56910432884176	0.0001528991533223	0.173490308242993	1.08835892716496
Spon1	-0.397633743576284	14.5231305396672	-7.05827096379545	0.00017092641206206	0.173490308242993	0.937711432864344
Frzb	-0.707456082794312	16.3770702142538	-6.01309362231132	0.00028284716260723	0.220981639390061	0.618124307687484
F2	-0.51889599194897	21.4452535819226	-5.95032546025709	0.00030391725462178	0.220981639390061	0.561958020051951
Taok3	-0.475330799141558	14.4470500280351	-5.92962765006875	0.00031123806830943	0.220981639390061	0.543295590124096
Rab11fip1	-0.695653190530155	15.2744924618274	-6.37363174696703	0.00032657385131536	0.220981639390061	0.473704533572563
Igfbp3	-0.497145630028989	17.4777811585801	-5.64351598835976	0.00043498076167751	0.254669839804032	0.277998148068402
Tubb1	-0.41511870256657	17.9634247706447	-5.6356183750061	0.0004390859306966	0.254669839804032	0.270478632844794
Rpl18a	0.426987736080388	19.3235403092051	5.44328420716026	0.00055338434024417	0.261824750885111	0.0840265234937076
Basp1	-0.443698879146051	18.8047575977584	-5.38377066466005	0.00059506053455041	0.261824750885111	0.0250254462271666
Serpinc1	-0.471240128420082	21.6514835910892	-5.31468454066625	0.00064778973693441	0.261824750885111	-0.0442500399416286
Pcolce2	-0.443362819644422	15.2443884172838	-5.24441634140424	0.00070669779459473	0.261824750885111	-0.115581035229055
Hp1bp3	0.308683455752877	17.4623710663234	5.23656635040123	0.00071363335748836	0.261824750885111	-0.123604508436717
Vamp1;Vamp2;Vamp3	0.262829672779478	17.9546604998696	5.20431181990563	0.00074291981114264	0.261824750885111	-0.156687737449356
Jpt2	-0.424256776820526	14.4528782793236	-5.20112577651167	0.00074588302963286	0.261824750885111	-0.159965766669931
Smoc1	-0.808605236121263	15.0018766861093	-5.56591140814067	0.00075081306635954	0.261824750885111	-0.161750523318621
Svip	0.421919049365036	14.2555059129204	5.50817971502141	0.00079932485149503	0.261824750885111	-0.211175111116012
Extl2	0.225943216673713	17.1889971372296	5.12661485010196	0.00081899023980419	0.261824750885111	-0.23714885428033
F13a1	-0.50128032647569	17.92876485086	-5.04201919645388	0.00091158582500615	0.261824750885111	-0.325994657247079
Rap1b	-0.250102717471538	17.7921017103294	-5.02537186165877	0.00093111663246427	0.261824750885111	-0.343631335774631
Habp2	-0.500198924673565	17.8590937114716	-5.02203298244261	0.00093508839601825	0.261824750885111	-0.347174714095977
Fermt3	-0.567648623490143	16.6067823318291	-4.96710053921249	0.00100315005703235	0.269478498573838	-0.405763323611141
Dpep2	-0.645916901349668	12.8943961218811	-6.71469158278651	0.00091822912372798	0.261824750885111	-0.426549335624563

Atrn	-0.516924482120135	16.4881059241072	-4.87752518943991	0.00112597008283339	0.269478498573838	-0.502483413197116
Thbs4	-0.560829443377072	14.6728642037287	-5.51814478400782	0.00130479376030498	0.269478498573838	-0.603883888593042
Tpm1;Tpm2	-0.318098755617839	17.6084698807568	-4.78145349716823	0.00127610532605434	0.269478498573838	-0.607854119347763
Gramd1a;Gramd1b	0.239803364508765	15.0030764993661	4.76817318190939	0.00129851421531233	0.269478498573838	-0.622553428512084
Apob	-0.499891795691084	18.3506375347852	-4.74259303912748	0.00134288984800908	0.269478498573838	-0.650958337433036
Rpl34	0.259307033142662	20.2154156661743	4.73317966944453	0.00135963155600303	0.269478498573838	-0.661441553922445
Trex1	0.257895223932218	15.3179459690881	5.00738292480848	0.001401884170927	0.269478498573838	-0.663997770980063
Smn1	0.2608222322601	14.705760078085	4.99493930257111	0.00142221427844363	0.269478498573838	-0.675813498792755
Rpl3	0.238288688622873	20.0818366515219	4.67575463856628	0.0014667909094586	0.269478498573838	-0.725746836647823
Aldob	-0.718533050157387	17.2180751583683	-4.65070832948052	0.00151636555266764	0.269478498573838	-0.753984487924322
Ptpn6	-0.46082842431473	15.4957562698872	-6.02816864129127	0.00152836415175507	0.269478498573838	-0.766470444567908
Sytl4	-0.565881597250307	15.9600606079272	-4.61974130259256	0.00158018268639141	0.269478498573838	-0.789057251501323
Lect2	-0.837742208742402	15.9880134981894	-5.26916431236129	0.00166424257921509	0.269478498573838	-0.792697434079313
Lamc1	-0.388878154751531	20.9875279276994	-4.61240928675865	0.00159571454604095	0.269478498573838	-0.797387277711477
Man1a1	-0.481915475230531	15.1370501244149	-5.26177539278664	0.0016765049515562	0.269478498573838	-0.798457060753924
Epb41l1;Epb41l2; Epb41l3	0.648506433507457	15.2788758036424	4.86282869182292	0.00165934167999975	0.269478498573838	-0.802987951866377
Igfbp5	-0.336643139472542	16.7316451221238	-4.85202376410127	0.00168058617892495	0.269478498573838	-0.813529784958936
Krt10;Krt13;Krt14;Krt15; Krt16;Krt17;Krt18;Krt19; Krt24;Krt28;Krt31;Krt32; Krt33b;Krt35;Krt36; Krt40;Krt42	-0.706900427679301	19.0327366624298	-5.23743603806369	0.00171762569898385	0.269478498573838	-0.817494262108482
Cyp2j6	0.252602097504028	15.1886155742715	4.59064762548398	0.00164279475978137	0.269478498573838	-0.822169460606528
Hgfac	-0.610723446913685	16.3731607812422	-4.58446484688781	0.00165644352053606	0.269478498573838	-0.829226343697796
Slc9a9	0.245307939683357	16.2290942214485	4.57836459059085	0.00167003043514706	0.269478498573838	-0.836195947313405
Pitpna;Pitpnb	0.488085669949896	16.8063891499948	4.79767410903135	0.00179209838953045	0.269478498573838	-0.866880515177792
F10	-0.45841723855164	18.9595730907996	-4.5388411648852	0.00176103406280524	0.269478498573838	-0.881518098732426
Ptp4a1;Ptp4a2	-0.288261113105506	17.2372609263312	-4.53750582410951	0.0017642009155408	0.269478498573838	-0.883054384432214
Nell2	-0.308907885554731	15.2376269194743	-5.67522067953885	0.00202229282756057	0.28294568884805	-0.964428111505313
Slc39a11	0.356203394001655	14.1091477251583	4.69765418462304	0.00201925400316346	0.28294568884805	-0.966483409457953

Cdk19;Cdk8	-0.580065043754697	12.6294094290766	-5.62410670517755	0.00210831208976463	0.28294568884805	-0.994526244596354
Pla1a	-0.598736764255113	15.562371048884	-4.64398040723602	0.00215408950206647	0.28294568884805	-1.02069680233192
Tln1;Tln2	-0.322082833945043	18.8574325710407	-4.39146920339199	0.00215065224484245	0.28294568884805	-1.0530471829062
Pdcd10	-0.207650244285094	17.9757565317118	-4.37189206030908	0.00220905056113954	0.28294568884805	-1.07613346913043
Krt5;Krt77;Krt79;Krt8	-1.10119038484934	15.7900629172518	-6.83235368774358	0.00084506559045616	0.261824750885111	-1.09438781121111
Cxcl10	-0.401004527895452	14.6736435631644	-4.89512386753179	0.00243514395290327	0.28294568884805	-1.09599498274703
Mapk8	0.248385921548241	15.0559861609124	4.34616631860663	0.00228840410996492	0.28294568884805	-1.10657711093577
Hnrnpa1;Hnrnpa2b1	0.35241486600291	18.8618360060816	4.33831235910633	0.00231323860867728	0.28294568884805	-1.11589552877315
Lcat	-0.720225978362574	16.540994646273	-4.33235556221365	0.00233226788882958	0.28294568884805	-1.12297054863988
Kcna1;Kcna10;Kcna2; Kcna3;Kcna4;Kcna5; Kcna6;Kcng3	0.385483404371183	15.2787359566296	4.30847992145481	0.00241025016404167	0.28294568884805	-1.15139315195603
Gsta4	0.206690168790448	17.7826563317538	4.29295548114784	0.0024624600763413	0.28294568884805	-1.16992985316768
Mfsd1	0.380031892783233	14.2870932579625	5.32501295206121	0.00270610853255006	0.28294568884805	-1.17832278347296
Vil1	-0.539341854922057	14.6730610633953	-4.27851914830564	0.00251210473178665	0.28294568884805	-1.18720666730464
Cxcl12	-0.530141437035638	15.283837266371	-4.2628247879096	0.00256730087361762	0.28294568884805	-1.20603200054701
Vtn	-0.295869846147472	21.8035526071239	-4.25831070692389	0.00258341734322873	0.28294568884805	-1.21145490471988
Thbs1	-0.484209654529341	17.3950917454603	-4.24519518353956	0.00263086418328536	0.28294568884805	-1.22723194809498
Tagln2	-0.217721521208592	18.8380492813455	-4.2291650785508	0.00269013199908682	0.28294568884805	-1.24655733457915
Gfra3	-0.262251188083376	15.3509500139011	-4.22671100425451	0.00269933148489108	0.28294568884805	-1.24951999202636
Mfsd9	0.349963431690862	13.2859408116401	4.41316686740059	0.00285809218265685	0.28294568884805	-1.25995378974535
Pla2g4a	-0.548341815535231	14.278196131194	-5.19290375179241	0.00303156095194339	0.28294568884805	-1.2638423228917
Smap1;Smap2	0.796777944639901	15.6221254305812	4.69524585519434	0.00300774383020192	0.28294568884805	-1.26818750536083
Rnf220	-0.281318753636199	14.3876278975911	-4.20408793030356	0.00278574914392591	0.28294568884805	-1.2768827210294
Hspa12a;Hspa12b	0.356416818569276	18.4615976621253	4.20403168542366	0.00278596766495521	0.28294568884805	-1.27695086461932
C1qtnf3	-0.519856639028708	15.7966979097971	-4.39543381290564	0.00292181803860321	0.28294568884805	-1.27874825871538
Mta1;Mta2;Mta3	0.30509963557019	18.0290184983255	4.19229635083544	0.00283196707663588	0.28294568884805	-1.29118130170098
Kcna1;Kcna2;Kcna3	0.523444639517383	15.4873068249175	4.18640170987523	0.00285537999849465	0.28294568884805	-1.29833858765802
Tmem186	0.239494466419528	13.7841244575799	4.15472415452964	0.00298481500390984	0.28294568884805	-1.33690851118749
Il1rap	-0.504125024755524	17.9899895890245	-4.12408122621962	0.00311603697357329	0.287525229834263	-1.37438981483411
Arhgap18	-0.697855164656008	16.1712833654343	-4.10251870113037	0.00321208047824447	0.293057230149945	-1.40086477996503

Mgst1	0.309965387493193	17.0266544803543	4.08736779067289	0.00328146358824856	0.296060937073092	-1.41951690085064
Serinc1	0.216416447831133	16.5191402468488	4.07359223924624	0.00334594505285009	0.297927816547239	-1.43651118778124
Nipa1	-0.345305433732719	16.1839584510155	-4.06736540452197	0.00337553683772734	0.297927816547239	-1.44420398762841
Krt1;Krt2;Krt4;Krt5; Krt6a;Krt6b;Krt7;Krt71; Krt72;Krt73;Krt74;Krt75; Krt76;Krt77;Krt79; Krt8;Krt84	-1.03310879297707	16.9445683245769	-4.21974161979897	0.00364449517931055	0.301972457714303	-1.46814681431298
Lin7a;Lin7c	0.297359928954098	15.5962011551451	4.87910029091042	0.00400441443104438	0.314786075399084	-1.47825023600196
Lamb1	-0.412386929029569	20.5730488615863	-4.03148729089775	0.0035515991969674	0.301972457714303	-1.48866213402393
Ifitm3	0.299829307208277	15.3386817725628	4.02749948675532	0.00357176785247879	0.301972457714303	-1.49361759329861
Cuta	0.565679256027851	14.3452817210924	4.82065858361649	0.00263276482098487	0.28294568884805	-1.50381767852626
Rpl14	0.375388038229026	20.415883982501	4.01577820118333	0.00363176299893443	0.301972457714303	-1.50819925076312
Nenf	-0.201215654617345	15.9920889825493	-3.9850629560258	0.00379415839221039	0.308085661447484	-1.54652405835501
F8	-0.749330903687222	15.5971648646237	-3.97766618833166	0.00383441662567718	0.308271910896027	-1.5557779270167
Selenop	-0.712440424813924	17.8600901025905	-3.96705285579501	0.00389298231518714	0.309911925483525	-1.56907255557192
Nsa2	0.364473998344776	13.6822258301523	4.33454593083891	0.0044668154220134	0.326153344939464	-1.59753776278771
C5	-0.406066453769068	16.9899543837171	-3.94257372246077	0.00403174283762373	0.314786075399084	-1.5998104075182
Kcna1;Kcna2; Kcna3;Kcna5	0.466736547316092	14.6631272634047	4.69255169776494	0.00475319435705735	0.326153344939464	-1.61357518111428
Ranbp17	-0.412127024828866	14.016579970933	-4.66340052150305	0.00488427153205002	0.326153344939464	-1.63527080544671
Bclaf1;Thrap3	-0.371980484930138	15.981679111217	-3.89032099070107	0.00434595155314635	0.326153344939464	-1.66576804679544
F13b	-0.551361181486577	14.6387944538465	-4.25972202080947	0.00486029405435022	0.326153344939464	-1.66892598517668
Dhx36;Dhx57	0.333386483415008	16.3441023543363	4.01686644506799	0.00473116466276684	0.326153344939464	-1.69404099251394
Cst3	-0.200739253004375	16.9042576689065	-3.86763824137057	0.0044904037967898	0.326153344939464	-1.69454521123031
Shisa4	0.497048796665913	14.1467850105498	3.86147862345151	0.00453050979725262	0.326153344939464	-1.70237486629072
Abhd17c	0.325657720510675	13.8227703483442	4.21431399184106	0.00511787383769098	0.326153344939464	-1.71276950474901
Afap1	0.248968811759811	13.8879702610498	3.85057696719327	0.00460243216838281	0.326153344939464	-1.71624797131979
Dhrsx	-0.320377033783799	13.7861939536565	-4.19159200761636	0.00525245421603786	0.326153344939464	-1.73485659935077
Scn8a	0.271203375704005	14.7764746647932	3.82566185562985	0.00477142201857117	0.326153344939464	-1.74802927920392
Rdh5	0.229844971729351	15.2277611442465	3.8228963436577	0.00479058368542746	0.326153344939464	-1.75156334138289

Ngef	-0.27941947171878	14.2274857237168	-4.1694839584277	0.00538719495614488	0.326153344939464	-1.75644179397177
Sdhc	0.447353155283039	16.3945111112188	3.81614968042624	0.00483767515896125	0.326153344939464	-1.76019030197583
Fabp3	0.289255855897597	17.520856064051	3.79554636270164	0.00498456668158662	0.326153344939464	-1.78658273259556
Sphk1	0.392525623719024	15.0077419283837	3.78563323735945	0.00505693009944956	0.326153344939464	-1.79930635926139
Mt-Cyb	-0.208335266111321	15.9427417755555	-4.11823340417102	0.00571460956000951	0.326153344939464	-1.80684066148627
Neu1	-0.241004331469524	14.5551687590805	-3.76700422300081	0.00519596361114834	0.326153344939464	-1.8232608588428
Mrpl2	0.211900463192379	15.8443697907551	3.75548801645123	0.00528394471278702	0.326153344939464	-1.83809775634357
C8a	-0.47736425426465	16.3076846067921	-3.74154552337266	0.00539259031097043	0.326153344939464	-1.8560896036013
Clvs2	0.215975172636796	14.2687907396592	3.73681318705422	0.00543000520726171	0.326153344939464	-1.86220357098841
Igf2	-0.544593498875368	15.3155878794708	-3.73425108852538	0.00545037693863978	0.326153344939464	-1.86551520816919
Rab13;Rab3a;Rab3b;Rab3c;Rab3d;Rab8a;Rab8b	0.331842532095976	17.4246712590306	3.7334013353012	0.00545715143986544	0.326153344939464	-1.86661379121392
Rpl27a	0.344797747339616	20.4356794349346	3.73011491979699	0.00548343625812674	0.326153344939464	-1.87086365830084
Rps14	-0.202794081198967	21.7152847818222	-3.72629265615384	0.00551417638734803	0.326153344939464	-1.87580866790964
Tmem45b	-0.22406487825703	15.3894209742829	-3.72166940715109	0.00555160360578255	0.326153344939464	-1.88179310607644
Pgk2	-0.649590201427134	16.8794339651202	-3.8491637796131	0.00589754239283644	0.326153344939464	-1.88652871349724
Ube2d1;Ube2d2;Ube2d3	0.73452880070513	14.9680686434523	3.84856278571392	0.00590224614172861	0.326153344939464	-1.8872277772985
Cacnb2;Cacnb3;Cacnb4	0.40044622536856	13.3823243758751	3.84568352768153	0.00592483749632826	0.326153344939464	-1.8905777800569
Amz2	-0.350579021661657	14.6166307769116	-3.70668809921305	0.00567475223158682	0.326153344939464	-1.90120897418921
Napsa	-0.289472342741719	14.700321489619	-3.70398482461237	0.00569728137921028	0.326153344939464	-1.90471628581142
Slc27a1;Slc27a4	0.312052891701891	15.6921730279102	3.82321947421693	0.00610434907086767	0.326153344939464	-1.91676615491575
F5	-0.361881631243907	19.6840433755388	-3.67751125388933	0.00592300687648941	0.326153344939464	-1.93912578433777
Parvb	-0.255668015921319	17.1942696915271	-3.67168254300438	0.00597397062188503	0.326153344939464	-1.94671676944062
Gskip	0.272765149501394	14.8490393480221	3.66590416886604	0.00602495444835509	0.326153344939464	-1.95424752000157
Prg4	-0.710491769023555	18.6253936436854	-3.66006100135145	0.00607698033831214	0.326153344939464	-1.96186808830588
Sfswap	-0.371844305033267	12.9320290651342	-4.22946441891764	0.0074247614727359	0.346488868727676	-1.97647248845381
Serpina1a;Serpina1b;Serpina1c;Serpina1d	0.597327921818097	15.2777180194126	3.64639488622226	0.00620053187282831	0.326153344939464	-1.97971225267435
Slc7a6os	-0.267199143692325	14.0432800038626	-3.94421500442807	0.00700293587587607	0.336571141992354	-1.9817324083182
Mmp19	-0.748512599293186	18.8228417017181	-3.64425287178848	0.00622013783506202	0.326153344939464	-1.98251179346543

Igbp1;Igbp1b	-0.417331714292189	13.9066585159207	-3.7476594354253	0.00675273480813168	0.334919006517804	-2.00552012845164
Hspa1a;Hspa1b;Hspa1l; Hspa2;Hspa5;Hspa8	-0.213801103525242	23.095359819654	-3.62451688776838	0.00640391023180464	0.326153344939464	-2.0083398425754
Lbh	-0.452609051787816	14.7547713369397	-4.11718383197989	0.00572154236880586	0.326153344939464	-2.01100971041695
Glrx	0.493147223741579	15.1414262700945	3.61856919160439	0.00646041593695522	0.326153344939464	-2.01613536520368
Samd4a	-0.359705396707703	14.6247626703873	-3.73713508862255	0.00684880858943481	0.336571141992354	-2.01796319457826
Fbxo7	0.271413704248515	15.6874035418423	3.61370717292317	0.00650700023155089	0.326153344939464	-2.02251198957074
Tubb3;Tubb6	0.482165532283648	21.2986029357679	3.58749368473858	0.006764374023266	0.334919006517804	-2.05695427971152
Slc9a1	0.225103642031709	14.6742935285527	3.57522263375129	0.00688854504219941	0.336571141992354	-2.07311357467683
Mrps5	0.250307664329775	16.0233697534985	3.56392621640995	0.00700499051683594	0.336571141992354	-2.08800964385623
Mtss1	-0.237050270961353	16.0400738403975	-3.53995504055749	0.00725905314963239	0.346488868727676	-2.11968308092866
Fga	-0.372704604445543	15.5160223578457	-3.53393026172443	0.00732443017765393	0.346488868727676	-2.12765723215941
Ldb2	-0.256487310123532	14.61660242445	-3.64074033442875	0.00780078257289537	0.348831647641788	-2.132841428229
Mtatp6	0.41686964171101	16.1781726480349	3.79732062666083	0.00834397507316913	0.351052215513644	-2.13389080766967
Cox7c	0.368167432625313	18.7641532695914	3.52906411929658	0.00737768940446719	0.346488868727676	-2.13410180304071
Dnajb6;Dnajb7	0.324545559033076	15.6248896434732	3.52652689318531	0.00740562142171949	0.346488868727676	-2.13746342241662
Ttf2	-0.264478161279897	14.7558446757886	-4.02868340144682	0.00909510209904003	0.365605094278243	-2.14632530191781
Igfbp2	-0.678114778688881	14.6366285550185	-3.61455194088475	0.00808343539147853	0.350003170928272	-2.16433161424006
Mfsd5	0.234415062500492	15.3551294958757	3.49625385175626	0.00774766215218916	0.348831647641788	-2.17764597900447
Ttc26	-0.200623230368571	14.6269579211984	-3.49596874884782	0.00775096170401496	0.348831647641788	-2.17802504523802
Serpinb1a;Serpinb1b; Serpini2	0.75091561900148	13.9596311928676	3.49157733380888	0.00780197253862352	0.348831647641788	-2.18386526380095
Sh3bgr	-0.53066320750413	13.1710679903234	-4.29273132301791	0.00697340515550698	0.336571141992354	-2.18763883426532
Brix1	0.285887002608398	13.8657795883362	3.47921246141161	0.00794751906573039	0.348831647641788	-2.20032455042518
Ugt1a6	0.224801571158132	17.7918533685584	3.47405024085298	0.00800913004684288	0.349645892367549	-2.20720268639084
Podxl	-0.22308749229382	14.1007398398292	-3.46605858830148	0.00810550766082978	0.350003170928272	-2.21785830789087
Mtnd4	0.419805729000563	15.6288388063014	3.46025858114917	0.00817622137607971	0.350003170928272	-2.22559743838488
Hbb-b1;Hbb-b2	-0.468721686703269	21.6628840934159	-3.4591566714972	0.0081897293690113	0.350003170928272	-2.22706829356228
Ankrd13a;Ankrd13d	0.775955275164396	13.9265475919038	3.93063474394651	0.0100644595564718	0.369789192753624	-2.2321125816161
Sra1	-0.21537745359254	14.6593142567163	-3.45415651975526	0.00825132159913954	0.350789169555042	-2.23374478693709
Rbp4	-0.365246509065372	17.0645304851202	-3.6738445621226	0.00969272719495278	0.369016214465239	-2.26497883650458

Ces1;Ces1f	-0.525958529802963	21.6957078734003	-3.42211676390145	0.00865777786175644	0.357047246509821	-2.27660993513442
Itih1	-0.599716376397573	19.9307601891768	-3.41954347543573	0.00869132665025914	0.357047246509821	-2.2800589060908
Rpl10;Rpl10l	0.283450278768822	19.4403505659531	3.41839648576678	0.00870632448386015	0.357047246509821	-2.28159650935455
Dhx40	-0.399898817875178	13.0068586813621	-3.65113578662756	0.00996607710277344	0.369016214465239	-2.28940198277371
Macroh2a1	0.208190762013963	19.1090555856632	3.39696869753719	0.00899158589618474	0.364492446172449	-2.31035505468115
Smarcd3	-0.233480360289651	14.0560396229476	-3.39468715403096	0.00902253468973674	0.364492446172449	-2.31342086166497
Sncg	-0.208824536749091	22.5472555390655	-3.38042183990342	0.00921860451307501	0.368744180523	-2.33260583386857
Atp5f1e	0.358605397585627	19.0824929331725	3.37549717153262	0.00928732991234338	0.369016214465239	-2.33923526331313
Tuba1b;Tuba1c; Tuba4a;Tuba8	0.887169064574575	15.1638463888956	3.46846974828359	0.00987659173627092	0.369016214465239	-2.34212831422191
Mmd2	0.318619360546858	14.7277092783879	3.46835724139106	0.00987812738321229	0.369016214465239	-2.34226661844848
C4b	-0.40073506105816	20.4877201653683	-3.36839289341098	0.009387424874471	0.369016214465239	-2.34880456114258
Asphd1	0.261201292123364	13.1493333679183	3.36593435893753	0.00942232822303566	0.369016214465239	-2.35211772575529
Ino80c	-0.432754130613572	13.1168329397036	-3.67737288750476	0.00965100272449153	0.369016214465239	-2.37677996207388
Fubp1;Khsrp	-0.270989092845468	16.9463792009468	-3.99076210445553	0.00945679073144417	0.369016214465239	-2.38176435974243
Krt10;Krt14;Krt15;Krt16; Krt25;Krt27	-0.651399445190968	20.0538878536847	-3.33171132645085	0.00992262959567186	0.369016214465239	-2.39832049138208
Stxbp2	-0.338835927530919	15.6201639938104	-3.32671501861774	0.0099979762539843	0.369016214465239	-2.40507859682348
Fhip2a;Fhip2b	-0.235267650788686	14.9584987612229	-3.31690376260327	0.0101476907575043	0.370353157208513	-2.41835889568372
Fam169a	-0.202894198171997	17.3465769043205	-3.31538806839969	0.0101710288248151	0.370353157208513	-2.42041161143683
Slc17a7	0.249183748273239	14.6755938968523	3.71459925126309	0.0126457932307101	0.377514121446198	-2.42781075720367
Crtac1	-0.222167821036177	14.8444014953208	-3.51802056341351	0.0117493524797206	0.377514121446198	-2.43450849095442
Ankib1	-0.200766351387504	13.5978031737039	-3.28293147420331	0.0106845566754506	0.377514121446198	-2.46443794605844
Tubg1	-0.302373021523584	13.4926316544939	-3.28174924886864	0.0107037682341238	0.377514121446198	-2.46604410064329
Serpina1a;Serpina1b; Serpina1c;Serpina1d; Serpina1e	0.384666499319781	15.2529018597967	3.36094623591465	0.0114679639364	0.377514121446198	-2.47523824109666
mt-Nd2	0.341534167237402	15.8281185269683	3.27305192155773	0.0108462223517416	0.377514121446198	-2.47786550754341
Chd1	-0.295228190446919	13.1789681865271	-3.27219944460785	0.0108602918311319	0.377514121446198	-2.4790246985723
Mast1;Mast2	0.249191464979209	15.0252008986123	3.3544304696348	0.0115728457626747	0.377514121446198	-2.48336342853493
Kiaa1671	-0.421707017438898	13.3710634528235	-3.65115006921266	0.0135413821571058	0.38446161928566	-2.48704369255814

Ksr1	0.251948393531691	14.284687848999	3.26623253779543	0.0109593089084718	0.377514121446198	-2.48714095759281
Prss23	-0.3047470222069	13.3556087575486	-3.47046701987721	0.0124691522331792	0.377514121446198	-2.48714113525296
Surf6	0.261263270444456	15.4375755904293	3.26214152001983	0.0110277439132396	0.377514121446198	-2.49270813813299
Lum	-0.324929852029218	16.1423118054055	-3.2619634841059	0.011030732280767	0.377514121446198	-2.49295046133693
Serinc5	0.274585116653704	16.4813027818855	3.2615510400856	0.0110376584988195	0.377514121446198	-2.49351185036337
Fgb	-0.29078294485034	15.4881591601841	-3.2603584232386	0.0110577119313835	0.377514121446198	-2.49513527133467
Ppp1r1c	-0.345263649941563	15.8619353291598	-3.25504919554509	0.0111474496797957	0.377514121446198	-2.50236443520647
Amn1	-0.238727980363089	14.6981470432462	-3.25361072069252	0.0111718944065291	0.377514121446198	-2.50432368545435
Ckm	-0.246450332822857	14.9628288150716	-3.25250759886705	0.0111906784004593	0.377514121446198	-2.50582634394868
Strn3;Strn4	-0.344991624871266	14.3061362685823	-3.62661751978383	0.013906765035725	0.384524493678371	-2.51016037612057
Rem2	0.223188245009696	15.1972843419915	3.23904537451989	0.0114226008662727	0.377514121446198	-2.52417625188364
Rad23a;Rad23b	0.257987722915473	17.3871501288306	3.23852604666214	0.0114316479966932	0.377514121446198	-2.52488456650207
Mafk	-0.353277712579979	13.1160446580496	-3.31025273340935	0.0123115803795113	0.377514121446198	-2.53862625068868
Cacna1c;Cacna1d	-0.308989187054788	14.004435146678	-3.30576813329688	0.0123893413175887	0.377514121446198	-2.5442528192543
Ist1	-0.20408301076894	17.1692097691639	-3.22145404601117	0.0117332773747972	0.377514121446198	-2.54818703232433
Tmem258	0.302425719710055	16.646939750222	3.21614280987269	0.0118288084680484	0.377514121446198	-2.55544362849311
Rac3	-0.291119000618089	14.8803942282656	-3.2116297636832	0.0119106230865555	0.377514121446198	-2.56161227056925
Srgap1;Srgap2	0.248594932730828	16.5005945626427	3.20955528949528	0.0119484287482081	0.377514121446198	-2.56444855388925
Ythdf1;Ythdf3	-0.207901847757672	16.3316389370367	-3.2035082753912	0.0120593495490648	0.377514121446198	-2.57271905786275
H2ac11;H2ac12;H2ac13; H2ac15;H2ac20;H2ac21; H2ac25;H2ac4;H2ac6; H2ac7;H2ac8;H2aj;H2ax; H2az1;H2az2;Hist1h2af; Hist1h2an;Hist1h2ao; Hist1h2ap;Hist2h2aa1	-0.244803624759623	23.8105720937026	-3.27270189015103	0.0129791391956898	0.379628413116699	-2.58583263941839
Calm1;Calm2; Calm3;Calml3	-0.269264252481623	22.6887737420398	-3.19088359793161	0.0122944139058819	0.377514121446198	-2.58999938813165
Serpina1a;Serpina1b; Serpina1c;Serpina1e	0.412546348028895	13.2122141533982	3.37722759243284	0.0140249054146143	0.384524493678371	-2.59153190520313
Ube2g1	0.242063953350211	15.7355936143395	3.18463419043579	0.0124125440399061	0.377514121446198	-2.59856013436634

Krt2	-0.690607133104901	19.46383598377	-3.18235358813637	0.0124559486339298	0.377514121446198	-2.6016853152601
Clca1	-0.946078820467998	14.6197407183069	-3.66932875651794	0.0132776440055594	0.379628413116699	-2.60780261411376
Nid1	-0.262783367559543	20.6881994381394	-3.17649405493502	0.012568197316098	0.377514121446198	-2.6097174986227
Mtnd1	0.274716077772062	17.2471513717708	3.17601971680407	0.0125773301907598	0.377514121446198	-2.6103678844155
Ptcd2	0.218804136172995	14.4747958752354	3.169440531533	0.0127047236126026	0.377884086938948	-2.61939148058014
Bclaf3	-0.377776622190831	14.5355297095517	-3.64212974471271	0.0136744500015927	0.384476095970916	-2.62788099743021
Ilrun	-0.252880831605788	13.7320957917501	-3.23934680697099	0.0136045376264284	0.384476095970916	-2.62794016961259
Cers6	0.208152348560635	14.4916792967603	3.15901548973016	0.0129093545932847	0.379628413116699	-2.63369962594211
Prkd1;Prkd2;Prkd3	0.345104114860167	13.6512090548746	3.49311530692153	0.0161016022957367	0.392514377676741	-2.6380509986382
Fmnl1;Fmnl2	0.264781672769262	15.6307265770123	3.14586039979058	0.0131725002923122	0.379628413116699	-2.65177167180495
Ybx1;Ybx3	-0.449566767603626	15.1239047124788	-3.37316579747015	0.0140973446185215	0.384524493678371	-2.65251902743723
Cfb	-0.558973479433423	19.2996148528578	-3.14292988316983	0.0132318800268603	0.379628413116699	-2.65580007347358
Cryzl2	0.232487764862478	14.4131942632641	3.14240421045671	0.0132425610381088	0.379628413116699	-2.65652278118209
Git1;Git2	0.476055615329683	15.2086632161851	3.20422207114696	0.0142979696273058	0.384524493678371	-2.67245649104488
Krt76	-0.62790764307271	18.9968713279879	-3.12838729180617	0.0135307135560476	0.38446161928566	-2.67580445745326
Mug1;Mug2	-0.261320911554634	16.3624146899894	-3.1210601177245	0.0136839398689156	0.384476095970916	-2.68589198400423
Nedd8	-0.205048351685946	16.6007884097905	-3.11701269840002	0.0137693551760894	0.384524493678371	-2.69146658588725
Tepsin	-0.25763687880945	13.0989413826999	-3.27950729063554	0.0158863492447424	0.392514377676741	-2.70259936952376
Cdkn1b	-0.207715631628307	15.840089752878	-3.10751666597907	0.0139719470098512	0.384524493678371	-2.70455234405757
Ddx3x;Ddx3y	-0.336090120011839	16.4424278974374	-3.10312451288078	0.0140667001420328	0.384524493678371	-2.71060796786216
Acta2;Actc1;Actg2	-0.31077219925271	19.6594472838406	-3.09548066892505	0.0142332041623167	0.384524493678371	-2.72115149586743
Pak2;Pak3	0.326612844698401	15.6274301740629	3.26201519104932	0.0162471547477821	0.392689177405767	-2.72265603991517
Exosc4	0.284875180245963	14.3850951558238	3.09381301214625	0.0142698026172506	0.384524493678371	-2.72345256095094
Mcl1	0.267024156218367	13.6632703757791	3.40524889700507	0.0177591278197023	0.408510248997119	-2.72414753261518
Dmd;Drp2	0.325392351080069	16.4330073420833	3.16073352543643	0.0152090361914473	0.391519286358406	-2.72781500815709
Rrm1	0.202608389622029	14.1744094277463	3.08241959931758	0.0145224817413973	0.388843050632556	-2.73918085632699
Tubb2a;Tubb2b;Tubb4a;Tubb4b;Tubb5	0.292092679730501	19.9183041736058	3.080849313465	0.0145576708611203	0.388843050632556	-2.74134960419872
Tmem254	0.232279840216028	15.2643687643727	3.07552355682365	0.0146776807449118	0.390763172618635	-2.74870690306158
Rpl24	0.223931570674416	19.9457573568179	3.06968636557802	0.0148103997223536	0.39084974965523	-2.7567739136642
Slc44a1	0.293173631669852	16.1619866463083	3.0635675211431	0.0149508649850695	0.39084974965523	-2.76523371694077

Cnrip1	0.211385667688262	17.7645913714409	3.05783654511232	0.0150836844228618	0.391519286358406	-2.77316052364902
Atp6v1g2	-0.220672315105656	18.2517033221387	-3.0552234395822	0.0151446521287648	0.391519286358406	-2.77677588371493
Bpgm	0.207330004030963	14.7602688071369	3.05262979216712	0.0152054195069357	0.391519286358406	-2.78036496287169
Gpm6b	0.276799725192717	16.2534465306347	3.04926292922976	0.0152846814994599	0.391519286358406	-2.78502496190691
Steap4	-0.575165525379482	13.9597415977461	-3.10277797813829	0.016520170497877	0.39516685048847	-2.79514948242589
Hcn1;Hcn2;Hcn3;Hcn4	0.232192985832798	14.7350555893821	3.33320458513767	0.0192622377371494	0.418206872795864	-2.7958716861712
Mtif3	-0.33434225685424	14.3650646676696	-3.03863650855868	0.015537677956142	0.392514377676741	-2.79973970751559
Des;Vim	-0.227768047852447	23.222719638791	-3.03188184046859	0.0157007556114996	0.392514377676741	-2.8090985435097
Kcna1;Kcna10; Kcna2;Kcna3	0.224541603320944	15.4764114391672	3.02781865265262	0.0157997093045958	0.392514377676741	-2.81473024553218
H1-2	0.33016975673338	19.7908234883189	3.02382121044518	0.0158976946501025	0.392514377676741	-2.82027228246791
Rbl2	0.352788523146332	14.2026530425371	3.30645880917747	0.0198562222793653	0.418910037228488	-2.82275619787891
Rnase4	-0.416642118100018	16.9883481556236	-3.015654413693	0.0160998474726002	0.392514377676741	-2.83159915523772
Gpatch11	0.352485684280991	14.3190501708797	3.01441975659173	0.0161306406024983	0.392514377676741	-2.83331207002468
Efemp1	-0.451454364040755	15.4358715117733	-3.00585553569073	0.0163459288131957	0.392689177405767	-2.84519743262974
Nckap5l	-0.295611349876301	13.4337258611033	-3.15500481595409	0.0186580782946902	0.411694553676316	-2.84648302154774
Serpinb1a;Serpinb1b	0.301004040977734	15.9909879810869	3.34051168780366	0.0191034460924533	0.418113159759355	-2.86072211569972
Kbtbd3	0.200992457056328	14.2214723210156	2.99198995917961	0.0167008311198674	0.397685480039072	-2.86445348933789
Ppp1r1a	-0.30947004484479	14.8826521500857	-3.03450336157989	0.0182201109397804	0.40896280718404	-2.87081146456089
Pnpla6;Pnpla7	0.304668724855087	14.9175707569003	2.97509372564018	0.0171441434515613	0.401182838117227	-2.88794045479111
Tubgcp6	-0.362540712006624	13.7540803438818	-3.11823984134543	0.0195738973431556	0.418910037228488	-2.88946241288886
Stk11	-0.307153277996424	14.3139223476297	-3.11478547339367	0.0196624174924528	0.418910037228488	-2.89351188486059
Unc13a;Unc13b;Unc13c	0.256964621349068	14.1791309031388	3.23172264375185	0.0216278437991973	0.427140289445907	-2.89861317700704
Ramac	-0.231259394518322	15.276035344294	-3.0205981608234	0.0185884788133097	0.411694553676316	-2.90791934138197
Gstm1;Gstm2; Gstm4;Gstm7	0.368607871261808	18.8331613500315	2.95990459434526	0.0175530832949556	0.408398384971459	-2.90907447308422
Cotl1	0.21345637011763	18.748850972727	2.95801465233814	0.0176046692817165	0.408428327335824	-2.91170541844126
Ppp1r14b	-0.390515119959236	13.9368420613585	-3.21746469004254	0.0219855657152096	0.430175406283137	-2.91320678762695
Clec2l	0.22348626034308	14.9604482904935	2.954849522111	0.0176914136947945	0.408510248997119	-2.91611215837151
Slc25a18	0.277606831736447	14.3573279407798	2.94743756311554	0.0178962849741037	0.40896280718404	-2.92643474181602
Ppia	-0.201443374904851	23.0191988648526	-2.94422869149658	0.0179857410413617	0.40896280718404	-2.93090504003326

Iqsec3	-0.266131387545268	13.7450053615369	-2.93949082085005	0.018118669621135	0.40896280718404	-2.93750684341116
Lama1	-0.360006522979774	20.6716472280827	-2.93593123929743	0.0182192083625944	0.40896280718404	-2.94246793098919
Arhgap6	-0.236258047621893	13.2845885624917	-3.06695234163995	0.0209337568856187	0.424157032064912	-2.94978029480613
Mif	0.381783063329362	17.6882069036861	2.9262684220528	0.018495052154861	0.411694553676316	-2.95594007119967
Tsc22d3	-0.24876090620787	14.4324084494483	-3.05024345338046	0.0213985837494941	0.426762122658931	-2.9695202721838
Josd2	-0.435621591806543	13.7883277788654	-3.18725182395994	0.0227656635790224	0.439090708460005	-2.98624203365788
Ecm1	-0.354220766815519	15.7256125030741	-2.90055123028882	0.0192504501064445	0.418206872795864	-2.99182879505065
Yod1	-0.225765380520121	13.4538564754845	-2.94992260584539	0.0205862187028547	0.423307806817296	-2.99967199815399
Tmem209	-0.202743806285222	15.5548026234444	-2.88598698643425	0.019692325295781	0.418910037228488	-3.01217393672604
Lims1;Lims2	-0.405685440691371	16.3905012905766	-2.88564501747892	0.0197028255341233	0.418910037228488	-3.01265181345966
Srgap1;Srgap3	-0.223993493882091	14.8344407635383	-2.88197937208202	0.0198157438790189	0.418910037228488	-3.01777477385696
Otud3	-0.440748493647847	13.54533782978	-2.92179339408107	0.0214431757309191	0.426762122658931	-3.03634668439532
Cyp2j5;Cyp2j6	0.234040525978353	13.9245484337122	2.99037369064839	0.0231578367418016	0.445596289913339	-3.04060084767717
Emg1	-0.236794837049224	13.9701722599193	-2.86350469878061	0.020395100410065	0.423276094598822	-3.04360753906316
Aida	-0.222730942729553	15.092284319064	-2.86285588296859	0.0204157618074879	0.423276094598822	-3.04451515976459
Igfals	-0.324020847024672	14.9228400295706	-2.91446204065577	0.0216726353758268	0.427140289445907	-3.04591924527885
Fosl2	-0.219929412619173	13.6273755525601	-2.98477369385353	0.0233301968754942	0.447851533401922	-3.0472769455511
A2m	-0.399036997869022	19.7914826659756	-2.85312056844516	0.0207283860806287	0.423307806817296	-3.05813689882998
Fads2	0.201597334935556	16.4859855949085	2.85250439261422	0.0207483383144438	0.423307806817296	-3.05899925243575
Ints14	0.238926237276948	13.5526894536383	2.97066642286899	0.0237705550771176	0.452030227696006	-3.06411553236989
Gria1;Gria3;Gria4	0.213855944007177	13.8915506876979	2.83957710601809	0.0211715292741937	0.426762122658931	-3.07709653598749
C3	-0.362920596414025	21.5374133669151	-2.83667567490227	0.021267727462856	0.426762122658931	-3.08115967880071
Hp	-0.493451726703956	22.2676748712133	-2.83349797335728	0.0213736023053898	0.426762122658931	-3.08561026275061
Cwc25	-0.216843132137791	16.0380244452026	-2.81971299513054	0.0218392133931724	0.42867454956307	-3.10492360473879
Fhl3	0.236035138762634	14.8800968375418	2.81921971658922	0.0218560669358511	0.42867454956307	-3.10561490247681
Rtn2	0.503112916942426	13.569761243706	2.9266140091766	0.0252042099811648	0.466223438626807	-3.1168823531204
Hexd	-0.255966263425204	13.0365077277341	-2.82659392977628	0.0246324236135562	0.461225705288068	-3.16107232649027
Rrs1	0.206466628352304	15.0541974556733	2.77422430052185	0.0234510619848326	0.448053231333742	-3.16872525719649
Ctbp2	0.210990708819347	15.6307033868447	2.76897681148717	0.0236447063554741	0.45069252489777	-3.17609163497329
Zcrb1	-0.319400301785002	12.7960670959653	-2.80929824692325	0.025263339038891	0.466223438626807	-3.1838252732097
Krt10;Krt13	-0.708360827566921	17.7247511399127	-2.76338531458523	0.0238528523924518	0.452535423894179	-3.18394225462311

Mpv17	0.2426107159963	13.8829685692029	2.80314270251701	0.0254919414366183	0.466343079243219	-3.1919294824228
Abca8a;Abca9	0.321958139754909	14.0389805597499	2.79868760593036	0.0256587416806444	0.467150184858369	-3.19779699633566
Ess2	-0.465698157909747	12.2094325642427	-2.80302457363322	0.0297451113146747	0.488347798444553	-3.2171739643954
Nfe2l1	-0.353799465326533	13.2127582373437	-2.91359879650309	0.0314229917539135	0.496508242448214	-3.22231231534536
Cisd1	-0.226970248704095	20.5691934684905	-2.73479800243886	0.0249467788539348	0.465225157199487	-3.22409969113654
Tbp	-0.419932126489265	13.4245878247024	-2.91118216994769	0.0315141675365006	0.496883573585214	-3.22446383019035
Jam3	0.381338341081461	15.9474152469902	2.7339482889436	0.0249800700171153	0.465225157199487	-3.22529379074835
Mapk10	-0.375760340423065	14.9761353345384	-2.83552956570749	0.0284716128288961	0.480643443182197	-3.22683926096003
Hba	-0.289543088913856	20.5290482618138	-2.72810028371332	0.0252104285213744	0.466223438626807	-3.23351267908348
Rpp38	0.238846985211593	13.7188891509968	2.7276127116616	0.0252297324477666	0.466223438626807	-3.234197976179
Ednrb	0.260762274248295	13.7367589807895	2.77094950897712	0.0267232472367156	0.476288794476238	-3.23436700101852
Itih2	-0.44050264243927	20.8490513864872	-2.72383741445471	0.0253797171115462	0.466302923465783	-3.2395045491403
Gpaa1	0.236432726399478	16.941989017125	2.71969263751	0.0255454321111957	0.466343079243219	-3.24533102515452
Frmd4a;Frmd4b	0.213589908446052	13.2267275205369	2.71318395580028	0.025807898395331	0.468177259404468	-3.2544816833159
Tgs1	-0.222540366392185	14.7643879285567	-2.69877732328438	0.0263987113874027	0.474242337313518	-3.27474090741895
Cyth1;Cyth2	-0.378228281529868	14.3372615100023	-2.87456106429096	0.0329322036952751	0.501297970843976	-3.27551811654022
Ifit2	0.257147783291535	13.5268162083268	2.87368111179459	0.032967132565355	0.501297970843976	-3.27647472639448
Pef1	0.205617858506663	14.7396677452653	2.68322365227085	0.0270521055512844	0.476288794476238	-3.29661980374802
Pllp	0.641622385731457	15.5269642540216	2.68190499506593	0.0271082553707746	0.476288794476238	-3.29847501225772
Tbc1d12	-0.357474596143874	13.3255727444404	-2.82728364303806	0.0348679877921841	0.507727253375469	-3.29986198222701
Adipoq	-0.445029063480124	18.1364398402229	-2.67996803150385	0.0271909492624555	0.476288794476238	-3.3012001893707
Eno3	-0.348614132102114	16.9172425133182	-2.71555347593135	0.0289893888785335	0.4820800472459	-3.30758496751549
Gpsm2	0.311641668064468	14.0307507244383	2.8322357077518	0.0346594614641922	0.507727253375469	-3.32167744282081
Nip7	0.290006503010801	13.4522171926848	2.70475414399946	0.0294540037004507	0.485297775280568	-3.32188504758914
Atf3	-0.345657871533284	17.9855203542488	-2.70451204397289	0.0294645077848916	0.485297775280568	-3.32220572058688
Plaur	-0.227815308280338	14.3271554434866	-2.65857174968098	0.0281217301064686	0.478489120628612	-3.33130903834497
Ambp	-0.386264032524515	20.1051574067317	-2.64764338430746	0.0286096136006947	0.480973214156607	-3.34669101829791
Ypel5	-0.216485062808982	14.434670016552	-2.64276970225804	0.0288299670590508	0.4820800472459	-3.35355153195118
Krt5;Krt6a;Krt6b;Krt75	-0.521548872981956	19.2859404161434	-2.6404947202007	0.0289334170074041	0.4820800472459	-3.35675407540915
Ssbp2;Ssbp3	-0.242828387955262	15.5532224053965	-2.6389999101606	0.0290015961277088	0.4820800472459	-3.3588539624246
Rab22a;Rab31	0.256408571739613	15.7367463497513	2.62239671708456	0.0297699704716815	0.488347798444553	-3.38223361788363

Bgn	0.847851436194116	15.6201403274237	2.62076936741749	0.0298463887606185	0.48836220675094	-3.38452490236847
Antxr1	-0.344374247198399	13.2343694068257	-2.70352109301235	0.0340358854029523	0.507727253375469	-3.38806887767855
Mrpl34	0.26716014043142	15.0049080487488	2.61778206818661	0.0299871885120432	0.48836220675094	-3.38873104754634
Col6a1	0.917878362453632	19.5685060478919	2.61414263140584	0.0301596389099541	0.488814906085483	-3.39385552575599
Masp1	-0.274152806902071	15.6470300098068	-2.63374320725156	0.0374347101845869	0.51259670606888	-3.39541614226
Rasa4	-0.21358191602674	14.149926974728	-2.60485076347399	0.0306045126474875	0.49405296758966	-3.4069393685296
Hypk	-0.214813369393895	16.0229703358524	-2.59612617159558	0.0310282988049804	0.496508242448214	-3.41922495584392
Plg	-0.381920029141376	20.9786750506191	-2.58798312133446	0.0314292163323131	0.496508242448214	-3.43069195156544
Hbb-b1	-0.224972285835307	21.5488263310133	-2.57803321051047	0.0319262425879163	0.497044376387676	-3.44470356333518
Clcn2	0.332506874074799	13.3659965229887	2.65736827143117	0.036245335869253	0.507727253375469	-3.44490470501812
Luzp2	-0.27114350404775	14.5999447706421	-2.57780102865265	0.0319379355125088	0.497044376387676	-3.44503052615476
Fkbp14	0.34318181721483	13.721577609957	2.66946540073458	0.0422921972574998	0.533249443681519	-3.44528569983655
Dph2	-0.227928758667078	15.3611272274016	-2.57750494771023	0.0319528527677792	0.497044376387676	-3.44544747284622
Cpb2	-0.607822468814987	17.6188085172159	-2.56731211492326	0.0324707255266963	0.501204006569932	-3.45980115440918
Clvs1;Clvs2	0.293557572229052	14.5496680347397	2.55636896470181	0.0330362009576104	0.501409255655694	-3.47521111317799
Pzp	-0.239976399256893	23.0250876197924	-2.55517881110556	0.0330982996641407	0.501414539688102	-3.47688703297507
Arl6ip1	0.207657593929142	16.7932363981927	2.54438342614813	0.0336670005168681	0.506087153563346	-3.49208816452965
Gpx3	-0.303896948761089	17.0986646979227	-2.54259625429382	0.0337620990967139	0.506087153563346	-3.4946046170131
Tspan15	0.264932261222226	15.7968022523256	2.52178941038361	0.0348894824485042	0.507727253375469	-3.52389944042289
Dapk1	-0.220234906766139	14.2810393119149	-2.519236547661	0.0350304026649168	0.507727253375469	-3.52749333339309
Nras	0.22152977734253	14.8006029938338	2.51912293530017	0.0350366875215433	0.507727253375469	-3.5276532733749
Fmnl3	-0.204365705368867	14.0737295084099	-2.54067358337487	0.0375456961034507	0.513250929899024	-3.53999058233138
Ubqln1;Ubqln2	0.229454330330393	14.8889150399693	2.52630905620935	0.0383556090106036	0.51478933085306	-3.55914180856291
Stk25;Stk26	-0.241852556445821	16.4334964881938	-2.49570223118225	0.036356914803603	0.507727253375469	-3.56061940806791
Col6a2	0.906876326844124	19.3717105042587	2.49368496232053	0.0364729518541477	0.507727253375469	-3.5634583356579
C8b	-0.586249562352954	14.6166678922981	-2.49293226057226	0.0365163443314377	0.507727253375469	-3.56451759912701
Tox4	-0.264470849069284	13.5674962546185	-2.48989427216964	0.0366920112481771	0.50842855176655	-3.56879277440325
Entpd2	0.269118629697179	17.9778645546491	2.47425694926453	0.0376097903373133	0.513263021073923	-3.59079465288236
Krt1;Krt71;Krt73; Krt74;Krt77	-0.453686845082057	20.9384524390109	-2.46463741481817	0.0381858349131883	0.51478933085306	-3.60432615208474
Trim24	-0.245652558164775	13.920766666757	-2.52449267292591	0.0434963331214369	0.538445784027205	-3.60967413457021

Rsrc1	0.297441483396165	13.8597203822671	2.57066717734086	0.0478097976109012	0.554722803736037	-3.61315101686913
Cdh6	-0.295717642869555	14.4047473926022	-2.45248089061912	0.0389265274845129	0.519335659014953	-3.62142231207137
Des;Ina;Nefh;Nefl;Nefm;Vim	-0.229661568958932	23.5502132883413	-2.44964441820902	0.0391014229016165	0.519645751163873	-3.62541064702498
Fn1	-0.369309663444742	19.2852247391861	-2.43821130231046	0.0398144321629287	0.523653528599465	-3.6414837491703
Dkk3	-0.304002995021376	14.0995397901315	-2.43473786670616	0.0400336254967283	0.523653528599465	-3.64636587522016
Col1a2	1.5778058184737	19.9579894127534	2.43451253741746	0.0400478868547127	0.523653528599465	-3.64668257325525
Krt10	-0.652841138723673	20.2628779027317	-2.42546121356438	0.0406249955926252	0.528621145661093	-3.65940244840302
H1-5	0.232351164940493	19.8281836535266	2.42346636916418	0.040753305071902	0.528621145661093	-3.66220536419501
Commd8	-0.223294017169005	14.1186595720369	-2.41985613182873	0.0409865527669171	0.530250075701137	-3.66727760849144
Abhd16a;Abhd16b	0.336878969793641	15.3225013865147	2.41544436645592	0.0412734048439867	0.530284885020842	-3.67347520354047
Itih4	-0.372217327878719	17.5995878672777	-2.41056649281186	0.0415929084566548	0.531172388643585	-3.68032657349125
H2bc12;H2bc14;H2bc3;H2bc4;H2bc7;H2bc9;Hist1h2bp;Hist2h2bb	-0.494165959072124	23.0205928176824	-2.40926173839594	0.0416787903908561	0.531172388643585	-3.68215902338979
PEDS1	0.319209450212426	14.7663521946742	2.4088145196352	0.0417082682633287	0.531172388643585	-3.68278709741453
Krt1	-0.391199848032308	19.186438983148	-2.40365484225661	0.0420498776728197	0.531172388643585	-3.69003267013303
Dolk	0.26691161578016	13.9735022948203	2.38223626733458	0.0434981822442226	0.538445784027205	-3.72009599275311
Gltp	0.238529466697763	15.636666855966	2.38223174973747	0.0434984929292145	0.538445784027205	-3.72010233116972
Tspan18	0.440698136348425	14.2457788180278	2.4017637130183	0.0461750166693478	0.550061124052271	-3.72536630875524
Mycbp	-0.240754388673354	15.7332152170627	-2.36693052580909	0.0445636311589843	0.541701624267893	-3.74156417081251
Lsm6	0.304627120267384	15.380116958243	2.35526962302264	0.0453928333934962	0.545251194016552	-3.75791078993535
Fgg	-0.319117801924589	15.7616251312145	-2.353772065175	0.0455004348482763	0.5457363825229	-3.7600095065493
Serpina1d	0.260198583196061	13.3719498835084	2.34403168899612	0.046206534008155	0.550061124052271	-3.77365642259946
Tbca	-0.228318290711414	17.3783811648198	-2.31586138586794	0.0483107497143241	0.554722803736037	-3.81308853435424
Scn10a;Scn11a;Scn5a;Scn9a	-0.235242594758024	16.6157689329931	-2.31066509603398	0.0487091917179643	0.554722803736037	-3.82035587783823
A2m;Pzp	-0.303263182138188	21.2889865356969	-2.30125490421341	0.049439086388067	0.554722803736037	-3.8335113258245
Serpind1	-0.474566796810389	18.9641860223996	-2.29757854355405	0.0497271856717864	0.554722803736037	-3.83864897298692
Dnajc6;Gak	0.242155260682051	16.504678234183	2.29455028609869	0.0499657488525452	0.554722803736037	-3.84288008605617